CRYSTALLIZATION OF PSEUDOPOLYMORPHIC FORMS OF SODIUM NAPROXEN IN MIXED SOLVENT SYSTEMS

A Thesis
Presented to
The Academic Faculty

by

Krystle J. Chavez

In Partial Fulfillment
of the Requirements for the Degree
Doctor of Philosophy in the
School of Chemical & Biomolecular Engineering

Georgia Institute of Technology
August 2009

CRYSTALLIZATION OF PSEUDOPOLYMORPHIC FORMS OF SODIUM NAPROXEN IN MIXED SOLVENT SYSTEMS

Approved by:

Dr. Ronald W. Rousseau, Advisor
School of Chemical & Biomolecular Engineering
Georgia Institute of Technology

Dr. Amyn Teja
School of Chemical & Biomolecular Engineering
Georgia Institute of Technology

Dr. Carson Meredith
School of Chemical & Biomolecular Engineering
Georgia Institute of Technology

Dr. Angus P. Wilkinson
School of Chemistry & Biochemistry
Georgia Institute of Technology

Dr. Mark Prausnitz
School of Chemical & Biomolecular Engineering
Georgia Institute of Technology

Date Approved: May 27, 2009

To my grandfather, who thought I would forever be a student

ACKNOWLEDGEMENTS

I would like to express sincere gratitude to my thesis advisor, Dr. Ronald W. Rousseau, for his constant encouragement and help during my time at Georgia Tech. Sincere appreciation is extended to my thesis committee, Dr. Carson Meredith, Dr. Mark Prausnitz, Dr. Amyn Teja, and Dr. Angus P. Wilkinson for their helpful discussions.

I would also like to thank current and previous group members; Dr. Karsten Bartling, Dr. Stephanie Barthe, Cosmas Bayuadri, P.J. Dumont, Dr. Laurent Nassif, Quinta Nwasinske, and Aphichit Svang-Aryiskul for their thoughtful advice and discussions. I would also like to acknowledge my undergraduate student, Melissa Guevara, for her help with some of the laboratory work.

A big thank you should also be extended to all of my friends for their encouragement and for getting me through the tough times. To my friends at Georgia Tech, Vittoria Blasucci, who has been though it all with me from the beginning; Dr. Suchitra Konduri, Dr. Yeny Hudino, and Marifel Olarte for entertaining me and helping me release all the day-to-day tension. To my best friends: Rekha Nair, Alicia Smith, Dr. Seema Qayumi, and Ramona Kei, thank you for listening and encouraging me through the good and bad times, and for supplying much needed distractions. You have all kept me sane. I'd also like to acknowledge Peter Emanuele, who had to listen to my rants everyday for the past four years; he still manages to keep me going with his encouragement.

Finally I would like to thank my family for all of their continual encouragement and support. This includes my grandfather, William Forester, who jokingly said I would

start collecting social security before I was ever done with school; I finally did it. My parents, Joyce and Camilo Chavez, who I know at times, had difficulties raising three distinct children, but somehow they managed to ensure we all turned out just fine. My sister, Melissa Chavez, and my brother, Michael Chavez, who have put with up with me throughout everything and although we may argue from time to time we are still always there for each other. I would also like to thank my sister-in-law, Kristin Chavez, who for the past eight or so years has managed to keep a smile on her face when dealing with our crazy family. This would also include my extended family Aunt Marsha and Uncle Greg Widdows, and Aunt Catherine and Uncle Kenneth Ferruggia; we are closer than maybe a family should be and a little crazier, but I love it and don't know how I could survive with out it. Thank you for being there through everything and picking me up when I needed it the most. Last but not least, my cousin and closest friend, Chelsea Ferruggia. She has seen me through all the ups and downs of my entire life, and still continues to provide never-ending encouragement. And to the rest of my family, who I may not see as often, but who are still there providing support when they can, I would like to extend my appreciations.

It is to all of these people that I owe my upmost gratitude for their encouragement and assistance in seeing me through to this point, without them I might never had made it.

TABLE OF CONTENTS

LIST OF TABLES

LISTS OF FIGURES

LIST OF SYMBOLS

a	Scalar of Unit Cell in $\vec{a}$ -direction
a	Thermodynamic Activity
$\vec{a}$	Crystallographic Axis
A	Area of HPLC Peak
b	Scalar of Unit Cell in $\vec{b}$ -direction
b	Calibration Curve Fit Variable, Y Intercept
$\vec{b}$	Crystallographic Axis
$\beta_{\circ}$	Compressibility of Pure Water
c	Scalar of Unit Cell in $\vec{c}$ -direction
$\vec{c}$	Crystallographic Axis
C	Concentration
C_p	Heat Capacity
Δc_p	Heat Capacity Difference between Solid and Liquid-State
C_s	Molar Concentration of Electrolyte
C_{S_1}	Concentration of First Diluted Sample
C_{S_2}	Concentration of Second Diluted Sample
d_{hkl}	Distance between two lattice planes (hkl)
Δg	Change Gibbs Free Energy
f	Fugacity

f°	Standard State Fugacity
Δh	Change in Enthalpy
$\Delta \hat{H}_{\mathrm{d}}$ (Chapter 2)	Change in Enthalpy upon Dissolution per Mole
$\Delta \hat{H}_{\mathrm{d}}$	Heat of Dehydration per Mole
$\Delta \hat{H}_{f}$	Change in Enthalpy upon Fusion per Mole
(hkl)	Family of Lattice Planes
$\Delta \hat{H}_{\mathrm{mix}}$	Heat of Mixing
$\Delta \hat{H}_{sol}$	Heat of Dissolution per Mole
$\Delta \hat{H}_{\mathrm{vap}}$	Heat of Vaporization per Mole
k	Calibration Curve Fit Variable, Slope
K_1	Equilibrium Constant for First Reaction
K_2	Equilibrium Constant for Second Reaction
K_h	Equilibrium Constant
k_s	Salting-out Parameter
m	Degree of Hydration
M	Mass of Acetonitrile
n (Chapter 3)	Number of Samples
n	Degree of Hydration
P_e	Effective Pressure
R	Ideal Gas Constant
S	Sample Standard Deviation

Δs	Change in Entropy
$\Delta \hat{S}_d$	Entropy Change of Dissolution per Mole
$\Delta \hat{S}_f$	Entropy Change Upon Fusion
T	Temperature
T_d	Dehydration Temperature
T_t	Triple Point Temperature
$U_{(eq)}$	Isotropic Atomic Displacement Parameter
V_c	Unit Cell Volume
$\bar{V}_i^\circ$	Partial Molar Volume of Non-electrolyte at Infinite Dilution
V_s	Volume of Pure Electrolyte
$\bar{V}_s^\circ$	Partial Molar Volume of Pure Electrolyte at Infinite Dilution
x	Mole Fraction
$\bar{X}$	Mean of Sample Set
X_i	Sample Value of *i*th Sample
Z'	Number of Formula Unit in Unit Cell Divided by the Number of Independent General Positions
α	Crystallographic Angle between b and c-axis
β	Crystallographic Angle between a and c-axis
γ (Chapter 2)	Crystallographic Angle between a and b-axis
γ	Activity Coefficient
Λ	Adjustable Wilson Parameters
λ	Energies of Interaction in Wilson Equation

θ	Angle of Incidence
υ	Molar Liquid Volume

Subscripts

A	Acetonitrile
I	Internal Standard
(l)	Liquid Phase
ROH	Alcohol with R-chain
S	Sample
(s)	Solid Phase
SD	Standard Deviation
(v)	Vapor Phase
W	Water
0	Initial Preparation
1 (Chapter 3)	First Dilution
1 (Chapter 4)	Water
2 (Chapter 3)	Second Dilution
2 (Chapter 4)	Organic Alcohol

LIST OF ABBREVIATIONS

A	Anhydrate
ASN	Anhydrous Sodium Naproxen
CBZA	Anhydrous Carbamazepine
CBZH	Hydrated Carbamazepine
DSC	Differential Scanning Calorimetry
DSN	Dihydrated Sodium Naproxen
dTGA	Derivative of Thermogravimetic Analysis
EtOH	Ethanol
FTIR	Fourier Transfer Infrared Spectroscopy
^{1}H-NMR	Proton Nuclear Magnetic Resonance
HPLC	High Performance Liquid Chromatography
IR	Infrared Spectroscopy
MeOH	Methanol
MSN	Monohydrated Sodium Naproxen
mol %	Mole Percentage
NSAID	Nonsteroidal Anti-inflammatory Drug
PLM	Polarized Light Microscopy
PXRD	Powder X-Ray Diffraction
SEM	Scanning Electron Microscopy
TGA	Thermogravimetric Analysis
TSN	Tetrahydrated Sodium Naproxen

UV	Ultraviolet

SUMMARY

Incorporation of solvent molecules into the crystal structure of an organic compound has strong effects on the solvate's chemical and physical properties; and hence, pharmacokinetics. Therefore, a study on pseudopolymorphic transitions and the ability of solvents to form pseudopolymorphs with pharmaceutical compounds is important for the pharmaceutical industries.

The main goals of this study were to provide quantitative descriptions of the crystallization and solid-state transformation of pseudopolymorphs of sodium naproxen in mixed alcohol-water solvents. Furthermore, organic alcohol solvates of sodium naproxen were discovered, and characterized qualitatively and quantitatively.

Several pseudopolymorphic forms of sodium naproxen were crystallized from methanol-water and ethanol-water solutions, including hydrated and alcohol-solvated forms. Results showed that the transitions of the pseudopolymorphic forms occurred at temperatures that depended upon the solvent concentration. Results also revealed that water activity was a controlling factor for the transitions because regardless of which alcohol solvent mixture was used, the water activity was the same for similar transitions.

A methanol-solvated form of sodium naproxen was discovered and fully characterized using a variety of analytical techniques. The methanol solvate was crystallized from pure methanol at 10°C and was determined to be in a one to one ratio of sodium naproxen to methanol. For further analysis, a single crystal study of crystals obtained by slowly evaporating methanol at approximately 4°C was performed and revealed a solvate with a two to three ratio of sodium naproxen to methanol. The 1.5 solvate was shown to not be representative of the entire sample, but still provided insight

into the bonding of the methanol solvent in sodium naproxen. Hydrogen bonding was determined to be the main force in solvation, along with Na-O coordination between methanol and sodium naproxen.

The heats of solution for each pseudopolymorph were estimated by fitting the solubility data with the van't Hoff equation. The stability of hydrated forms over solvated forms at higher temperatures was proven for enantiotropic systems from a thermodynamic cycle.

Additionally, the ability of sodium naproxen to solvate with other alcohol solvents was explored, specifically looking at comparisons between ethanol, 1-propanol, 2-propanol, 1-butanol, and isobutanol solvents. It was shown that as the size and/or branching of the alcohol increased the ability to solvate decreased in relation to the molar amount of the alcohol present in the crystal structure. Additionally larger, branched alcohols required more energy to desolvate based on the energy per mole of alcohol. This is related to the fact that these solvates had a smaller amount of alcohol present in the solvate; and hence, had strong bonding with the sodium naproxen molecule.

CHAPTER 1

INTRODUCTION

Incorporation of solvent into the crystal structure of organic compounds can lead to changes in both physical and chemical properties. These solvates often have different unit cells leading to changes in physical properties, such as density, solubility, bioavailability, and dissolution rate. The changes in physical properties are similar to those seen in polymorphs (chemical species with the same molecular formula, but different crystal structures); hence solvates are often termed pseudopolymorphs (Kuhnertb and Gasser, 1971). In the present student, a number of pseudopolymorphic forms of sodium naproxen were examined. This includes the previously studied anhydrous, monohydrated, and dihydrated forms, as well as, newly discovered organic alcohol-solvated forms. Organic alcohol solvents were studied because they are often used in manufacturing processes for organic compounds, such as sodium naproxen. The alcohol solvates examined include those of methanol, ethanol, propanol, and butanol incorporated in sodium naproxen.

Crystalline solvates and hydrates play an important role in the pharmaceutical industry (Morris, 1999). The formation of pseudopolymorphs of pharmaceuticals can be of great significance because changes in the physical properties of the crystal can affect the safety and efficacy of a drug. Bioavailability and/or physiochemical stability of pseudopolymorphs can raise issues during the development of new pharmaceuticals. For example, hydrated compounds can convert to amorphous forms upon dehydration. Cephradine dihydrate dehydrates to become amorphous and undergoes subsequent

oxidation (Florey, 1973). Dihydrophenylalanine anhydrate crystallized from ether is stable to oxidation; however, the dihydrated form oxidizes in air producing 70% phenylalanine in ten minutes (Byrn and Lin, 1976; Ressler, 1972). Also, stability and instability of various solvates play important roles in pharmaceutical development. For example, aripiprazole is known to exist in five reproducible pseudopolymorphic forms, but only four of them are stable. The dichloromethane solvate form is reproducible but highly unstable. Additionally, a number of other solvates disclosed in patent literature have been seen but are not reliably reproducible (Braun et al., 2009). Therefore, a comprehensive understanding of pseudopolymorphic formation is important in developing reliable and stable pharmaceuticals.

Furthermore, technical and industrial uses of solvates concern issues such as purification, preparation of a specific polymorphs with high chemical and physical purity, or particle size control due to the fact that desolvation of stoichiometric solvates often leads to products with a small and homogenous particle size distribution (Griesser, 2006). Purification of dirithromycin, a macrolide antibiotic, is achieved by the formation of the acetone solvate followed by heating in water to convert it to a nosolvated, stable polymorphic form (Wirth and Stephenson, 1997). Both prilocaine hydrochloride and zanoterone exhibit specific polymorphic forms only via transformation from a solvated form (Schmidt et al., 2004; Rocco et al., 1995). Solvent adducts can often crystallize more easily than solvent-free molecules, because of more efficient packing achieved with the addition of the solvent molecules, as is the case for R-cinacalcet hydrocholoride, a therapeutic agent marketed as Sensipar®, Mimpara®, and Parareg® (Braum et al., 2008). As illustrated, formation of solvates can play a crucial role in pharmaceutical

development due to the fact that they can be the only pathway to certain polymorphic forms or they can reduce the need for additional processing steps, such as milling.

Formation of pseudopolymorphs is affected by a number of variables such as temperature, pressure, and solvent choice; thus, changing operating variables during crystallization may result in changes to pseudopolymorphic forms or the discovery of new forms. One of the most unusual cases can be seen in the polymorph Ritonavir (Bauer et al., 2001). Form I of Ritonavir was the only form seen during the development stages of the pharmaceutical, but during manufacturing a second form (Form II), which had a significant lower solubility, was discovered. Form II was both unusually stable and difficult to crystallize, but did hinder production. Recognition of the variables that can affect polymorphic and pseudopolymorphic transitions is important in preventing unwanted changes to pharmaceuticals.

The present study was motivated by pseudopolymorphic transitions seen in varying solvent concentrations of sodium naproxen and the thermodynamic reasons for these transitions. It was previously shown that sodium naproxen transitions from a dihydrate to an anhydrate in pure water solutions with changing temperature, and that the addition of methanol to the solvent at a 64 mol% concentration produces a transition from a dihydrated form to a monohydrated form (Kim and Rousseau, 2005). Since some work had begun on mixed-solvent systems and pseudopolymorphic transitions of sodium naproxen prior to this work, one aim was to determine what thermodynamic factors controlled pseudopolymorphic transitions in these mixed-solvent systems. Additionally, understanding how changes in solvent concentrations affected these pseudopolymorphic transitions was another aim.

In the present work, two main areas were addressed; these were derived from the above mentioned motivations and goals: (1) solvent-mediated transitions of pseudopolymorphic forms of sodium naproxen in mixed alcohol-water systems, and (2) the ability of organic alcohols to form solvates with sodium naproxen based on the carbon chain length and branching. An outline of the remaining chapters is presented below:

- ◊ Chapter 2: basic background information is discussed that relates to the information presented in this work.
- ◊ Chapter 3: solubility of anhydrous sodium naproxen in methanol-water and ethanol-water solvents was studied, along with the observation of changes in pseudopolymorphic forms across the studied temperature range. Methanol created a general salting-in effect, while ethanol solutions created a salting-out effect.
- ◊ Chapter 4: determination of the actual transition point for the pseudopolymorphic forms was determined based on van't Hoff plots of solubility and temperature. The data was also manipulated to determine the role of water and alcohol activity in determining when a transition would occur in reference to changes in the alcohol solvent used. It was found that water activity played an effective role in determining pseudopolymorphic transition points, while alcohol activity did not. This was explained by the equation for the equilibrium constant of the transition and its squared dependence on the activity of water.

- ◊ Chapter 5: the stability of dihydrated versus alcohol solvated sodium naproxen in mixed solvent systems, based on the heats of dissolution of the pseudopolymorphs, is analyzed using slight modifications of a previously developed method. The analysis gives validation to the fact that the dihydrated form of sodium naproxen is seen at higher temperatures than the alcohol solvated forms of sodium naproxen, as presented in chapter 4. It can also provide an estimate of the heat of dissolution of pseudopolymorphs in mixed solvent systems.
- ◊ Chapter 6: a novel methanol solvate form of sodium naproxen was characterized using a variety of analytical techniques including thermal gravimetric analysis, differential scanning calorimetry, proton nuclear magnetic resonance, polarized light microscopy, and powder x-ray diffraction.
- ◊ Chapter 7: the crystal structure of a methanol solvated form of sodium naproxen is discussed based on single crystal x-ray diffraction techniques. Comparison is made between its crystal structure and the other solved crystal structures of pseudopolymorphs of sodium naproxen. Additionally, this methanol solvate is compared to the methanol solvate discussed in chapter 6.
- ◊ Chapter 8: other organic alcohol solvates are discussed in terms of their similarities and differences to the hydrated forms of sodium naproxen. These solvates were analyzed by thermal gravimetric analysis, differential scanning calorimetry, proton nuclear magnetic resonance, polarized light microscopy, and powder x-ray diffraction. Desolvation endotherms were compared to the size and bulkiness of the organic alcohols present in the crystal structure.

◊ Chapter 9: conclusions and recommendations for further work in this area.

CHAPTER 2

BACKGROUND

This chapter provides a basic background for the work being presented in this thesis.

2.1 Crystallography

2.1.1 Lattice and Unit Cells of Crystal Systems

A true solid crystal is comprised of a rigid lattice of molecules, atoms, or ions, the locations of which are characteristic of the substance (Mullin, 2004). Ideally a crystal is constructed using identical structural units that repeat in space. A three-dimensional array is referred to as a lattice (see Figure 2.1). It is purely a mathematical abstraction and refers to the fact that a three-dimensional grid of lines can be used to connect the lattice points. The lattice points can represent a single atom, as with a monatomic element, or can contain one or more molecules, as with an organic species. The crystal structure is only formed when the fundamental unit is attached identically through the lattice and extended along each crystal axis through translational repetition (Brittain and Byrn, 1999).

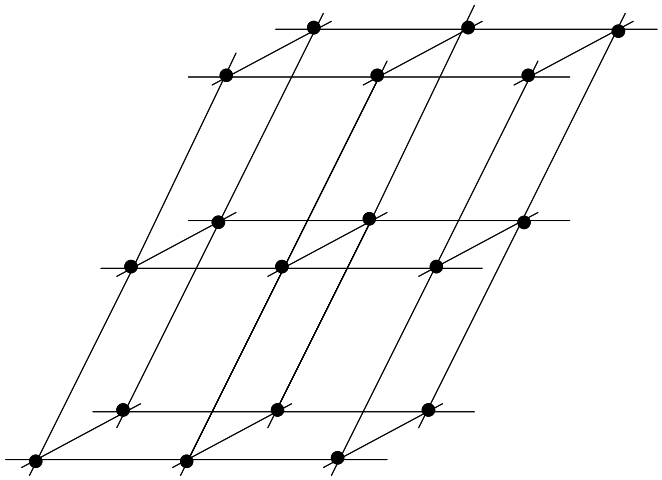

Figure 2.1. Three-dimensional lattice with lattice points.

The axes which form the smallest parallelepiped, repeated block is termed a unit cell. The unit cell can be described by six scalars, a, b, c, α, β, and γ, as seen in Figure 2.2. By elementary vector analysis, the volume of the unit cell is defined by

$$V_c = \left|\vec{a} \times \vec{b} \cdot \vec{c}\right| \tag{2-1}$$

Several kinds of unit cells are possible by varying the six scalars. For example, if a = b = c and α = β = γ, a cubic unit cell exists, such as with iron and chromium. Only seven unit cells are necessary in order to include all possible lattices. These are listed in Table 2.1.

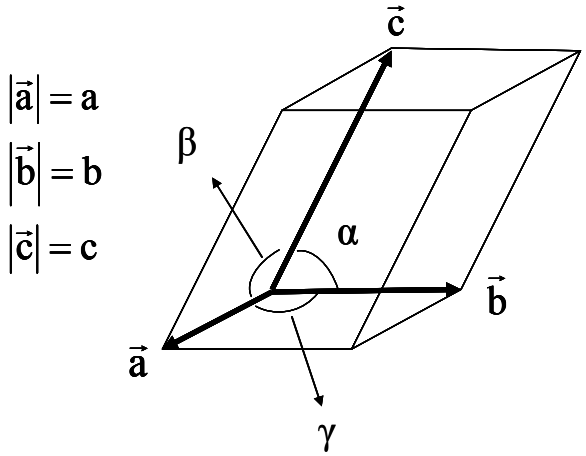

Figure 2.2. Unit cell and its six scalars.

Table 2.1. Seven crystal classes based on the fundamental unit cells.

Crystal Class	Relationship between Cell Edges	Relationship between Cell Angles
Cubic	$a = b = c$	$\alpha = \beta = \gamma = 90°$
Tetragonal	$a = b \neq c$	$\alpha = \beta = \gamma = 90°$
Orthorhombic	$a \neq b \neq c$	$\alpha = \beta = \gamma = 90°$
Monoclinic	$a \neq b \neq c$	$\alpha = \gamma = 90°$ $\beta \neq 90°$
Triclinic	$a \neq b \neq c$	$\alpha \neq \beta \neq \gamma \neq 90°$
Hexagonal	$a = b \neq c$	$\alpha = \beta = 90°$ $\gamma = 120°$
Trigonal	$a = b = c$	$\alpha \neq \beta \neq \gamma \neq 90°$

2.1.2 Space Groups

Although there are seven different crystal systems, there are more possible arrangements of the points that do not violate the lattice constraints. Auguste Bravais postulated in 1949 that there were only 14 possible basic types of lattices that could fit

within the constraints of the seven crystal systems. These fourteen lattices are shown in Figure 2.3.

Crystal structures can be carried into themselves by various point symmetry operations. These symmetry operations are defined as an operation that moves the system into a new configuration that is equivalent to and indistinguishable from the original one. There are seven symmetry operations: *identity*, *reflection*, *inversion*, *proper rotation*, *improper rotation*, *screw operation*, and *plane glide*. *Identity* leaves the system unchanged and in an orientation identical to the original. The second symmetry operation is *reflection* through a plane. This changes the sign of the coordinates perpendicular to the plane while leaving the coordinates parallel to the plane unchanged. *Inversion* through a point changes the sign of all coordinates of the lattice points. *Proper rotation* is defined as a simple rotation about an axis. Finally, *improper rotation* is merely a proper rotation followed by an inversion. These first five operations are described as macroscopic operations. Performing these operations on each of the 7 crystal systems leads to the 32 point groups.

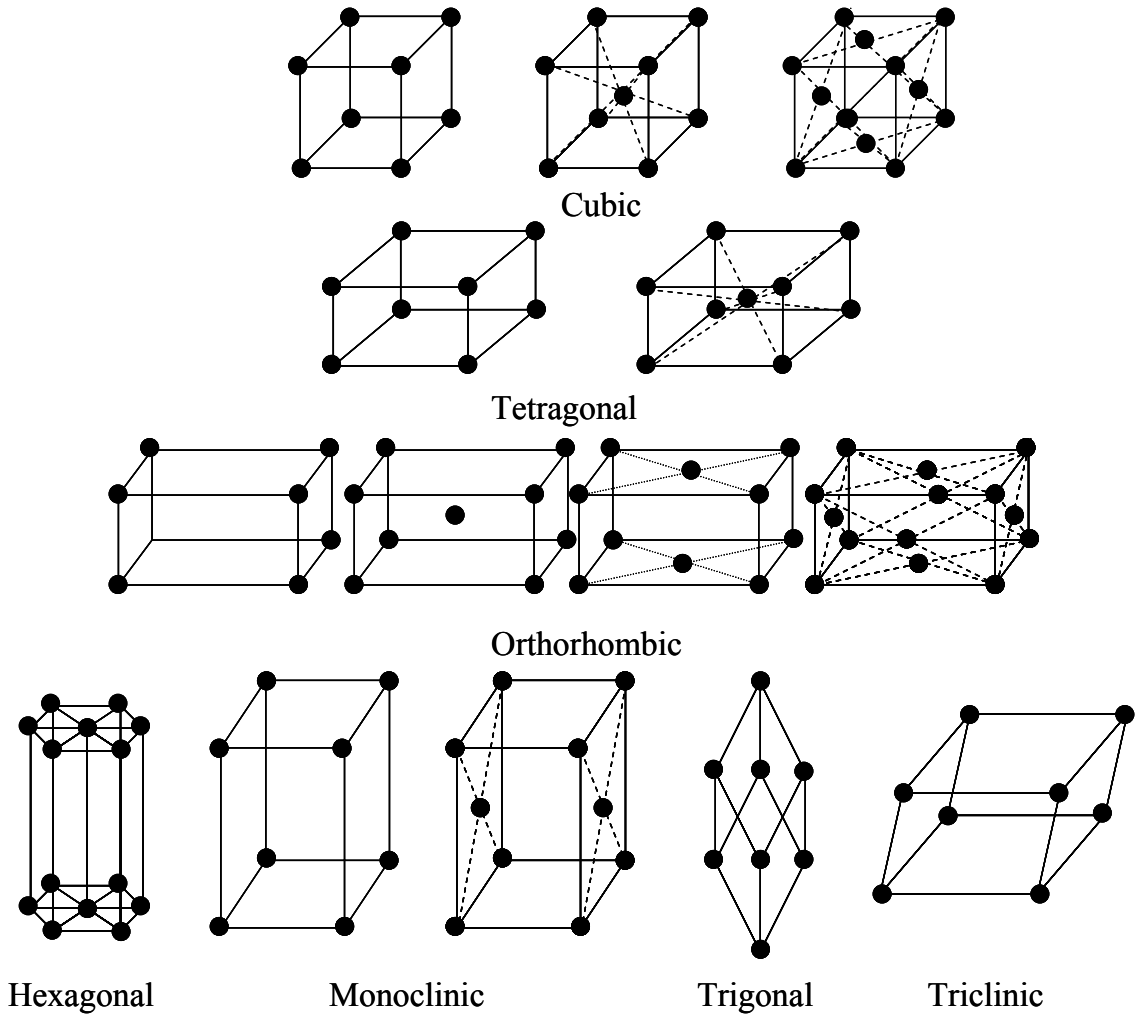

Figure 2.3. The fourteen Bravais lattices (Mullin, 2004).

The remaining two symmetry operations are termed microscopic operations. The *screw operation* couples a proper rotation with a translation parallel to the axis of rotation. A *glide plane* operation combines a reflection with a translations operation. Combining the 14 Bravais Lattices with the 32 point groups and performing these remaining two operations leads the 230 space groups. The relationship between the 7 crystal systems, 14 Bravais lattice, 32 point groups and 230 space groups can be seen in Figure 2.4.

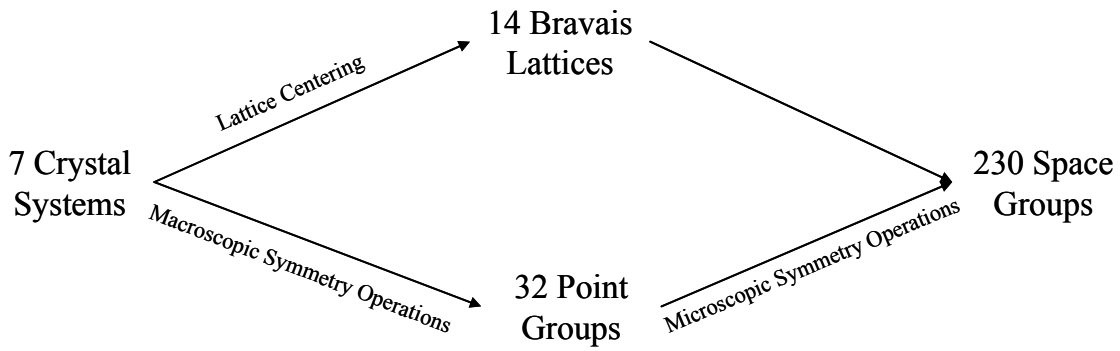

Figure 2.4. Schematic of the relationship between the 7 crystal systems, 14 Bravais lattices, 32 point groups, and 230 space groups.

2.1.3 Plane Spacing

Wilhelm Röntgen discovered x-rays in 1895 and seventeen years later, Max von Laue suggested that they may diffract when passed through a crystal. He realized that their wavelengths are comparable to the separation of lattice planes. Under von Laue, Walter Friedrich and Paul Knipping confirmed this (Atkins, 1998). If one regards a lattice plane as a mirror and a crystal as merely stacks of reflecting lattice planes of separation d, one can calculate the angle the crystal must make with the incoming beam

of x-rays for constructive interference. W.L. Bragg was able to express the necessary conditions for diffraction in a simple mathematical form known as Bragg's law:

$$\lambda = 2d_{hkl} \sin\theta \qquad (2\text{-}2),$$

where λ is the wavelength of the x-ray, d_{hkl} is the distance between the two lattice planes of the crystal, and θ is the angle of incidence. Figure 2.5 shows the relationship between the planar spacing and the angle of diffraction for a crystal with hkl planes.

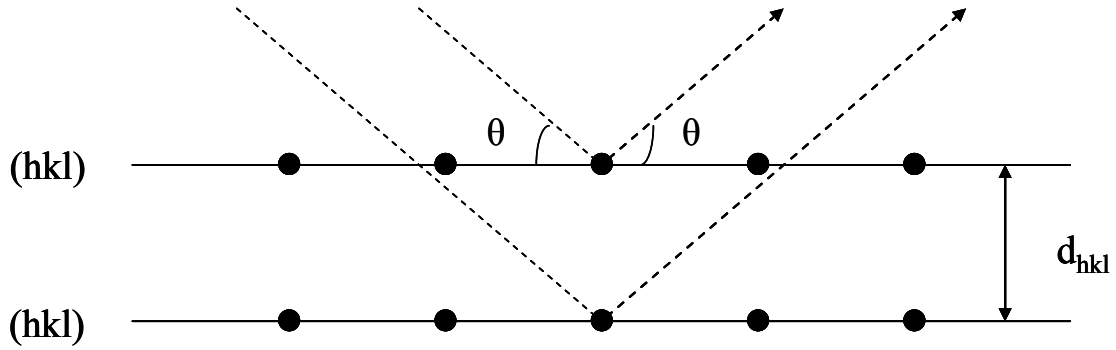

Figure 2.5. Diagram of Bragg's angle determination between interplanar spacing of hkl planes.

Braggs' equation gives an easy way to understand powder x-ray diffraction. Powder x-ray diffraction data has information on peak positions and intensities. Peak positions can be related to unit cell constants and intensities to the contents of the unit cell. Interplanar spacing is a function of the cell constants. Therefore, if the cell constants are known for a crystalline compound, peak positions can be obtained from the Bragg equation (λ is dependent on the machine). Reversing this process one would be able to determine cell parameters from powder x-ray diffraction patterns.

2.2 Solid-State Phases

During crystallization and pharmaceutical formulation processing, a number of solid-state phases can occur. These can include polymorphs, solvates, desolvated solvates, and amorphous material. Polymorphs are defined as crystal species with the same chemical formula but different crystal structures. Solvates are the incorporation of a solvent into the crystal structure. Removal of the solvent creates desolvated forms of the solvates. Amorphous materials have no long-range atomic order. Figure 2.6 shows the possibilities for solid-state phases. A reproducible production of the solid state demonstrates control over the manufacturing process of the pharmaceutical ingredient, which is important in regulatory guidelines.

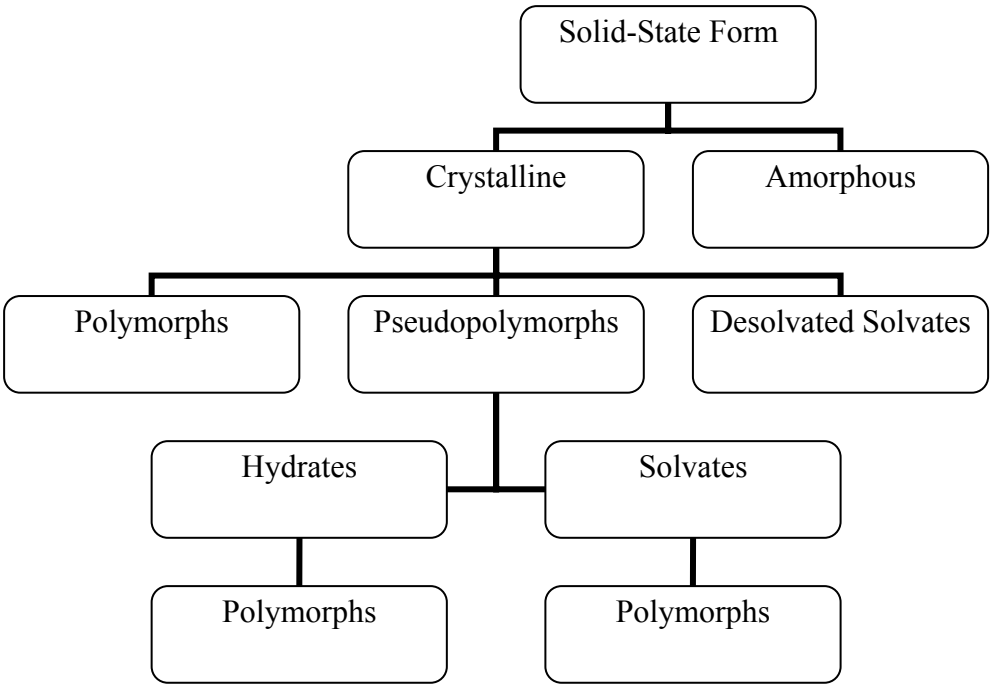

Figure 2.6. Solid state phases (Brittain and Byrn, 1999).

2.2.1 Polymorphism and Pseudopolymorphism

Many organic and inorganic pharmaceutical compounds can crystallize in two or more solid forms while having the same chemical composition. These solid forms are referred to as polymorphs. Due to their varying crystal structures, polymorphs have varying physical properties, such as solubility, hygroscopicity, dissolution rate, and compactability.

Solvents are often used in the production of crystalline pharmaceutical species and during processing. These solvents can become incorporated into the lattice of the crystal in a specific stoichiometric ratio, thus forming solvates or hydrates (also known as pseudopolymorphs) (Bechtloff et al., 2001). The properties of pseudopolymorphs differ from those of the unsolvated species, which should not be surprising because their compositions are different. Accordingly, transformations among pseudopolymorphic forms often produce variations in physical properties such as density, solubility, dissolution rate, and bioavailability. These changes in physical form can interrupt downstream processing during manufacturing. Furthermore, the formation of pseudopolymorphs of pharmaceuticals can be of great importance because changes in the physical properties of the crystal can affect the safety and efficacy of a drug. For example, some hydrated compounds may convert to an amorphous form upon dehydration and may become chemically labile. Some examples of how pseudopolymorphism can affect the efficacy of a drug include cephradine dihydrate and ampicillin. Cephradine upon dehydration becomes amorphous and then undergoes oxidation (Florey, 1973). Due to the aqueous solubility differences between the anhydrous and trihydrated form of ampicillin, blood serum concentrations of the

anhydrous form are higher and reach optimal levels earlier than the trihydrated form (Poole et al., 1968). Thus, knowing the presence or existence of crystal pseudopolymorphs is of importance in developing robust, large-scale crystallization processes in the pharmaceutical industry and is becoming more important within the current regulatory climate.

2.2.2 Types of Polymorphism

There are two forms of polymorphism: *packing polymorphism* and *conformational polymorphism* (Brittain and Byrn, 1999).

Packing polymorphism represents molecules that exist as a rigid group of atoms with definite symmetry that can be stacked differently to occupy the points of different lattices. This form of polymorphism is readily available to compounds for which hydrogen bonding is important, and for which there exists multiple possibilities to achieve the necessary intramolecular and intermolecular interactions. Figure 2.7 shows the three polymorphic forms of ethyl maltol (Brown et al., 1995). Each polymorph has a different mode of hydrogen bonding; Form 1 contains nearly planar chains of molecules, Form 2 has three-dimensional or spiral chains, and Form 3 contains hydrogen bonded dimers.

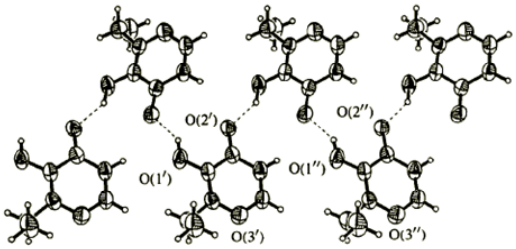

Form 1

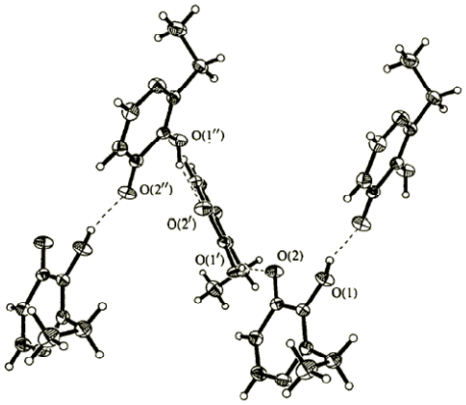

Form 2

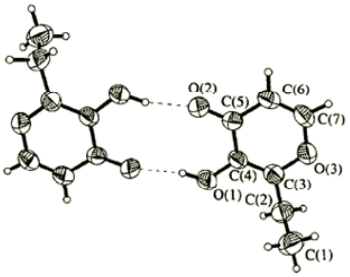

Form 3

Figure 2.7. Three polymorphic forms of ethyl maltol (Brown et al., 1995).

Packing polymorphism usually represents different modes by which molecules in their most favorable conformational state are assembled into different solid structures. When different conformational states are possible, *conformational polymorphism* may result. Conformations arise from rotation about single bonds, corresponding to potential energy minima. The various conformations cannot differ too greatly in free energy content from the equilibrium structure of the molecule. It is this proximity of molecular conformation energies that makes possible the existence of different molecular conformations in a single-crystal structure. For example, lomeridine dihydrochloride has been reported to exist in two conformational polymorphic forms as shown in Figure 2.8 (Hiramatsu et al., 1996). Although the molecular conformations are similar for the two forms, torsion around the C—N4 bond is sufficient to yield the conformational polymorphs.

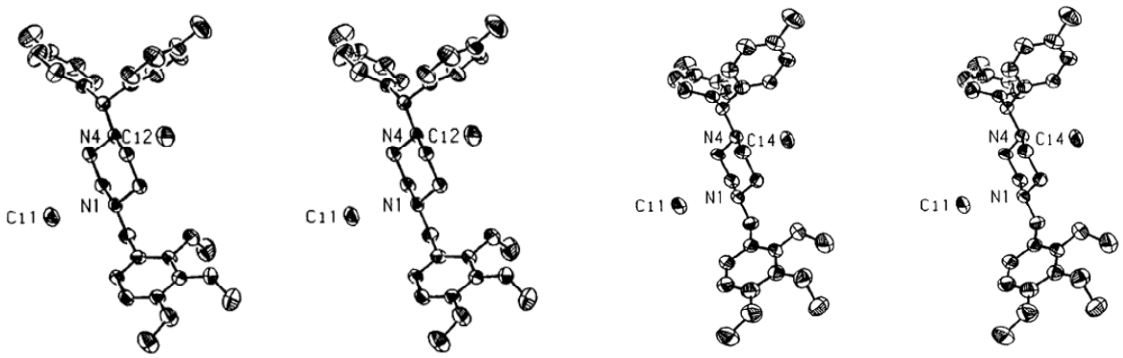

Form I Form II

Figure 2.8. Two polymorphic forms of lomeridine dihydrochloride (Hiramatsu et al., 1996).

2.2.3 Classification of Hydrates

Water is small enough to fill many commonly occurring periodic "voids" formed when larger molecules are packed, and it interacts through hydrogen bonding to overcome energy barriers. This characteristic gives rise to a series of water arrangements in crystal structures. Table 2.2 lists the classification of crystalline hydrates.

Table 2.2. Classification of crystalline hydrates (Morris, 1999).

Class	Description
1	Isolated Lattice Sites
2	Lattice Channels
-a	Expanded Channels (Non-Stoichiometric)
-b	Lattice Planes
-c	Dehydrated Hydrates
3	Metal-ion Coordinated Water

Isolated site hydrates represent hydrates where water molecules are isolated from each other and surrounded by intervening molecules of the host structure. This means that water molecules on the surface of the crystal can be easily lost, but does not leave other water molecules accessible. Similarly, there is no network of hydrogen bonding that solely involves water molecules on any axis through the crystals. These types of hydrates should yield sharp DSC endotherms and a narrow TGA weight loss.

Hydrates in the second class, *lattice channel hydrates*, contain water molecules that lie next to one another along an axis of the lattice forming "channels" through the crystal. For TGA and DSC data, early onset of dehydration is present, followed by a broad water loss step. This is due to the fact that dehydration begins at the "ends" of the

crystal and continues towards the center along the channels. Additionally, some channel hydrates may take up additional moisture when exposed to high humidity, such as chromylin sodium (Cox et al., 1971). Upon water addition, such hydrates may expand, which is why they are termed *expanded channels*. Planar hydrates have the water molecules localized in a two-dimensional order or plane, hence the term *lattice planes*. *Dehydrated hydrates* dehydrate at relatively high partial pressures of water, or they dehydrate shortly after removal from the mother liquor. The dehydration leaves an intact anhydrous structure similar to the hydrated structure but with a lower density.

Ion associated hydrates contain metal ion coordinated water. The metal-water interaction can be quite strong; hence, dehydration only takes place at very high temperatures. In DSC and TGA thermograms, very sharp peaks corresponding to loss of the water bonded with the metal ions are expected at high temperatures.

2.3 Solubility Behavior

2.3.1 Polymorphs and Pseudopolymorphic Systems

Polymorphs and pseudopolymorphs are classified as either monotropic or enantiotropic, depending on if one form can change reversibly to the other (Ostwald, 1897). For monotropic systems, as shown in Figure 2.9 (a), the transition temperature from Form I to Form II does not appear before the melting temperature; therefore, Form I cannot transform to Form II reversibly. In Figure 2.9 (b), Form II is stable until a transition temperature is reached, here the two solubility curves meet and then Form I is stable above the transition temperature. This is an example of an enantiotropic system; at the transition temperature, reversible transformation between the two forms exists. By examining kinetic effects on thermodynamic properties of solubility, Figure 2.9 (c) is

established. The dotted lines represent metastable behavior of the two forms. If X identifies the initial conditions of the system and crystallization is allowed to occur isothermally, the Ostwald rule of stages suggests that, Form I, which is metastable, would crystallize first, and then reform into a stable Form II. The Ostwald rule of stages states that an unstable system does not necessarily transfer to the most stable system, but instead transforms to the system that allows for the smallest loss of free energy (Prausnitz et al., 1999).

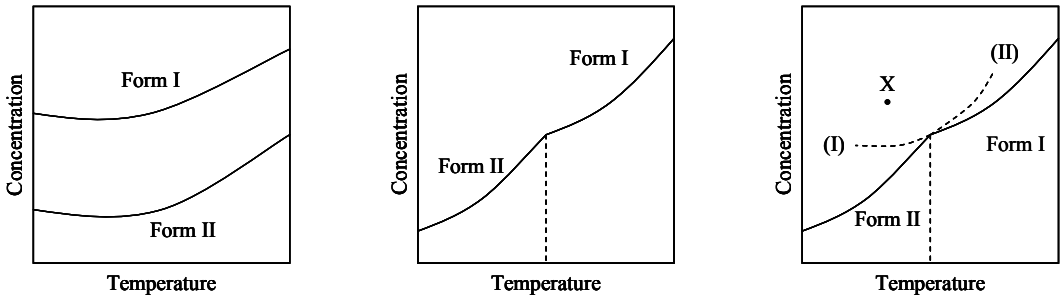

Figure 2.9. Solubility curves exhibiting (a) monotropy, (b) enantiotropy, and (c) enantiotropy with metastable phases (Ostwald, 1897).

Thermodynamic rules were also developed by Burger and Ramberger in 1979 to determine if two polymorphs were monotropes or enantiotropes. These rules are presented in Table 2.3, where Form I is the stable form.

Table 2.3. Relative thermodynamic properties of monotropic and enantiotropic polymorphs (Burger and Ramberger, 1979).

Monotropes	**Enantiotropes**
$T_{transition} > T_{fusion}$ Form I	$T_{transition} < T_{fusion}$ Form I
Form I stable	Form I: stable for $T > T_{transition}$ Form II: stable for $T < T_{transition}$
Transition Irreversible	Transition Reversible
Exothermic Transition of II→ I	Endothermic Transition of II → I
Solubility I < Solubility II	Solubility I > Solubility II for $T < T_{transition}$ Solubility I < Solubility II for $T > T_{transition}$
$\Delta H_f(\mathrm{I}) < \Delta H_f(\mathrm{II})$	$\Delta H_f(\mathrm{I}) < \Delta H_f(\mathrm{II})$

Intermolecular forces between solute and solvent are a strong influence on solubility (Prausnitz et al., 1999). However, other factors besides the intermolecular forces between the solute and solvent can play a role in determining the solubility of the solute, e.g. solubility can also depend on the fugacity of the pure solid and the fugacity of the standard state to which the activity coefficient would refer.

The solid-liquid equilibrium equation is

$$f_{(\text{pure solid})} = f_{(\text{solute in liquid solution})} \tag{2-3}$$

or

$$f_{(\text{pure solid})} = \gamma_{\text{solute}} x_{\text{solute}} f^{\circ}_{\text{solute}} \tag{2-4}$$

where x_{solute} is the solubility (mole fraction) of the solute in the solvent, γ_{solute} is the activity coefficient in the liquid-phase, and $f^{\circ}_{\text{solute}}$ is the standard-state fugacity. From the previous equation the solubility becomes

$$x_{\text{solute}} = \frac{f_{(\text{pure solid})}}{\gamma_{\text{solute}} f^{\circ}_{\text{solute}}} \tag{2-5}$$

Thus the solubility of the solid depends on both the activity coefficient and the ratio of the two fugacities.

The two fugacities are independent of the solvent; they depend only on the properties of the solute. The standard-state fugacity is usually defined as the fugacity of the pure, subcooled liquid at the temperature of the solution and at some specific pressure. The ratio of the fugacities is also related to the Gibbs energy change for the solute, as follows:

$$\underset{\text{a}\to\text{d}}{\Delta g} = RT \ln \frac{f^{\circ}_{\text{solute}}}{f_{(\text{pure solid})}} \tag{2-6}$$

where the path $\text{a} \to \text{d}$ is designated by Figure 2.10. The Gibbs energy change can also

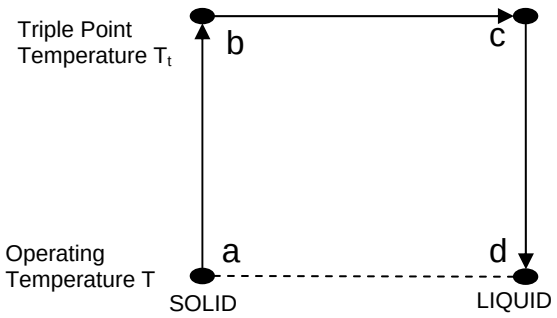

Figure 2.10. Thermodynamic cycle.

be related to the corresponding enthalpy and entropy changes as follows:

$$\underset{a\to d}{\Delta g} = \underset{a\to d}{\Delta h} - T\ \underset{a\to d}{\Delta s} \tag{2-7}$$

Using the thermodynamic cycle presented above (assuming the heat of mixing from b→c is zero) and the above equations, a general expression for solubility can be established,

$$\ln \frac{1}{x_{\text{solute}}\gamma} = \frac{\Delta h_{\text{f}}}{RT_{\text{t}}}\left(\frac{T_{\text{t}}}{T} - 1\right) - \frac{\Delta c_{\text{p}}}{R}\left(\frac{T_{\text{t}}}{T} - 1\right) + \frac{\Delta c_{\text{p}}}{R}\ln\frac{T_{\text{t}}}{T} \tag{2-8}.$$

After a series of assumptions, one is led to the van't Hoff equation,

$$\ln x = -\frac{\Delta \hat{H}_{\text{f}}}{RT} + \frac{\Delta \hat{S}_{\text{f}}}{R} \tag{2-9}.$$

The first assumption is the difference between the triple-point temperature and the melting temperature is small, therefore differences in the enthalpies of fusion at these temperatures are taken to be small. So one can substitute the melting temperature for the triple-point temperature and use the enthalpy of fusion at the melting temperature. Second, Δc_{p}, the differences in the heat capacity of the solute in its solid-state and its liquid-state, is relatively small. Additionally as $\frac{T_{\text{t}}}{T}$ goes to one, $\ln\frac{T_{\text{t}}}{T}$ goes to $\frac{T_{\text{t}}}{T} - 1$. This allows the second and third terms of the equation on the right-hand side to be neglected. Third, the solution is assumed to behave ideally, and γ is taken to be one.

To account for non-ideality of the solution, i.e. to eliminate one of the assumptions made in the van't Hoff equation, the enthalpy of fusion can be replaced by the heat of solution, $\Delta \hat{H}_{\text{d}}$, and the entropy of fusion by the entropy of solution, $\Delta \hat{S}_{\text{d}}$ (Beiny and Mullion, 1987). Thus the van't Hoff equation can be re-written as follows:

$$\ln x = -\frac{\Delta \hat{H}_{\mathrm{d}}}{RT} + \frac{\Delta \hat{S}_{\mathrm{d}}}{R} \qquad (2\text{-}10).$$

van't Hoff plots ($\ln x$ vs. $1/T$) have been used to show discontinuities in solubility between pseudopolymorphs of enantiotropic pharmaceuticals, such as carbamazepine (Qu et al., 2006), and theophylline (Khanhari and Grant 1995). Since each pseudopolymorph has distinct $\Delta \hat{H}_{\mathrm{d}}$ and $\Delta \hat{S}_{\mathrm{d}}$ values, a van't Hoff plot should show distinct lines for each pseudopolymorph. The point where the two lines crossed is referred to as the transition point.

2.3.2 Salting-Out Effects

A solution can be made supersaturated, with respect to a given solute, by the addition of a substance that reduces the solubility of the solute in the solvent. In the pharmaceutical industry, the precipitation of organic substances from water-miscible organic solvents is controlled by the addition of water to the solution. This is generally termed 'watering-out'. In contrast, the addition of a water-miscible organic solvent to an aqueous solution has been termed 'drowning-out', 'quenching', and 'solventing-out'. The term 'salting-out' is generally used to encompass all of the above examples.

Salting out has many advantages. For example, highly concentrated initial solutions can be made by dissolving an impure crystalline material in a suitable solvent. If the solute is highly soluble in the solvent, dissolution may be affected at low temperatures which are advantageous for the processing of heat sensitive materials. Additionally, a slight dilution of the salting-out agent with the solvent can be beneficial in avoiding excessive nucleation in the regions of primary contacts.

There are four basic theories with regard to the salting-out/in effect as described by Long et al. (1951): hydration theories, electrostatic theories, van der Waals forces, and an internal pressure concept. Hydration theories stem from the idea that water molecules are removed from their solvent role due to "hydration" of the ions; that water dipoles are oriented in the hydration shell around an ion. So there is a preferred orientation of water molecules toward a polar non-electrolyte, which means that ions of one sign should promote its solubility while those of the opposite sign should have an increased salting-out effect. Although this theory does not explain variations in the effects of different salts on non-polar solutes, it does attempt to explain that local solvent structure should play a significant role.

Electrostatic theories, which stem from Debye and McAulay, relate salt effects to the influence of non-electrolytes on the dielectric constant of the solvent. The amount of work necessary to discharge the ions in the pure solvent and to recharge them in a solution containing the non-electrolyte yields the electrostatic contribution to the chemical potential of the neutral solute. The solvent is simply treated as a continuous dielectric and only departures from non-ideality are considered. For this theory, these departures arise from electrostatic interactions involving the ionic charges only and do not preclude the possibility that other types of forces may be important. Partially due to this reason, the theories can not reasonably account for the variation in the effect of different electrolytes and even fails whenever there is a shift from salting-out to salting-in of a particular non-electrolyte.

To expand upon the short range nature of the electrostatic interactions between an ion and a neutral molecule from the electrostatic theories, other short range forces, such

as dispersion forces, were considered. It was suggested that van der Waals interactions may be responsible for salting in by large ions and by simply adding terms for the potential of dispersion forces to the electrostatic equations, these forces could be taken into consideration. As a result, these theories were able to predict salting-in effects by large ions, but fail to indicate low salting-out effects, generally observed for lithium and hydrogen ions, and do not fit data for some non-electrolytes. One reason for the failure was thought to be the lack of accounting for the water molecules displaced by the ions. Although the theories account for water molecules displaced by neutral solutes, there are no terms for similar displacements from ions.

The internal pressure concept relates salt effects to other properties of the salt solutions themselves. A connection can be seen between the order of increasing volume contractions on dissolving salts and the order of increasing salting out of certain solutes. A similar correlation can be seen between salt effects and the relative effects of salts in decreasing the compressibility of the solution. By considering that neutral molecules merely take up space and hence modify the ion-water interaction, the free energy transfer of non-polar non-electrolyte from pure water to the salt solution can be calculated and a limiting law for k_s, the salting out parameter, can be obtained. Furthermore, the parameter can also be expressed in terms of P_e, the "effective pressure" exerted by salts in solution, as follows:

$$k_s = \lim_{C_s \to 0} \frac{\bar{V}_i^{\circ}}{2.3RT} \frac{dP_e}{dC_s} = \frac{\bar{V}_i^{\circ}(V_s - \bar{V}_s^{\circ})}{2.3RT\beta_{\circ}} \qquad (2\text{-}11)$$

Where C_s is the molar concentration of the electrolyte, $\bar{V}_i^{\circ}$ is the partial molar volume of the non-electrolyte at infinite dilution, R is the gas constant, T is absolute temperature,

V_s is the molar volume of the pure electrolyte, $\overline{V}_s^{\circ}$ is the partial molar volume of the pure electrolyte at infinite dilution, and $\beta_{\circ}$ is the compressibility of pure water. The expression corresponds to the idea that the non-ideal free energy of transfer relates to $P_e\overline{V}_i$. According to this final concept, salting-out and salting-in of a non-polar solute is determined by the extent to which the solvent medium is compressed or loosened when ions are present.

None of the theories provide a complete picture of salting-in and salting-out effects for every system, but together they create a comprehensive overview of the properties necessary to consider when looking at a particular system.

2.4 Naproxen and Sodium Naproxen

Naproxen[1] was introduced into the market in 1976 by Syntex and is a nonsteroidal anti-inflammatory drug (NSAID); sodium naproxen (the sodium salt of naproxen) was introduced in 1980 (Harrington and Lodewijk, 1997). Naproxen is used for the reduction of moderate to severe pain, fever, inflammation, and stiffness caused by conditions such as osteoarthritis, rheumatoid arthritis, psoriatic arthritis, gout, menstrual cramps, and the treatment of dysmenorrheal (Chen et al., 1992). Both naproxen and sodium naproxen are available in prescription strength; sodium naproxen is also available as an over-the-counter medication as of 1994.

The first large scale production of naproxen was in 1970 and produced 500 kg of material. The synthesis began with a Friedel-Craft acylation of 2-methoxynaphthalene (nerolin) to produce 2-acetyl-6-methoxynaphthalene (Harrington and Lodewijk, 1997).

[1] (S)-(+)-6-Methoxy-α-methyl-2-naphthaleneacetic acid

This was then converted, using a Willgerodt reaction, to naphthylacetic acid. An α-methylation will yield the D, L-acid, which is then resolved using cinchonidine.

Sodium Naproxen has a much higher solubility in water than naproxen, thus making its applicability as a pharmaceutical compound greater than its acid free form. (Kim et al., 2004) Producing crystals with a chiral purity of 99% or more and significantly larger than 70 μm was a major improvement in 1999 (Phan and Young, 1999; Phan and Allen, 1999). Phan et al. showed that chiral purity of 99% or more could be achieved while neutralizing (s)-2-(6-methoxy-2-naphthyl)propionic acid having a chiral purity of less than 99% (at least about 82%, but below 99%) with less than stoichiometric amount of aqueous sodium hydroxide, then, by removing the water either with a suitable organic solvent or simple distillation. Crystal size can be improved by a process that forms a solids-free liquid mixture of naproxen, water, an organic solvent, and at least one water-soluble inorganic basic sodium compound in an amount proportioned to neutralize from about 50% to 97% of the acid. Water removal leaves the monohydrate form of sodium naproxen with an average particle size of 120 μm and a chiral purity of at least 98% (S)-enantiomer. This process has the advantage of producing larger crystals which can reduce centrifugation cycle time and simplifying product handling during other operations, such as drying, flowing, screening, or tableting. This procedure does require an addition dehydration step to produce the commercially available anhydrous sodium naproxen from the monohydrated form. The optically pure (S)-(+)-sodium naproxen was used in the studies presented here.

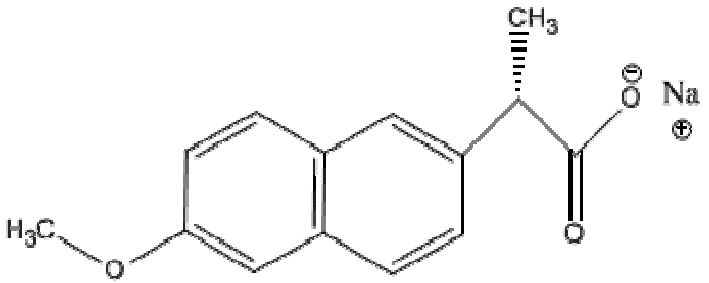

Figure 2.11. Schematic diagram of sodium naproxen.

The crystal structure of sodium naproxen was solved my Kim et al. (2004) to show the crystal parameters illustrated in Table 2.4.

Table 2.4. Unit cell parameters of anhydrous sodium naproxen.

Parameter	Value
Crystal Class	Monoclinic
Space Group	$P2_1$
Crystal Habit	Prism, colorless
Unit Cell Lengths	a = 9.969 Å b = 5.9346 Å c = 20.823 Å
Unit Cell Angles	α = 90° β = 102.025° γ = 90°
Cell Volume	1204.9 Å

2.4.1 Hydrates of Sodium Naproxen

Currently, sodium naproxen has been shown to exhibit 4 hydrate forms; anhydrous, monohydrate, dihydrate and tetrahydrate. Each of the hydrates has been thoroughly characterized in previous research and the conditions leading to transitions of these hydrates are illustrated in Figure 2.12 (Kim et al., 2004; Di Martino et al., 2001;

DiMartino et al., 2007). These works mostly looked at when the transitions occur from the anhydrous form to the other forms through changes in relative humidity, or slow cooling crystallization in water or a 64 mole % methanol-in-water mixture. They also examined how one could transition from a more hydrated to a less hydrated form either through heating or desiccation.

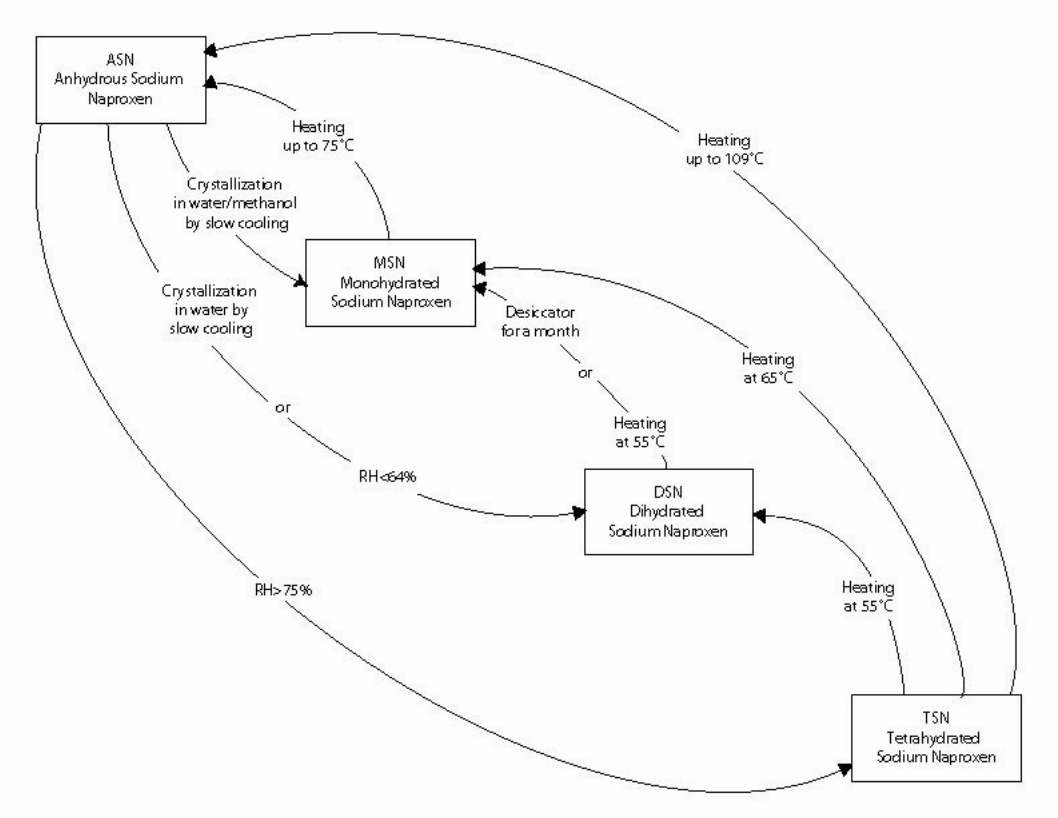

Figure 2.12. Schematic showing transitions of 4 known pseudopolymorphic forms of sodium naproxen.

The structure for the monohydrated form of sodium naproxen has been solved, while those of the dihydrated and tetrahydrated form have not been determined. Table 2.5 shows the cell parameters for the monohydrated form compared to those of the anhydrous form shown in the previous section (Kim et al., 1990).

Table 2.5. Comparison of anhydrated and monohydrated sodium naproxen unit cell parameters.

Parameter	Anhydrate	Monohydrate
Crystal Class	Monoclinic	Monoclinic
Space Group	$P2_1$	$P2_1$
Crystal Habit	Prism, colorless	Prism, colorless
Unit Cell Lengths	a = 9.969 Å b = 5.9346 Å c = 20.823 Å	a = 21.177 Å b = 5.785 Å c = 5.443 Å
Unit Cell Angles	α = 90° β = 102.025° γ = 90°	α = 90° β = 91.41° γ = 90°
Cell Volume	1204.9 $Å^3$	666.61 $Å^3$

The dihydrated form of sodium naproxen has been characterized as a channel hydrate (Kim and Rousseau, 2004). Upon dehydration, small crack can been seen in the crystal, using scanning electron microscopy (SEM), where the water being removed has created small channels to escape from the center of the crystal. Highly hydrated forms of sodium naproxen have shown to have multiple steps for dehydration, passing through other known pseudopolymorphic forms before arriving at the anhydrous form (Kim and Rousseau, 2005; DiMartino et al., 2006). In addition, each of the hydrated forms has exhibited dehydration at low temperatures, which is another indication that they are indeed channel hydrates.

CHAPTER 3

SOLUBILITY OF SODIUM NAPROXEN IN ALCOHOL-WATER SOLVENT SYSTEMS

One way to increase the yield of a solid product or to alter the solid state is to add organic alcohols to aqueous solutions during the crystal process, creating a salting-out effect, and/or forming a different polymorph or pseudopolymorph. Some work has been done on the solubility of sodium naproxen in 64 mole % methanol-in-water solution (Kim, 2005), but little has been done beyond that work. In this chapter, solubilities of sodium naproxen in 10 mole % methanol-in-water, 25 mole % methanol-in-water, 47 mole % methanol-in-water, pure methanol, 14.5 mole % ethanol-in-water, 44 mole % ethanol-in-water, 67 mole % ethanol-in-water, 79 mole % ethanol-in-water, and pure ethanol were obtained by measuring equilibrium concentrations over a temperature range of approximately 10°C to 40°C.

3.1 Experimental Section

3.1.1 Apparatus

The apparatus to determine the solubility of sodium naproxen in mixed solvent systems included two equilibrium cells in series along with a circulating cooling/heating bath to control temperature. The equilibrium cells were merely capped 100-mL, UV-coated Pyrex bottles. UV-coated bottles were used because degradation of sodium naproxen in aqueous solutions has been reported; the degradation is fostered by light, especially UV (Moore and Chappuis, 1988). The bottles were submerged in water at a

desired temperature that was controlled by a jacketed vessel. A magnetic stirring bar was inserted into each equilibrium cell to create mixing by placing the cells on a stirring plate. The jacketed vessels containing the immersed equilibrium cells were connected to a circulating bath with temperature control. A diagram of the apparatus is given in Figure 3.1. The equilibrium cells were placed under a prepared UV-protecting set-up or wrapped in aluminum foil to prevent the samples from degrading.

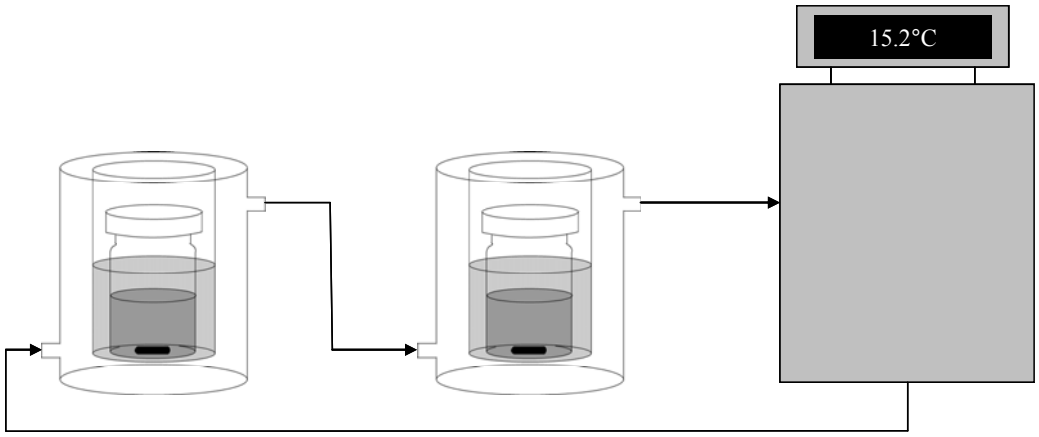

Figure 3.1. Schematic of equilibrium apparatus including equilibrium cells and circulating temperature controlling system.

Liquid samples from the equilibrium cells were withdrawn using a syringe, filter, and needle set-up. A 15 gauge, stainless-steel needle (inside diameter ~ 1.7 mm) was used to exclude any large crystal from entering the liquid sample. The needle was attached to a 0.2 μm syringe filter to remove any smaller crystals from the liquid sample collected in an attached 5 mL plastic syringe. A diagram of the sampling apparatus is given in Figure 3.2.

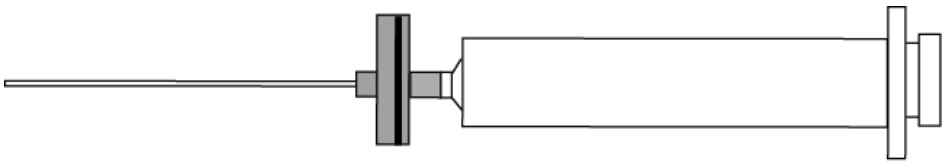

Figure 3.2. Sampling apparatus including a 5 mL plastic syring, 0.2 μm filter and 15 gauge needle.

3.1.2 Materials

The anhydrous sodium naproxen (ASN) used in the experiments was provided by Albemarle Corp., and was used without further processing or purification. Mixed solvents were prepared using HPLC-grade methanol (purchased from Fisher Scientific), water, and ethanol (purchased from VWR). The alcohols were dried overnight using class 3A molecular sieves. Solutions were prepared with the following molar methanol concentrations in water: 0, 0.10, 0.25, 0.44, and 1.00 mole/L. The following molar concentrations of ethanol-in-water were also prepared: 0.145, 0.44, 0.67, 0.79 and 1.00 mol/L. Preparation of the solvents for specific molar concentration was determined by weight and then converted to the corresponding molar concentration. Large batches of the solutions were prepared so as not to have varying concentrations across experiments. When not in use the lids of the solvents containers were paraffin wrapped and the solvent stored in a refrigerator to prevent evaporation of the solvent.

3.1.3 Experimental Procedure

The slurry solutions for equilibrium solubility studies were prepared by batch cooling crystallization. Approximately 50 ml of solvent was added to the equilibrium cell, which was heated or cooled to the appropriate temperature. The solvent was allowed to reach the desired equilibrium temperature, and then sodium naproxen was

slowly added until it no longer dissolved. The solution was stirred for at least twenty minutes; if all the sodium naproxen dissolved, more was added. Once the solution was considered saturated, the temperature was raised to about 10°C above the equilibrium temperature being measured, so that all the existing crystals were dissolved. The solution then was cooled, at an approximate cooling rate of 0.6° per minute, to the original temperature. The system conditions were then held constant for at least 15 hours to allow the system to reach equilibrium.

This procedure was carried out for each of the solvent concentrations across an approximate temperature range of 10°C to 40°C in 5° increment. Experiments were generally run in triplicate.

3.1.4 Sampling Protocol

Liquid sampling at temperatures greatly above or below room temperature, required heating or cooling of the needle prior to sampling so as not disturb the equilibrium concentration. To do this, the needle was place in a refrigerator or an oven prior to sampling. The sample was then withdrawn using the needle, filter, and syringe set-up and 2-3 drops of the sample were immediately placed in four individual pre-weighed HPLC vials with a known mass of HPLC water. Immediately after sampling, the temperature of the solution was measured and recorded using a K-type thermocouple attached to a thermometer.

3.2 High Performance Liquid Chromatography (HPLC)

3.2.1 Equipment

Solute concentration was measured using a Shimadzu® HPLC system that consisted of a SCL-10Avp system controller, a LC-10ATvp solvent-delivery system, FCV-10ALvp gradient flow control value , a DGU-14A on-line degasser, a SIL-10Avp auto injector, and a SPD-10Avp UV-VIS spectrophotometric detector. The system used a reverse-phase packed column (Microsorb-MV, 100-3 C_{18} 100 x 4.6mm from Varian) for separation. Two mobile phases were utilized; Solvent A was HPLC grade acetonitrile and Solvent B was a 2 vol% acetic acid mixture in HPLC grade water. Parameters were as follows:

Table 3.6. Acquisition parameters for HPLC.

Items	Parameters
Pumps Mode	Low Pressure Gradient Parameters
Total Flow Rate	1 mL/min
Pressure Limits	0.0 – 20.0 MPa
Lamp for Detector	Deuterium (D2)
Wavelength for Acquisition Channel	254 nm
Sampling Frequency	5 Hz
Acquisition Time	8 min
Injection Volume	10 µL
Sampling Speed	10 µL/sec
Solvent A Concentration	50%

The internal standard method for determining concentration using HPLC was used, with butyrophenone as the internal standard. A typical separation by HPLC is illustrated in Figure 3.3. The Y-axis is in minutes and the X-axis is in mVolts. The peak

for sodium naproxen was seen slightly before 3 minutes and the internal standard eluted at approximately 4.5 minutes.

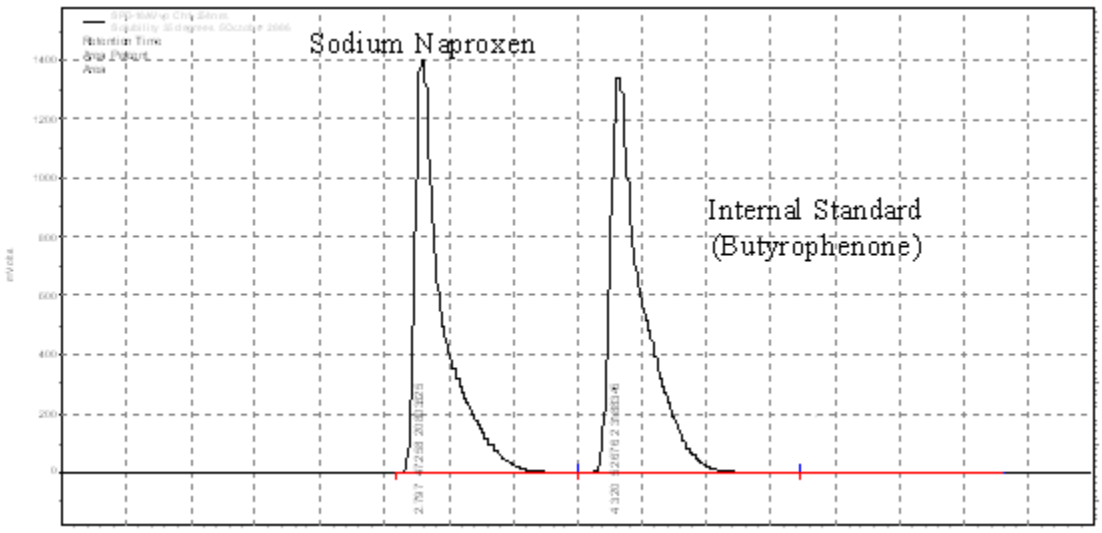

Figure 3.3. HPLC separation of sodium naproxen and butyrophenone.

Although there were slight tails on the measurements, the separation was still complete since the peaks do not overlap.

3.2.2 Calibrations

The internal standard method was used to determine the concentration of sodium naproxen in the samples. This was necessary since the efficiency of the column, sensitivity of the detector, and injection amount do not stay the same for every run. Butyrophenone purchased from Sigma Aldrich was used as the internal standard. The internal standard method assumes that the ratio of the peak areas for the sample to the internal standard is proportional to the ratio of the sample concentration to the internal standard concentration: i.e.

$$\frac{A_S}{A_I} = k\frac{C_S}{C_I} + b \tag{3-12}$$

Where A_i is the peak area, C_i is the concentration in g/kg of solution, and k and b are constants. Subscripts S and I refer to the sample and internal standard, respectively. By preparing solutions of known concentrations of sodium naproxen and butyrophenone and determining their peak areas using the HPLC, k and b can be determined. Stock solution of sodium naproxen with the proper solvent (C_{S_0} ~10 g/kg) and butyrophenone with acetonitrile (C_{I_0} ~8 g/kg) were prepared. Nine calibration samples were then prepared according to Figure 3.4 with concentration range of about 0.5 to 4 g ASN/kg (C_{S_1}) and about 0.8 to 2.6 g butyrophenone/kg (C_{I_1}). These ranges were determined based on the assumed range of solubility of sodium naproxen in the mixed solvents.

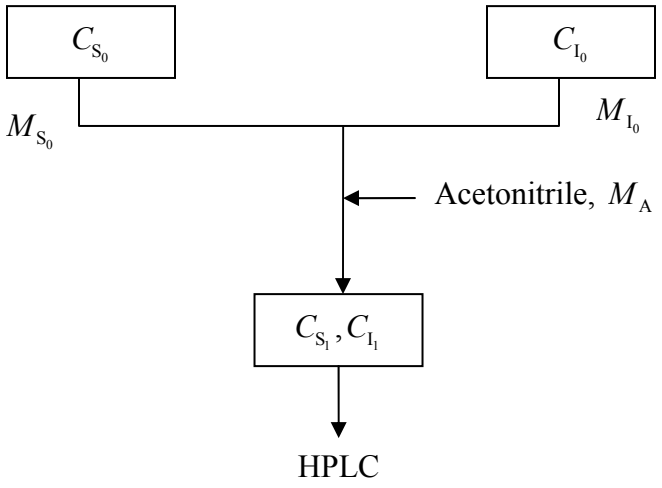

Figure 3.4. Dilution scheme for calibrations.

The equation for linear regression then becomes the following:

$$\frac{A_S}{A_I} = k\frac{C_{S_1}}{C_{I_1}} + b \qquad (3\text{-}13).$$

A_S and A_I can be obtained from the chromatogram and the concentrations can be computed as follows:

$$C_{S_1} = C_{S_0} * \frac{M_{S_0}}{M_{S_0} + M_{I_0} + M_A} \qquad (3\text{-}14)$$

$$C_{I_1} = C_{I_0} * \frac{M_{I_0}}{M_{S_0} + M_{I_0} + M_A} \qquad (3\text{-}15)$$

By plotting $\frac{A_S}{A_I}$ versus $\frac{C_{S_1}}{C_{I_1}}$ and fitting a least squares linear regression, k and b were obtained. Calibrations were performed routinely since the efficiency of the column degraded with time; they were also performed for each alcohol-water mixture. An example of a calibration plot is given in Figure 3.5:

Calibration curves for each of the alcohol-water mixtures are given in Appendix A.

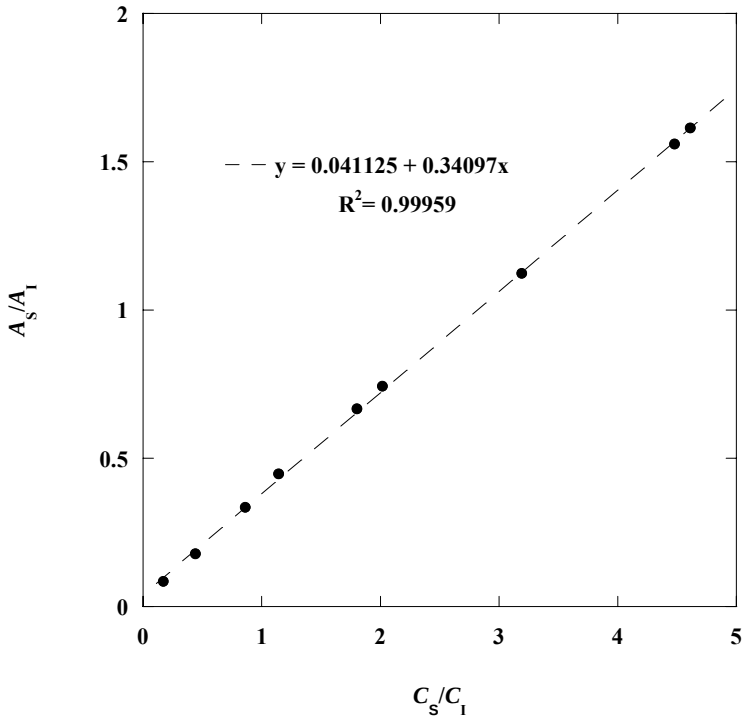

Figure 3.5. Example of calibration curve.

3.2.3 Dilution of Samples

Dilution of the samples was necessary to prevent crystallization and to increase the accuracy of the HPLC, since analysis was more reliable at lower concentrations. Approximately 0.1 g of the sample (M_{S_0}) was immediately diluted with approximately 1 g of water (M_W) as described in the sampling protocol. This solution was then vortexed for at least 7 minutes to ensure the solution was well mixed. Approximately 0.2 g of the diluted sample (M_{S_1}) was then added to an HPLC vial containing approximately 1 g of acetonitrile (M_A) and 0.1 g of the stock internal standard (M_I). The dilution scheme is illustrated in Figure 3.6.

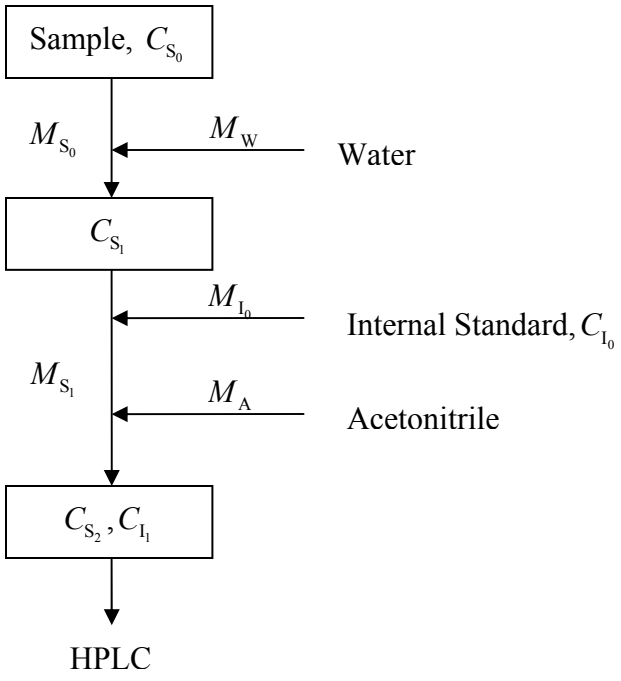

Figure 3.6. Dilution scheme for samples.

The concentration of the sample can then be calculated as follows:

$$C_{S_2} = \frac{\left(\frac{A_{S_2}}{A_{I_1}} - b\right)}{k} * C_{I_1}^2 \qquad (3\text{- }1)$$

$$C_{S_1} = \frac{C_{S_2}\left(M_{S_1} + M_{I_0} + M_A\right)}{M_{S_1}} \qquad (3\text{-}2)$$

$$C_{S_0} = \frac{C_{S_1}\left(M_{S_0} + M_W\right)}{M_{S_0}} \qquad (3\text{-}3)$$

Where C_{S_i} refers to the concentration of the solute at diluting step *i*, A_{S_2} is the area as reported by the HPLC of sodium naproxen in the solution, and A_{I_1} is the area as reported by the HPLC of the internal standard in the solution.

3.3 Results and Discussion

3.3.1 Solubility Analysis

The solubility of sodium naproxen in aqueous systems has been reported by Kim et al. (2005). In the present study, the solubility of sodium naproxen in both methanol-water and ethanol-water systems was obtained by the methods outlined above. The average solubilities of sodium naproxen (g anhydrous sodium naproxen/kg solution) at various temperatures and methanol-water solutions are given in

Table 3.7, Table 3.8, Table 3.9, and Table 3.10, along with the sample standard deviations. Sample standard deviations were calculated from a total of eight to twelve samples that were taken from three to four experimental set-ups and were computed using the following equation embedded in Excel

$$S = \sqrt{\frac{1}{n-1}\sum_{i=1}^{N}\left(X_i - \bar{X}\right)^2} \qquad (3\text{-}4),$$

where S is the sample standard deviation, n is the number of samples, X_i is the sample value of the i-th term, and $\bar{X}$ is the mean of the sample set. Standard deviations stem from the saturation of the solution, sampling technique, sample preparation, and HPLC analysis.

For comparison reasons, previous solubility data of anhydrous sodium naproxen in pure water solutions (Méndez del Rio, 2004) and aqueous solutions containing 64 mole % methanol-in-water (Kim, 2005) are shown in Table 3.11, and Table 3.12, respectively. The data are graphically presented in Figure 3.7 for water-methanol mixture and in Figure 3.8 for water-ethanol mixtures. Generally, the solubility of sodium naproxen increased with increasing methanol concentration, except at higher temperatures. For ethanol mixtures, solubility was greater in water except for water-ethanol mixtures at 14.5 mol% and 44 mol%. Ethanol solutions tended to show a traditional "salting-out" effect on sodium naproxen compared to methanol solutions.

Table 3.7. Experimental solubility of anhydrous sodium naproxen in aqueous solutions containing 10 mole % methanol.

Temperature (°C)	Solubility ± Standard Deviation (g Anhydrous Sodium Naproxen/kg Solution)
11.4	73 ± 6
15.6	108 ± 1
20.0	178 ± 4
24.8	263 ± 4
29.4	318 ± 5
33.0	386 ± 6
38.2	445 ± 10

Table 3.8. Experimental solubility of anhydrous sodium naproxen in aqueous solutions containing 25 mole % methanol.

Temperature (°C)	Solubility ± Standard Deviation (g Anhydrous Sodium Naproxen/kg Solution)
10.6	157 ± 10
15.3	225 ± 4
20.3	299 ± 10
25.0	318 ± 4
29.2	361 ± 1

Table 3.9. Experimental solubility of anhydrous sodium naproxen in aqueous solutions containing 47 mole % methanol.

Temperature (°C)	Solubility ± Standard Deviation (g Anhydrous Sodium Naproxen/kg Solution)
11.2	228 ± 7
15.6	259 ± 6
20.2	293 ± 5
25.0	325 ± 2
29.6	345 ± 4

Table 3.10. Experimental solubility of anhydrous sodium naproxen in pure methanol.

Temperature (°C)	Solubility ± Standard Deviation (g Anhydrous Sodium Naproxen/kg Solution)
10.4	214 ± 2
15.3	216 ± 5
20.4	224 ± 3
25.3	244 ± 3
29.9	242 ± 8
34.4	243 ± 8
38.9	243 ± 8

Table 3.11. Solubility of anhydrous sodium naproxen in pure water by Méndez del Rio (2004).

Temperature (°C)	Solubility (g Anhydrous Sodium Naproxen/kg Solution)
15.2	104.3
17.3	121.5
20.0	145.5
22.9	181.2
26.6	223.7
27.9	240.2
28.3	246.1
30.3	273.7
34.1	308.1
36.9	333.7
39.7	364.1

Table 3.12. Experimental solubility of anhydrous sodium naproxen in aqueous solutions containing 64 mole % methanol by Kim (2005).

Temperature (°C)	Solubility (g Anhydrous Sodium Naproxen/kg Solution)
10.2	224.5
15.2	260.7
17.0	279.4
24.8	323.8
27.7	333.6
29.7	341.2
34.5	365.2

Table 3.13. Experimental solubility of anhydrous sodium naproxen in aqueous solutions containing 14.5 mole % ethanol.

Temperature (°C)	Solubility ± Standard Deviation (g Anhydrous Sodium Naproxen/kg Solution)
10.5	118 ± 6
13.5	129 ± 1
16.6	167 ± 2
20.6	250 ± 4
23.5	276 ± 2
25.5	295 ± 12
29.6	337 ± 4
32.6	375 ± 7

Table 3.14. Experimental solubility of anhydrous sodium naproxen in aqueous solutions containing 44 mole % ethanol.

Temperature (°C)	Solubility ± Standard Deviation (g Anhydrous Sodium Naproxen/kg Solution)
103	148 ± 2
12.4	151 ± 3
15.2	164 ± 3
20.0	182 ± 2
24.6	201 ± 5
26.5	209 ± 3

Table 3.15. Experimental solubility of anhydrous sodium naproxen in aqueous solutions containing 67.4 mole % ethanol.

Temperature (°C)	Solubility ± Standard Deviation (g Anhydrous Sodium Naproxen/kg Solution)
10.8	71 ± 1
15.7	81 ± 4
18.1	87 ± 2
20.6	91 ± 4
22.6	97 ± 6
25.8	112 ± 3
29.8	125 ± 4
34.2	147 ± 6

Table 3.16. Experimental solubility of anhydrous sodium naproxen in aqueous solutions containing 79 mole % ethanol.

Temperature (°C)	**Solubility ± Standard Deviation (g Anhydrous Sodium Naproxen/kg Solution)**
10.8	47 ± 2
15.8	54 ± 3
20.3	62 ± 1
25.1	73 ± 4
29.8	78 ± 1
34.5	86 ± 2
39.1	96 ± 3

Table 3.17. Experimental solubility of anhydrous sodium naproxen in pure ethanol.

Temperature (°C)	**Solubility ± Standard Deviation (g Anhydrous Sodium Naproxen/kg Solution)**
11.0	14 ± 1
15.6	16 ± 1
20.5	19 ± 1
25.1	23 ± 1
29.7	26 ± 1
34.5	28 ± 1
39.4	30 ± 1

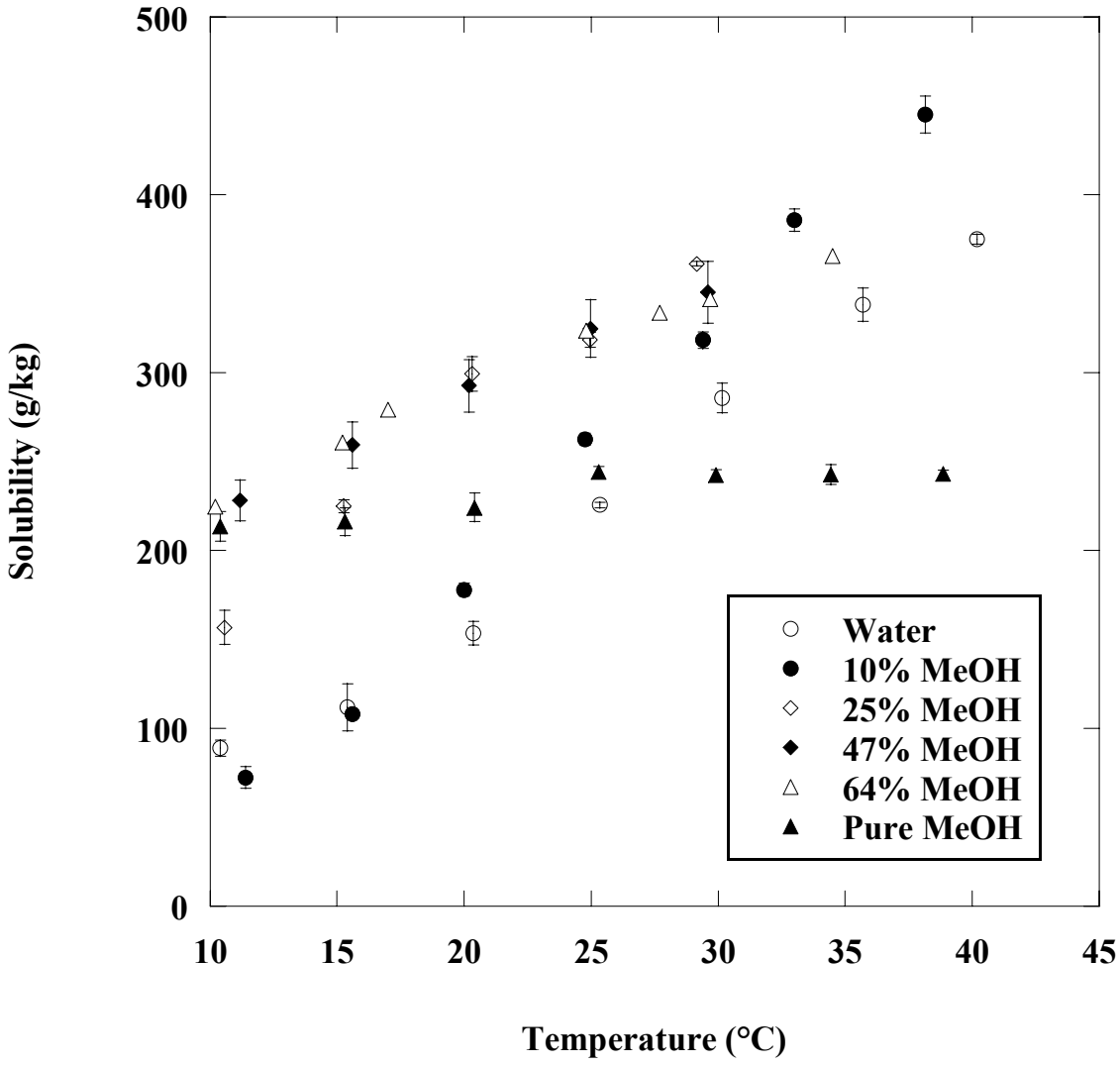

Figure 3.7. Anhydrous sodium naproxen solubility in water-methanol systems.

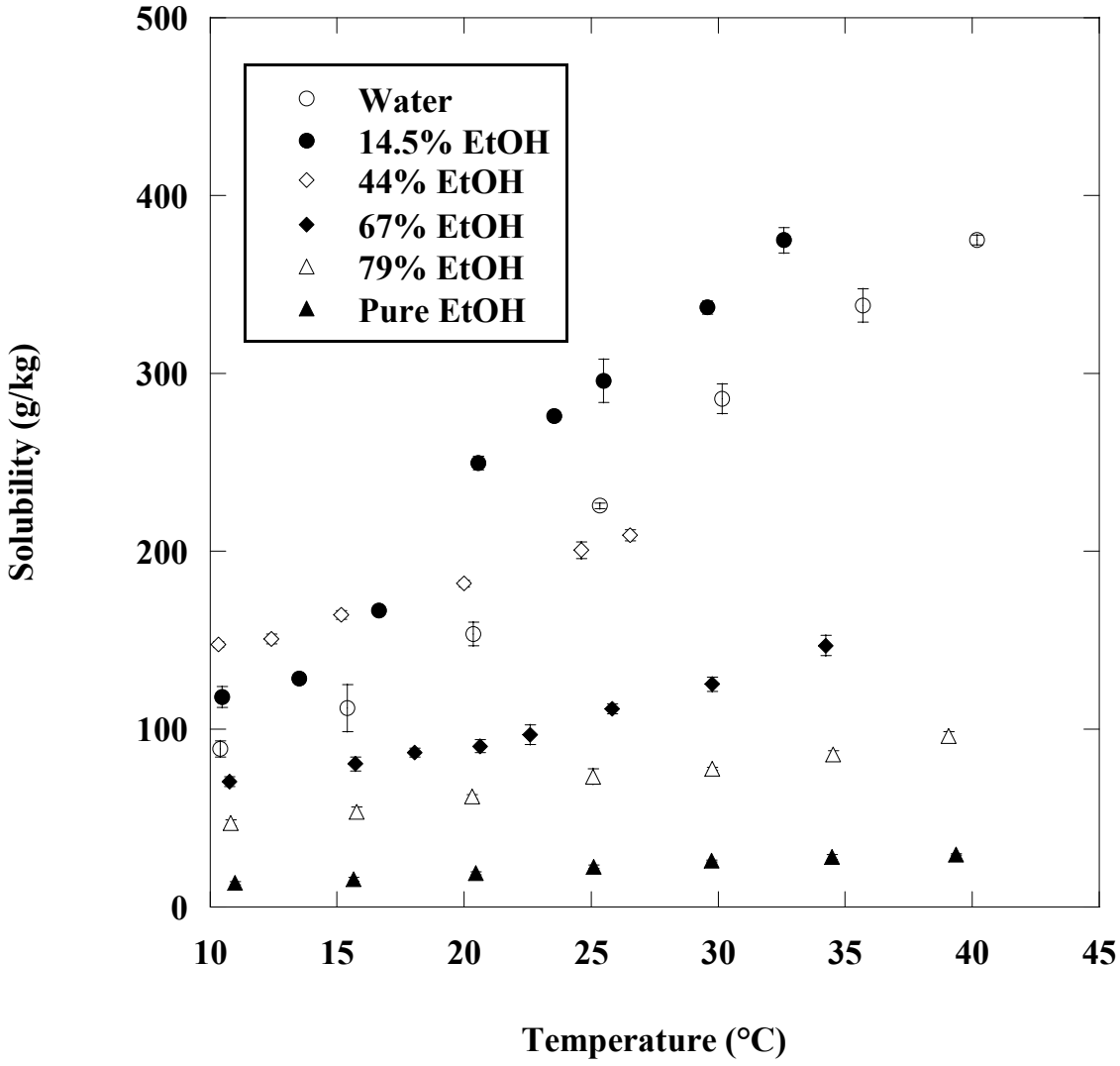

Figure 3.8. Anhydrous sodium naproxen solubility in water-ethanol systems.

3.3.2 Transitions between Pseudopolymorphs

Careful inspection of the plots of data in Figure 3.7 and Figure 3.8, revealed discontinuities in the data for each of the solvent concentrations. These discontinuities were be attributed to changes in the solid state of sodium naproxen in equilibrium with the solutions and are better observed in Figure 3.9, Figure 3.10, Figure 3.11, and Figure 3.12, which separates the data based on the solid state in equilibrium with the solution. Generally, at lower temperatures one pseudopolymorph was in equilibrium with a particular solution, but at higher temperatures the pseudopolymorphic phase changed. This was true in all of the solutions examined except for those containing 47 mole % methanol and 67 mole % ethanol-in-water. Changes in solid state were verified by thermogravimetric analysis (TGA), differential scanning calorimetry (DSC) and powder x-ray diffraction (PXRD), and will be further discussed in the next chapter.

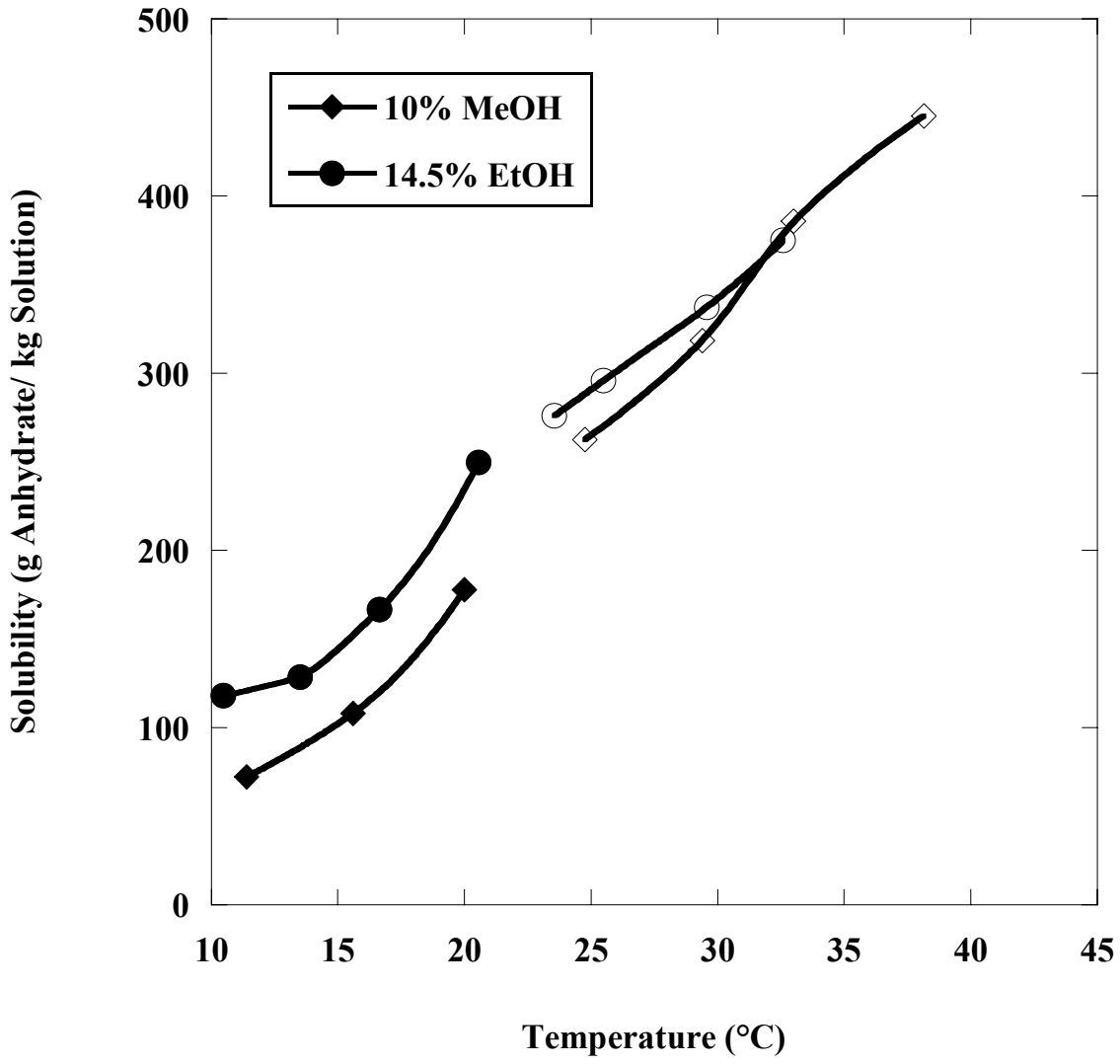

Figure 3.9. Empirical fits to the solubility data of 10 mole % methanol and 14.5 mole % ethanol-in-water.

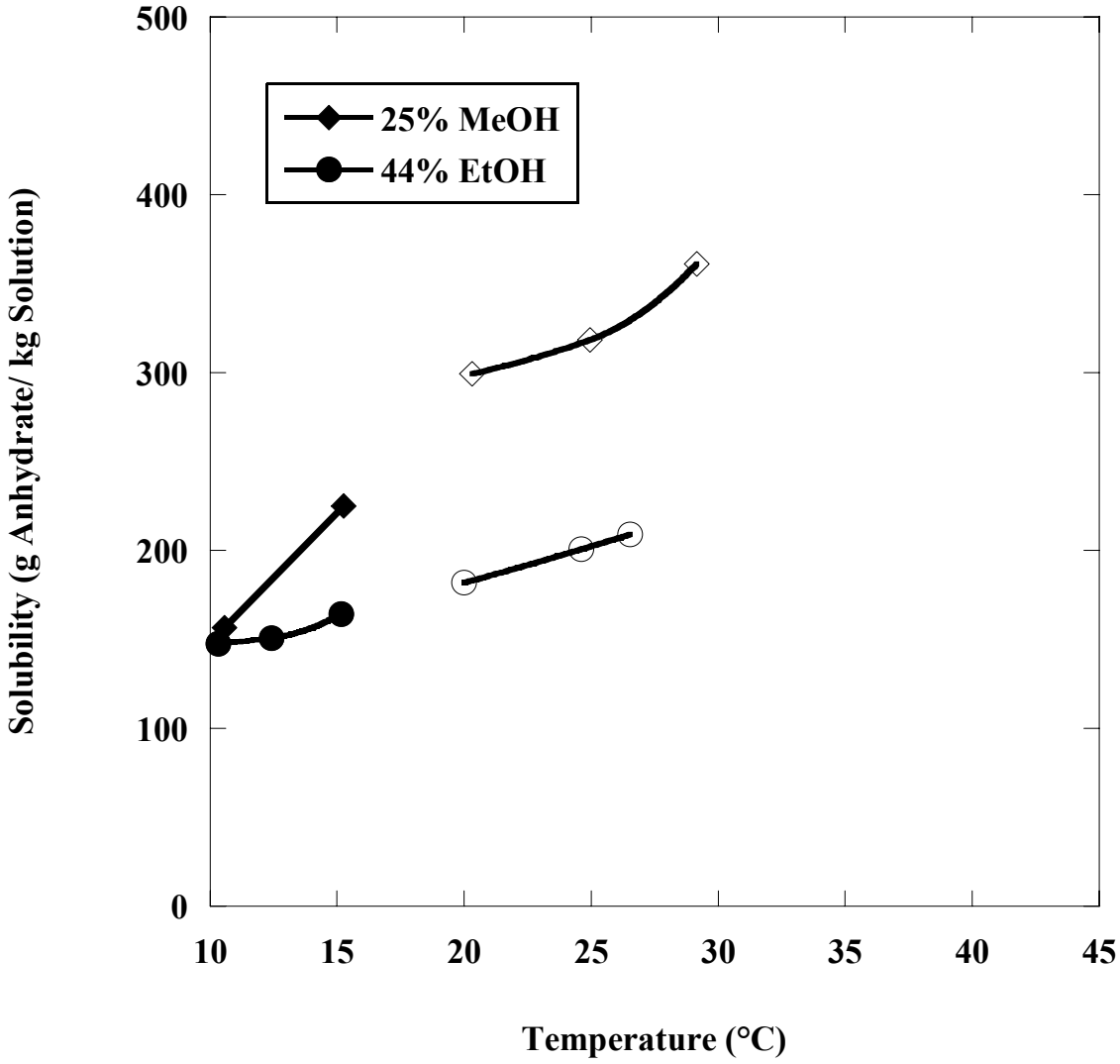

Figure 3.10. Empirical fits to the solubility data of 25 mole % methanol and 44 mole % ethanol-in-water.

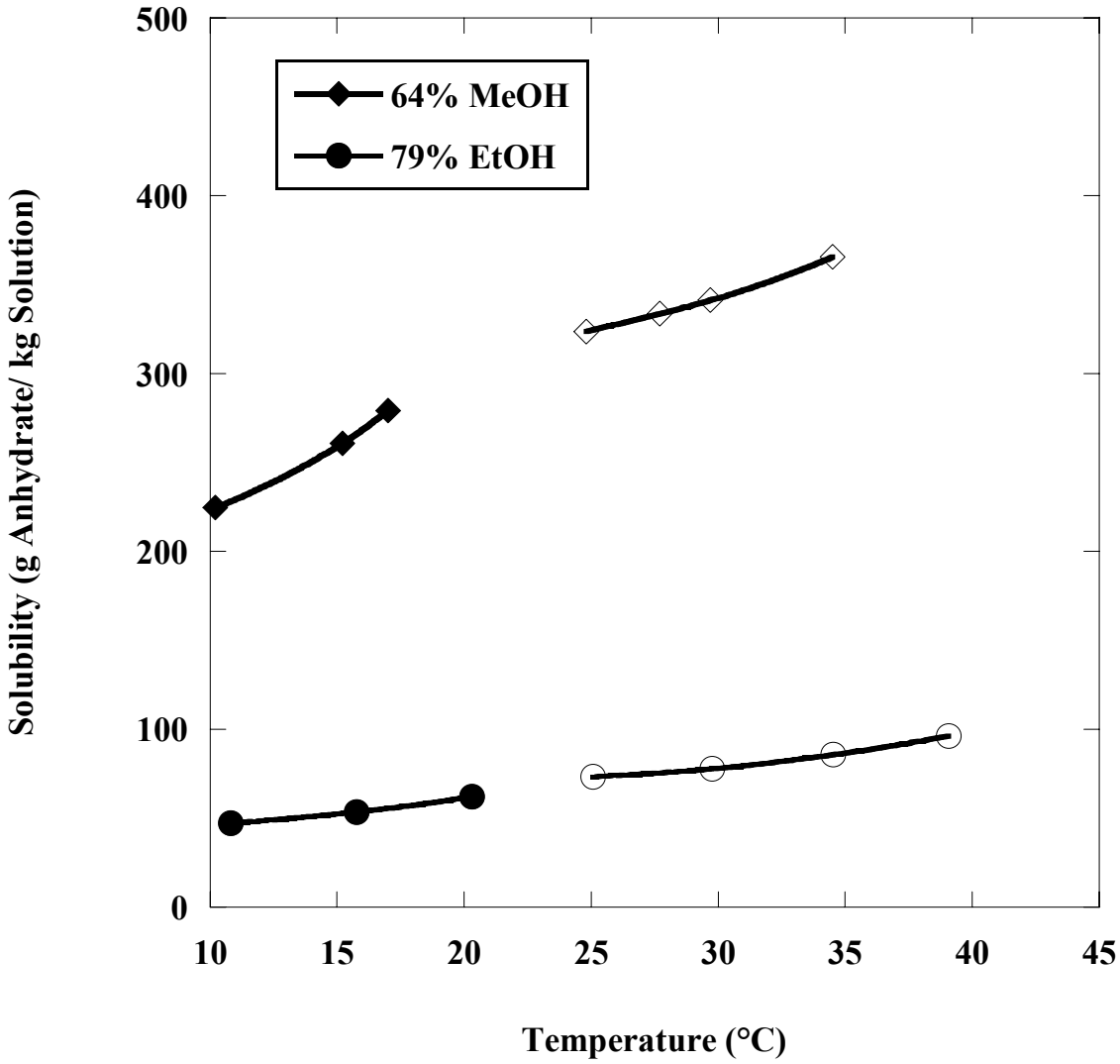

Figure 3.11. Empirical fits to the solubility data of 64 mole % methanol and 79 mole % ethanol-in-water.

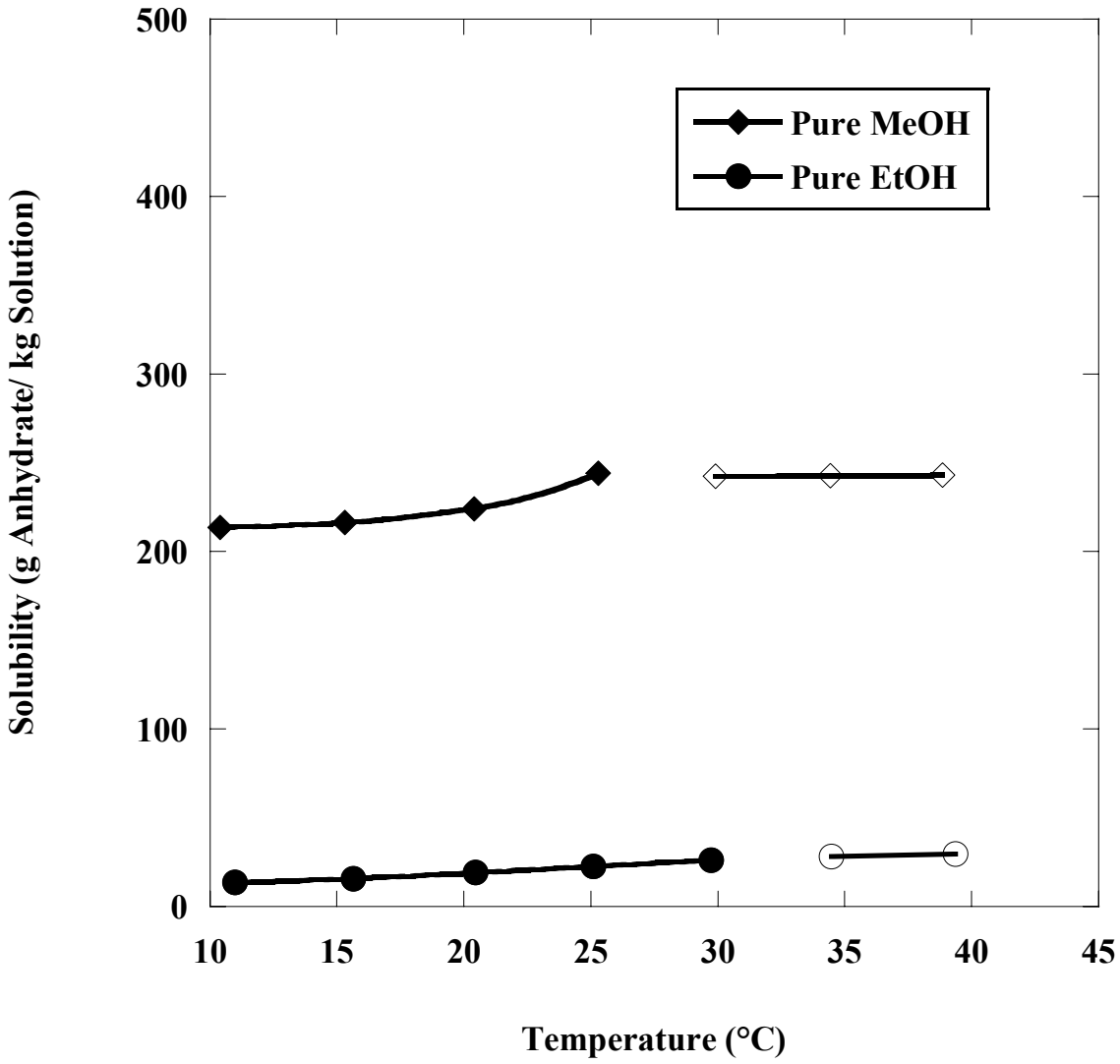

Figure 3.12. Empirical fits to the solubility data of pure methanol and pure ethanol.

Table 3.18 shows the pseudopolymorphic transitions of sodium naproxen in the solvent systems studied. As previously reported, a dihydrate to anhydrate solid-state transition was observed when the solvent was pure water (Mendez del Rio, 2004). In 10 mole % methanol-in-water and 14.5 % ethanol-in-water solutions, a solvate to dihydrate transition occurred. A dihydrate to monohydrate transition was apparent with 25 mole % methanol, 64 mole % methanol, 44 mole % ethanol, and 79 mole % ethanol-in-water. When the pure alcohols were used a solvate-to-anhydrate transition was observed. There appeared to be no transition in both the 47 mole % methanol and 67 mole % ethanol-in-water. These transitions are all given when going from lower temperatures to higher temperatures.

Table 3.18. Solid-state pseudopolymorphic transitions in water-alcohol systems.

Methanol Concentration (Mole %)	Ethanol Concentration (Mole %)	Pseudopolymorphic Transition Low T → High T
0%	0%	Dihydrate → Anhydrate
10%	14.5%	Solvate → Dihydrate
25%	44%	Dihydrate → Monohydrate
47%	67%	Dihydrate
64%	79%	Dihydrate → Monohydrate
100%	100%	Solvate → Anhydrate

3.4 Conclusions

The solubility of sodium naproxen in mixed alcohol-water solvents and pure alcohols was measured using cooling crystallization to generate the equilibrated solid in an equilibrium cell. Solution compositions were determined by reverse-phase HPLC. Addition of methanol to aqueous solutions generally caused a salting in effect, while addition of ethanol to aqueous solutions caused a salting out effect. Additionally, pseudopolymorphic transformations were seen in some of the solutions across the temperatures ranges measured. This shows that pseudopolymorphic forms can be controlled by varying the amount of organic alcohol present in the aqueous solutions.

CHAPTER 4

TRANSITIONS OF PSEUDOPOLYMORPHIC FORMS IN ALCOHOL WATER SOLVENT SYSTEMS

As discussed in the previous chapter, solid-state transitions have been found in some of the sodium naproxen-alcohol-water systems due to temperature changes. This can be observed by examining the discontinuities in solubility data and then proven through analysis of crystal samples. The identity of each of the solid states is confirmed by polarized light microscopy (PLM), thermogravimetric analysis (TGA), differential scanning calorimetry (DSC) and powder x-ray diffraction (PXRD). The solubility data measured previously can be correlated using the van't Hoff equation, as discussed in Chapter 2, based on the solid state present in solution to determine the actual transition temperature for each of the solvent mixtures. Finally, the transitions can then be related to water activity in the solutions at the transition point to determine what role the activity of water plays in the transitions.

4.1 Solid-State Analysis

The apparatus, materials, and experimental procedure were described in the previous chapter. This chapter deals with the solid-state identification of the crystals in the slurry mixture.

4.1.1 Sampling Protocol

After equilibration, the slurry solution was vacuum filtered until there was no visible liquid being removed. The crystals were then allowed to dry overnight in a dark

place at ambient conditions to remove any excess solvent on the surface of the crystals. They were then gently ground to a fine powder using a mortar and pestle so that they could be further analyzed for solid-state identification.

4.1.2 Polarized Light Microscopy

During recrystallization, crystals can change in size and shape. This can be caused by kinetic factors, such as mixing intensity and temperature ramping rates, and by thermodynamic factors, such as polymorphism and solvent composition. In this study, optical microscopy was used to observe changes in crystal size and shape based on pseudopolymorphism affected by temperature and solvent composition.

Analysis of crystal samples from the slurry solution was performed under a Leica DM LM microscope equipped with a Sony DKS-5000 digital camera and an objective lens of 20X. The microscope was equipped with a Sony DKC-5000 digital camera that converted the focused light into a digital signal, which was then visualized by Image-Pro Plus version 4.5.

A small amount of slurry was placed on a glass slide, which was cooled or heated according to the temperature of the slurry solution, and covered with a cover glass. The glassware was cooled or heated due to the instability of the crystals in solutions. For example, with crystal samples taken at low temperatures, the solid would quickly dissolve once placed under the microscope.

4.1.3 Thermogravimetric analysis

The TGA is used to determine how much solvent is bound in the crystals and gives information on the molecular ratio of solvent to solute in the pseudopolymorphic

forms. Mass loss of the sodium naproxen samples was measured using a TG/DTA 320 instrument manufactured by Seiko Instrument Inc. Crystal samples of 10 to 15 mg were heated from 22°C to 130°C in aluminum pans that were 5 mm in diameter. A ramping rate of 10°C/min was used with a nitrogen purge rate of 90 mL/min. As recommended by Di Martino et al (2001), all TGA runs were carried out with open pans.

4.1.4 Differential Scanning Calorimetry

Desolvation and melting endotherms were measured using a DSC 220C instrument (Seiko Instrument Inc.) The temperature range of the experiments was 22 to 290°C with a heating rate of 10°C/min and a nitrogen purge rate of 90 mL/min. Crystal samples of 10 to 15 mg were placed in open aluminum pans with a diameter of 7 mm. The use of open aluminum pans was necessary to obtain quantitative evaluations of the desolvation energy (Di Martino, 2001). The quantitative evaluation of energies associated with desolvation aided in the determination of the amount and type of solvent in the pseudopolymorphic forms.

4.1.5 Powder X-Ray Diffraction

Crystals were analyzed using PXRD analysis for final determination of solid-state. Each pseudopolymorph had a distinct diffraction pattern which can be used for quick and reliable identification. A PANanlytical X-Pert Pro Alpha-1 diffractometer with copper Kα1 radiation was used in conjunction with the X'Celerator detector. The PXRD pattern was made over a diffraction-angle (2θ) range of 10° to 80°, with a step size of 0.02° and a counting time of 1 second per step.

4.2 Results and discussion

4.2.1 Crystal Habit

Initial identification of pseudopolymorphs was based on crystal habit as determined by PLM images. Figure 4.1 shows PLM images of the anhydrate, monohydrate, and dihydrate forms of sodium naproxen.

The anhydrous form was thin and plate-like (Figure 4.1 (a)), which was in contrast to the monohydrate form (Figure 4.1 (b)) which was plate-like but larger and not as thin. The dihydrated form (Figure 4.1 (c)) was the easiest form to distinguish due to its slender, needle-like characteristics. Because of the instability of the solvated forms, sharp PLM images were not possible with these species. The methanol solvate form (Figure 4.1 (d)) of sodium naproxen was small in size and possibly prism-like in habit. The ethanol solvate form (Figure 4.1 (e)) could also have had a prism-like habit similar to the methanol solvate form, but elongated in a similar fashion to the anhydrate form.

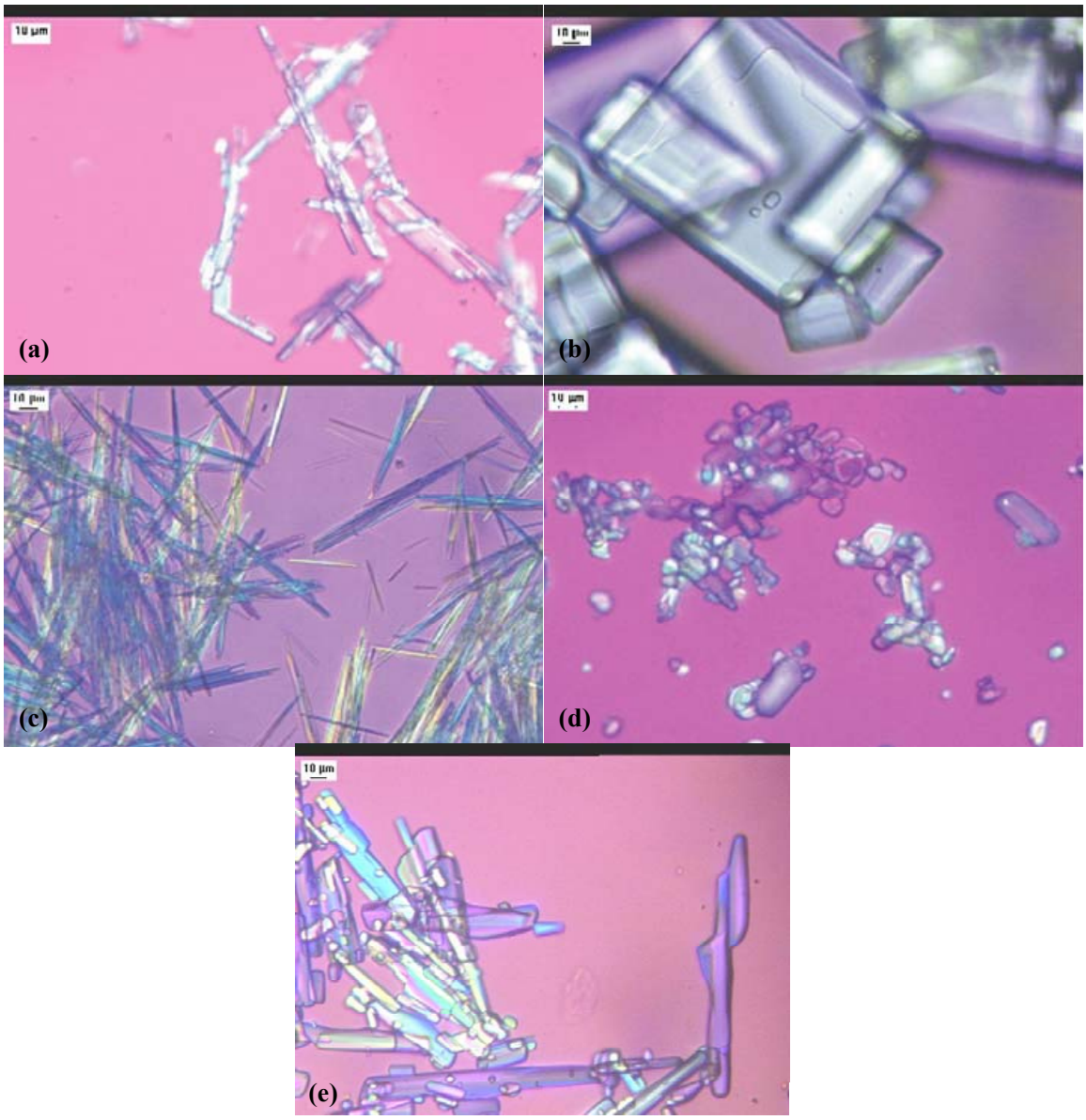

Figure 4.1. Photomicrographs of pseudopolymorphic forms of sodium naproxen (a) anhydrate (b) monohydrate (c) dihydrate (d) methanol solvate (e) ethanol solvate.

4.2.2 Thermal Analysis

Theoretical water contents for the monohydrate and dihydrate forms (the previously know pseudopolymorphic forms) of sodium naproxen was 6.67 wt% and 12.5 wt%, respectively. Additionally the dihydrated form was known to have two separate dehydration steps relating to the release of two structurally different water molecules (Kim and Rousseau, 2004). Of course the anhydrate form contained no water and no weight loss was to be expected. The heats of dehydration for the monohydrate and dihydrate have also been shown to be 207.3 J/g of the monohydrate and 376.8 J/g of the dihydrate (Kim and Rousseau, 2004). If the anhydrous species was used as the basis, the heats of dehydration become 220.5 and 427.6 J/g of the anhydrate, respectively. Based on this information the TGA and DSC data of each solid crystal form was analyzed and its pseudopolymorphic state determined.

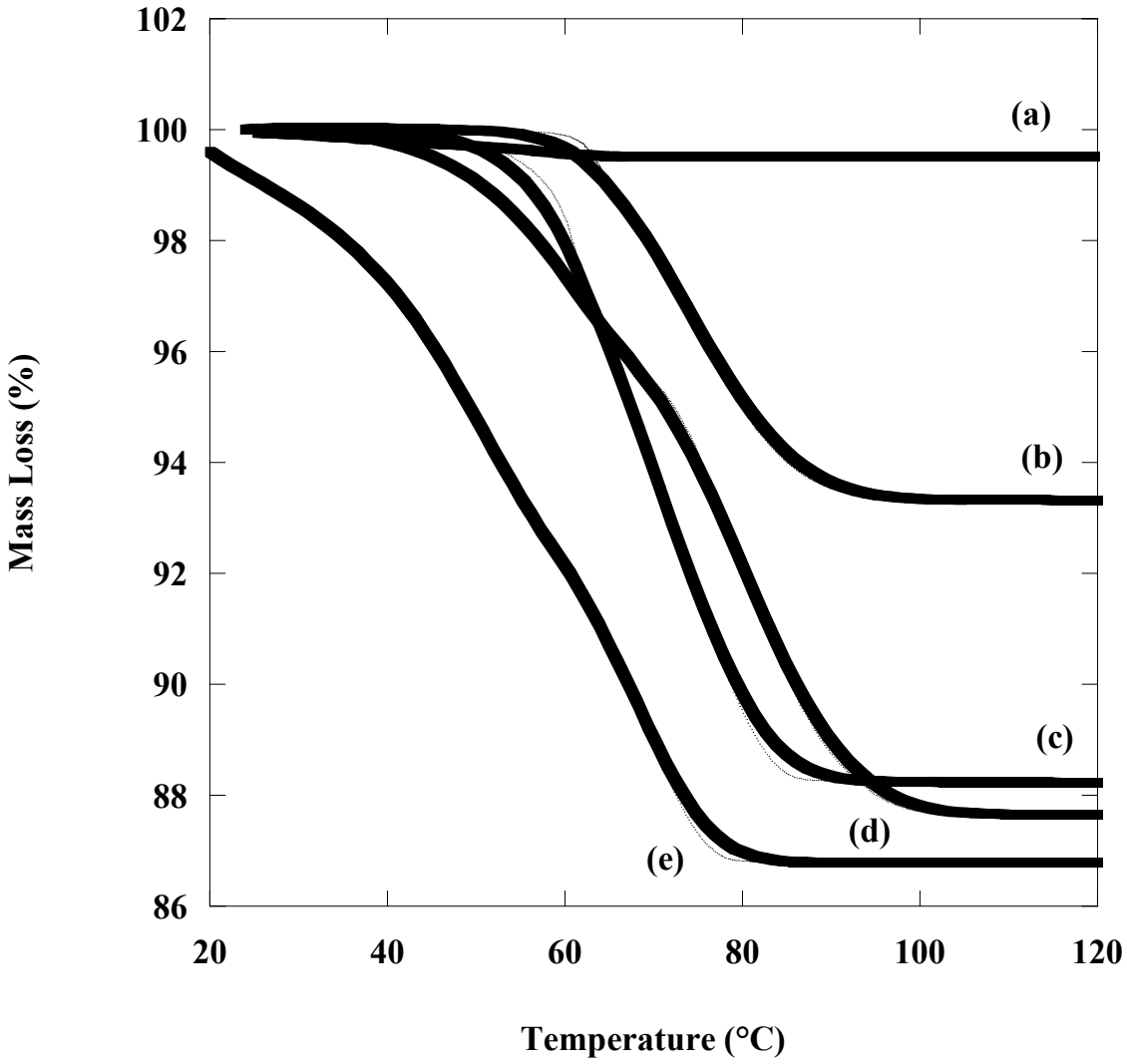

Figure 4.2. TGA curves of (a) anhydrous, (b) monohydrated, (c) methanol solvated, (d) dihydrated, and (e) ethanol solvated forms of sodium naproxen.

Figure 4.2 shows typical TGA curves for the pseudopolymorphic forms of sodium naproxen evaluated as part of the present work. A mass loss of 0.490 wt% was typical for the anhydrate, while the monohydrate and dihydrate saw typical mass losses of 6.70 wt% and 12.3 wt%, respectively. For the solvated species, mass losses were 11.8 wt% and 13.2 wt% for the methanol and ethanol solvated forms of sodium naproxen, respectively. The mass losses reported for the hydrated forms of sodium naproxen were in agreement with theoretical values. The mass losses reported for the solvated forms corresponded to a 1:1 ratio of methanol to sodium naproxen and a 0.86:1 ratio of ethanol to sodium naproxen. No alcohol solvated forms of sodium naproxen had previously been reported.

The monohydrated and methanol solvated forms showed a steady desolvation to the final anhydrous form, while the dihydrated and ethanol solvated forms seemed to have multiple steps for removal of solvent, as shown by the derivates of the TGA mass loss shown in Figure 4.3. There were two peaks evident for the dihydrate and ethanol solvate, but only one peak was seen during mass loss of the monohydrate and methanol solvate. Additionally, initial removal of solvent from the ethanol solvate forms took place immediately upon measurement, as opposed to the other desolvations which seemed to begin shortly after measurement initiates. This may have suggested instability of the ethanol solvate since desolvation began with a small elevation in temperature. The task here was merely to identify which pseudopolymorphic form was seen in equilibrium with various solvent mixtures, but solvated forms will be further explored in a later chapter.

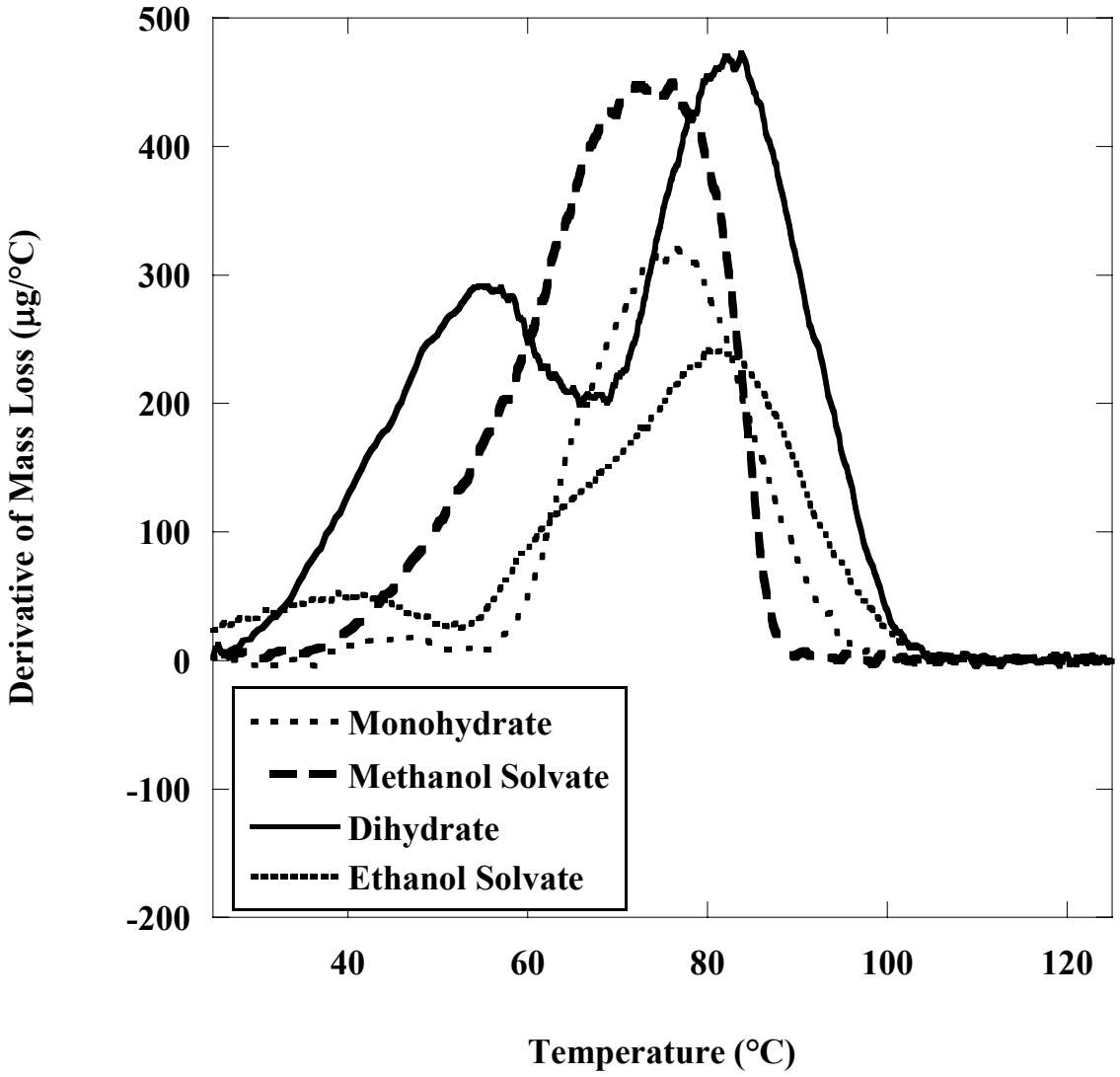

Figure 4.3. Derivative of TGA curves of the monohydrate, methanol solvate, dihydrate, and ethanol solvate of sodium naproxen.

Similar to the TGA curves presented in Figure 4.2, Figure 4.4 represents DSC endotherms of the pseudopolymorphic forms to aid in further identification. As can be seen, the endotherms for solvent removal took place between 25°C and 115°C. The endotherm above 250°C corresponded to the melting of sodium naproxen. Each pseudopolymorphic form had a distinct endotherm shape and energy associated with removal of the solvent. Since the endotherms of the monohydrated and dihydrated species had been reported previously and were 207.3 J/g monohydrate and 376.8 J/g dihydrate (Kim, 2004), comparison to experimental endotherms, in these studies, aided in distinguishing pseudopolymorphic forms. In the present study, additional endotherms were found for the methanol and ethanol solvated forms of sodium naproxen, they were found to be 204 ± 2 and 217 ± 17 J/g solvate, respectively. These values were converted to J/g anhydrate to make comparisons to other pseudopolymorphic forms easier and were 230 and 251 J/g anhydrate for the methanol and ethanol solvate, respectively. For the previously mentioned monohydrate and dihydrate species the energy of desolvation based on the anhydrate form was 220.5 and 427.6 J/g anhydrate, respectively.

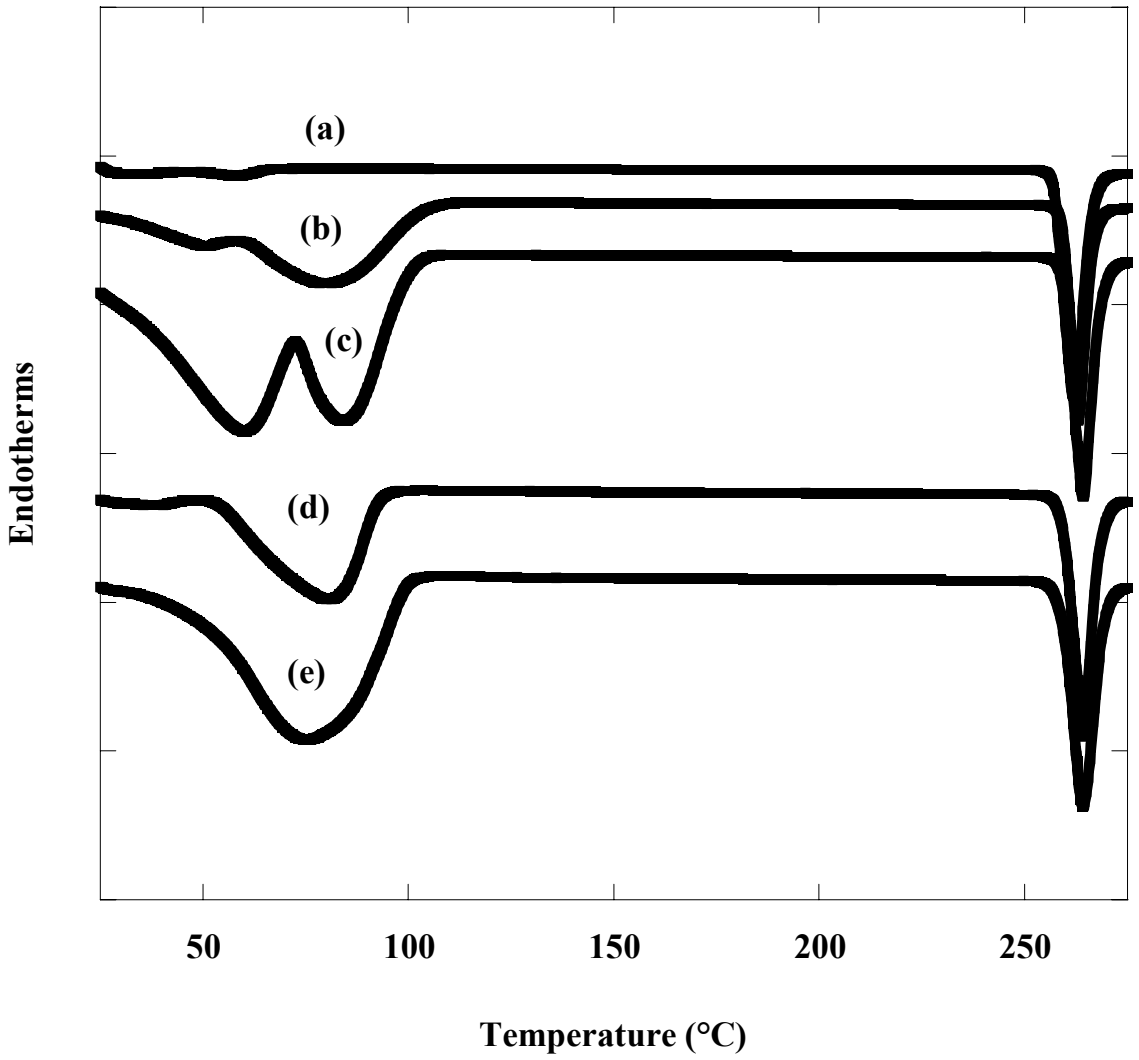

Figure 4.4. DSC endotherms for (a) Anhydrous, (b) monohydrated, (c) dihydrated, (d) methanol solvated, and (e) ethanol solvated forms of sodium naproxen.

4.2.3 Powder X-ray Diffraction Patterns

PXRD was the final step for solid-state identification. Each pseudopolymorphic form had a distinct PXRD pattern that was independent of the crystal habit. The PXRD diffraction patterns for the anhydrate, monohydrate, and dihydrate of sodium naproxen were known prior to the present research (Kim, 2004). The PXRD patterns determined here for the methanol and ethanol solvated forms of sodium naproxen were compared to the previously mentioned pseudopolymorphs in Figure 4.5.

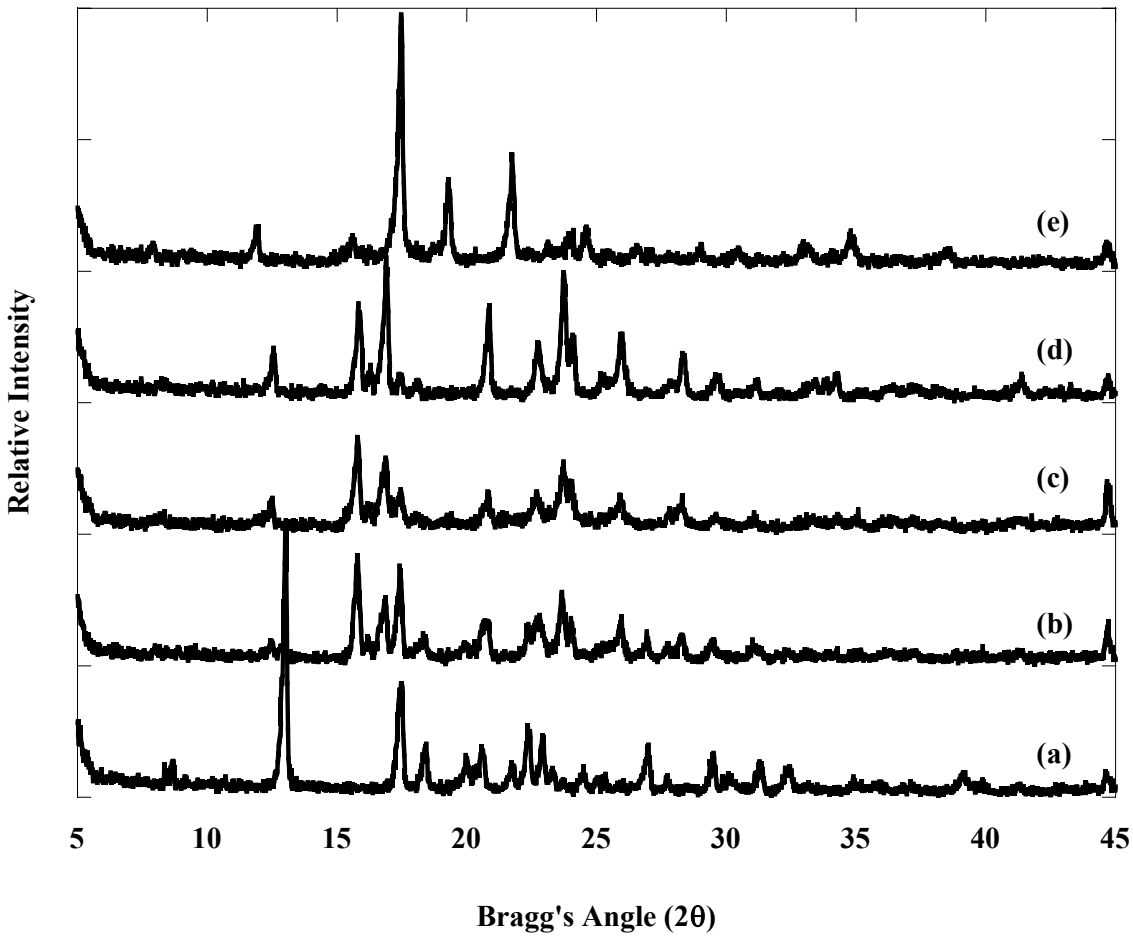

Figure 4.5. PXRD patterns for (a) anhydrous, (b) methanol solvated, (c) ethanol solvated, (d) monohydrated, and (e) dihydrated forms of sodium naproxen.

4.2.4 Pseudopolymorphic Forms From Crystal Analysis

Using the above mentioned solid-state identification techniques (PLM imaging, TGA, DSC, and PXRD), the solid states in equilibrium with the solvent systems studied here were determined and are listed in Table 4.1 and Table 4.2 for the methanol and ethanol systems, respectively. For example, for a methanol-water system with a methanol concentration of 10 mole %, a transition from the solvate to the dihydrate was seen when going from lower to higher equilibrium temperatures.

Table 4.1. Solid-state transition for methanol-water systems

Methanol Concentration (mole %)	Solid State (Lower T → Higher T)
0	Dihydrate → Anhydrate
10	Solvate → Dihydrate
25	Solvate → Dihydrate
47	Dihydrate
64	Dihydrate → Monohydrate
100	Solvate → Anhydrate

Table 4.2. Solid-state transition for ethanol-water systems

Ethanol Concentration (mole %)	Solid State (Lower T → Higher T)
0	Dihydrate → Anhydrate
14.5	Solvate → Dihydrate
44	Solvate → Dihydrate
67	Dihydrate
79	Dihydrate → Monohydrate
100	Solvate → Anhydrate

It is interesting to note that the same solid states were identified for 10 mol% methanol/14.5 mol% ethanol-in-water, 25 mol% methanol/44 mol% ethanol-in-water, 47 mol% methanol/67 mol% ethanol-in-water, 64 mol% methanol/79 mol% ethanol-in-water and pure methanol/pure ethanol solutions. Also the discovery of organic alcohol solvates of sodium naproxen should be mentioned since previous alcohol solvates were not known.

4.2.5 Determining Solid-State Transitions with the Van't Hoff Correlation

Using equation 2-10, as developed in Chapter 2,

$$\ln x = -\frac{\Delta \hat{H}_{\mathrm{d}}}{RT} + \frac{\Delta \hat{S}_{\mathrm{d}}}{R} \tag{2-10}$$

For systems that fit the assumptions leading to this equation, a plot of the natural logarithm of solubility (in mole fraction) versus the inverse of temperature should be linear with the slope and the intercept related to the enthalpy and entropy of dissolution, respectively. The enthalpy and entropy of dissolution are specific to the particular solid that is in equilibrium with the solution. So if different solids are present in the same solutions there will be distinct relationships for each solid. Figure 4.6 through Figure 4.15 show the van't Hoff correlations for each of the solvent systems studied.

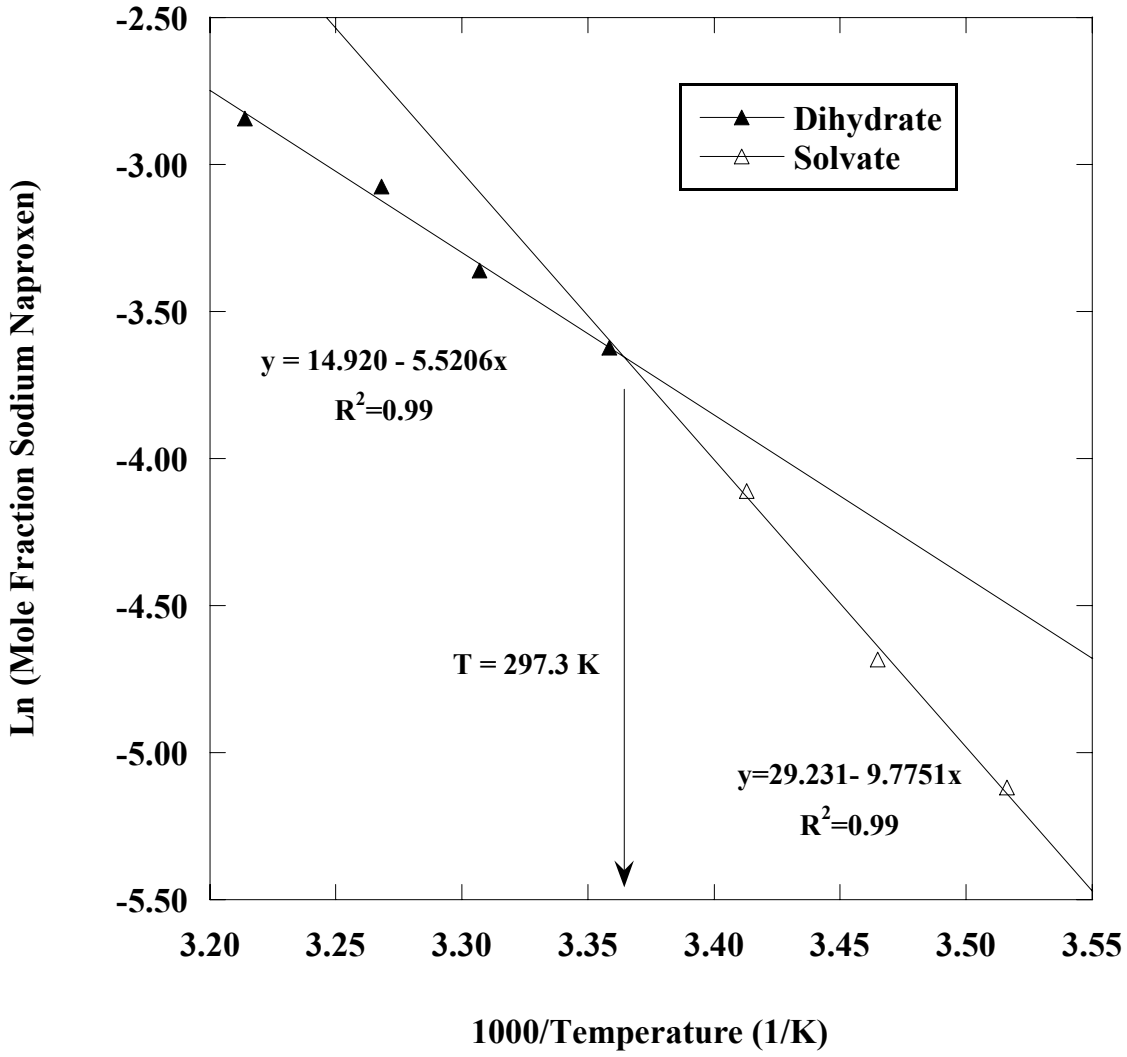

Figure 4.6. Van't Hoff plot of 10 mol% methanol-in-water solvent.

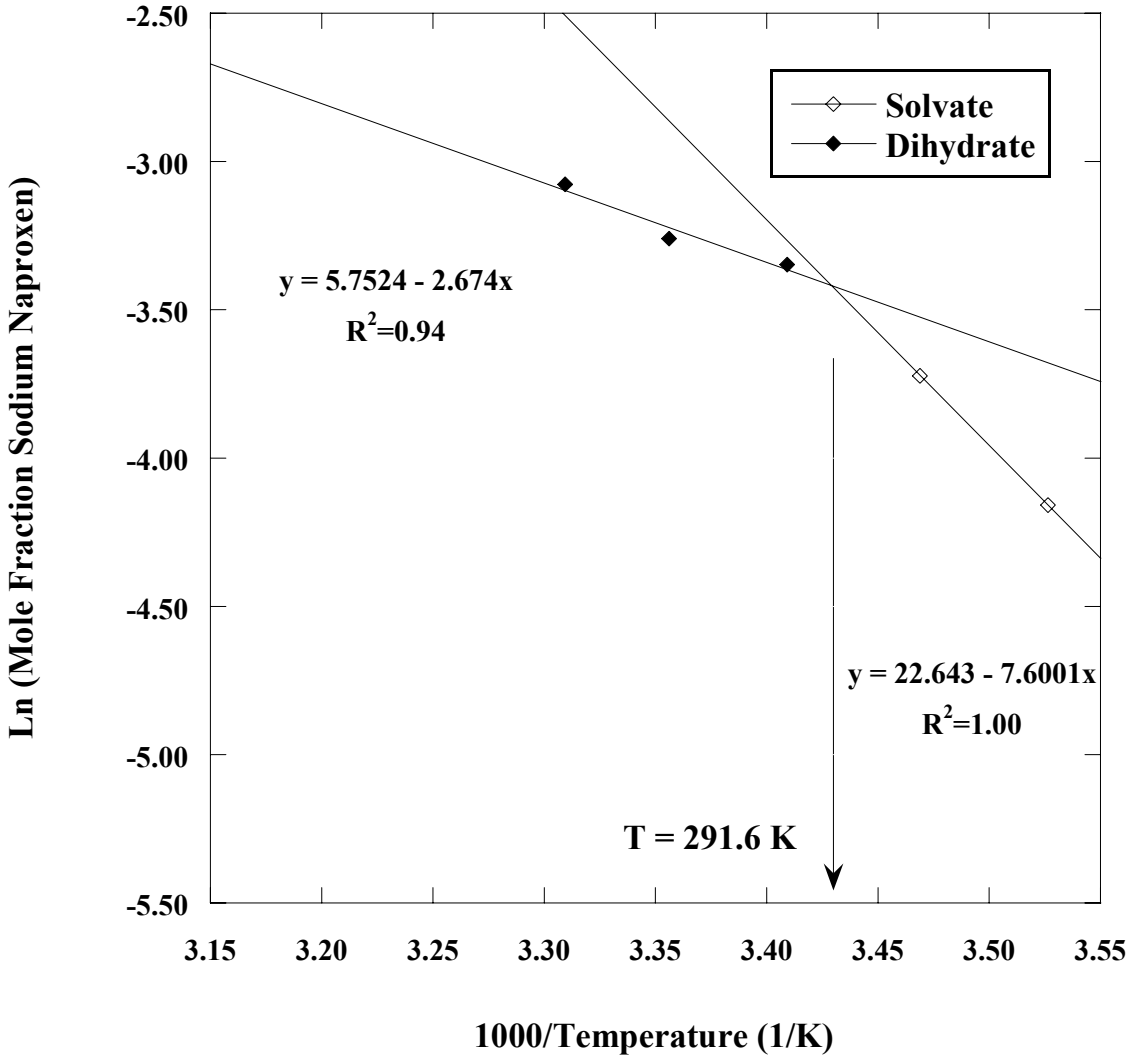

Figure 4.7. Van'f Hoff plot of 25 mol % methanol-in-water solvent.

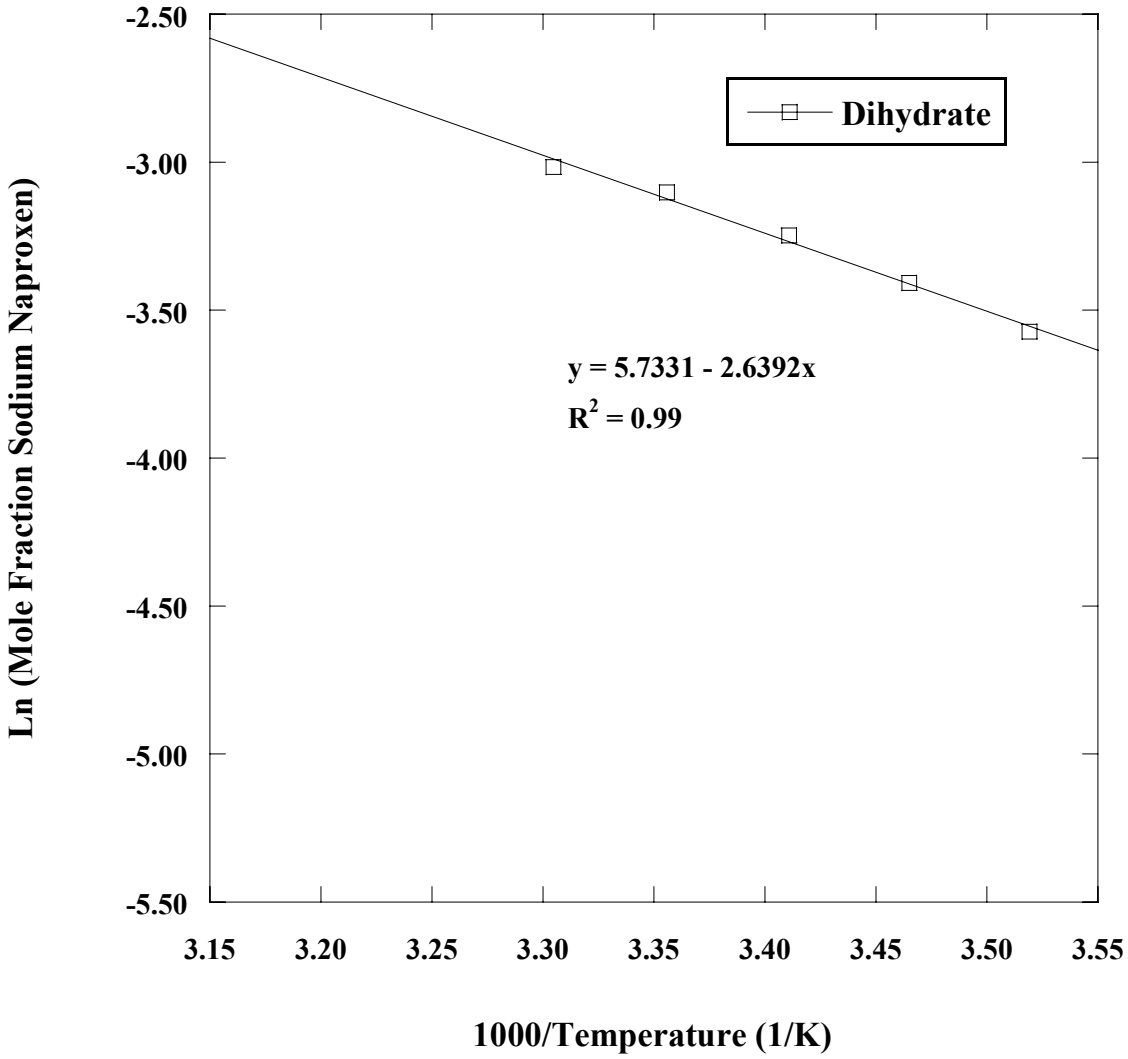

Figure 4.8. Van't Hoff plot of 47 mol % methanol-in-water solvent.

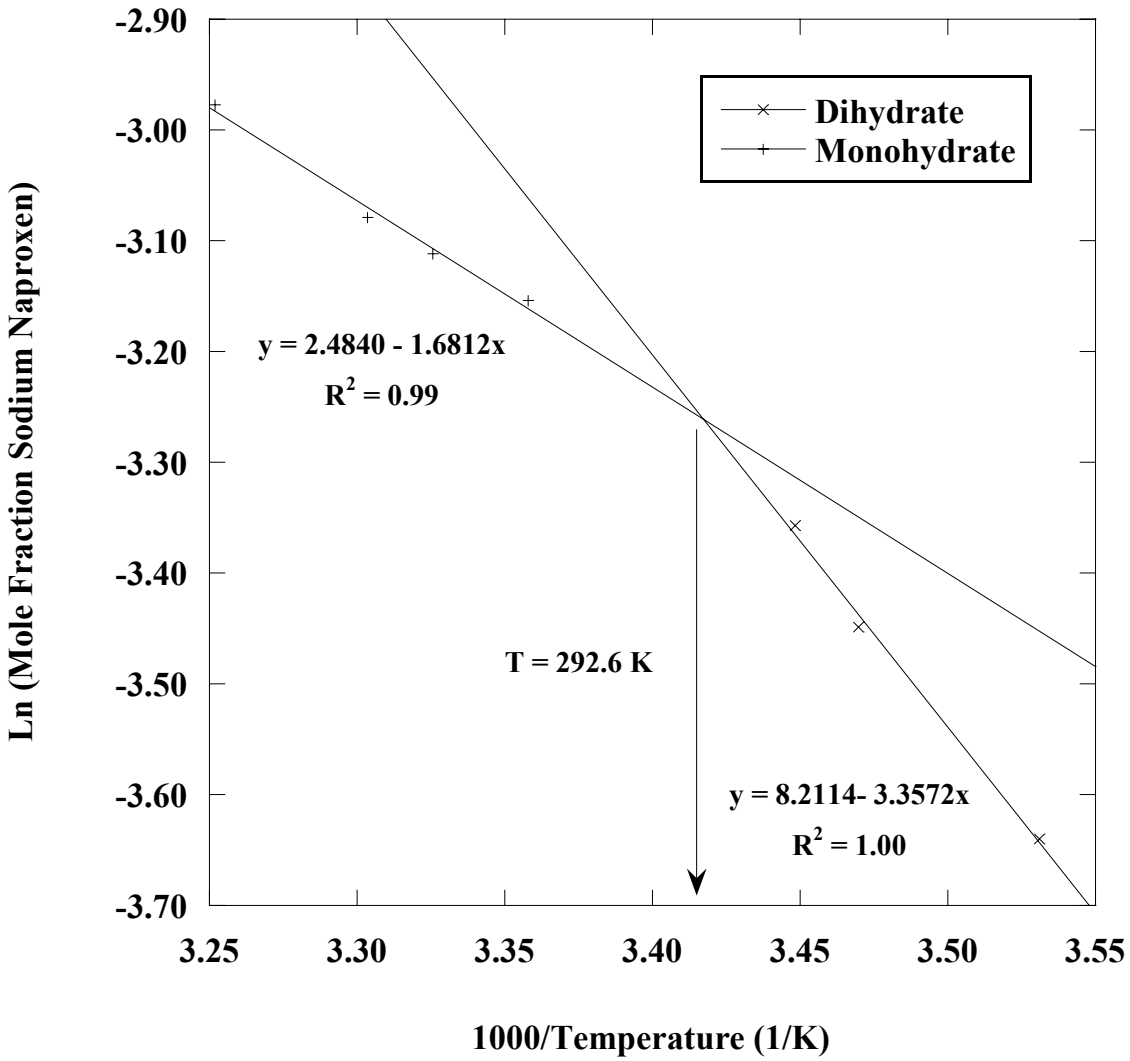

Figure 4.9. Van't Hoff plot of 64 mol % methanol-in-water solvent.

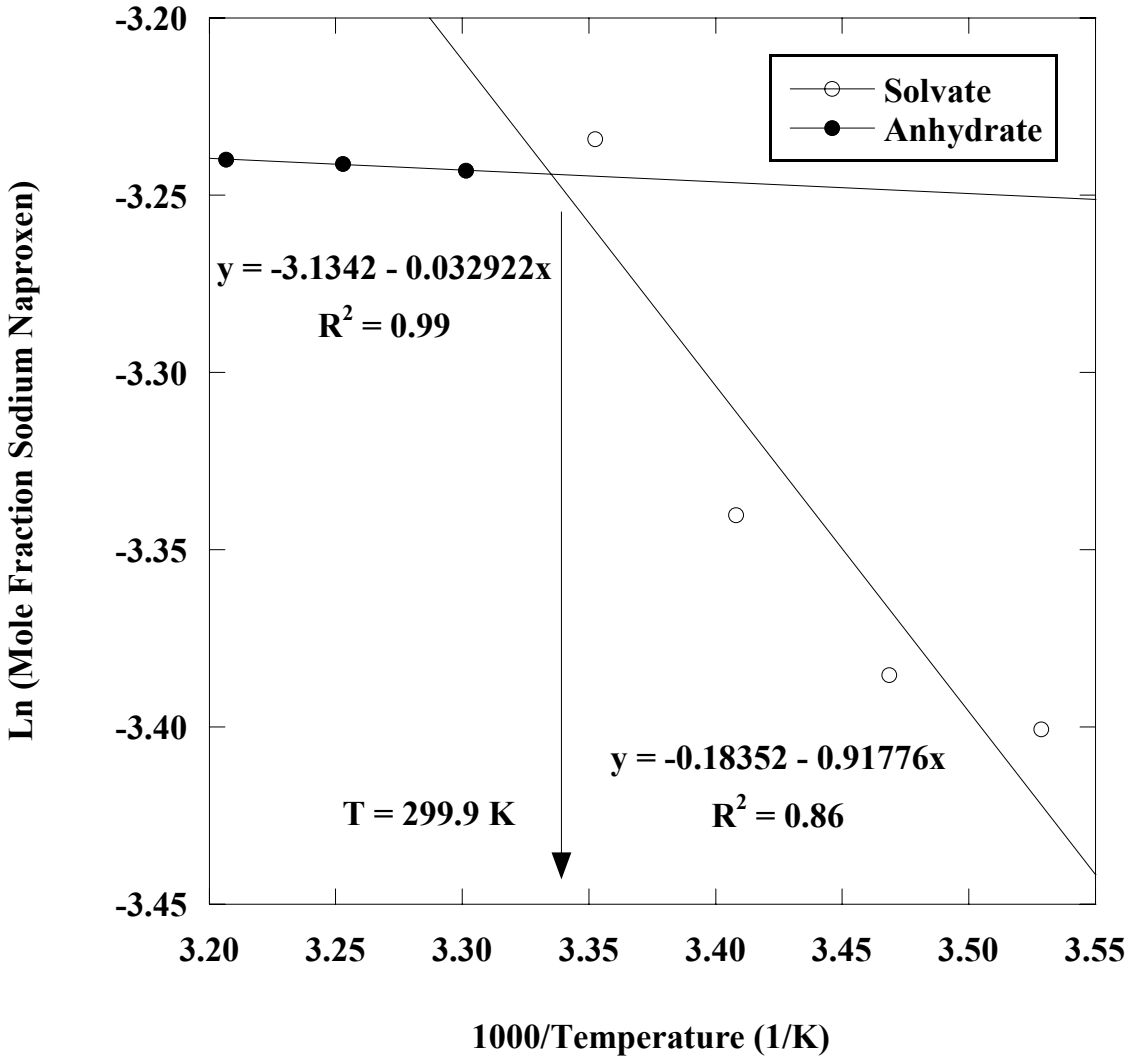

Figure 4.10. Van't Hoff plot of pure methanol solvent.

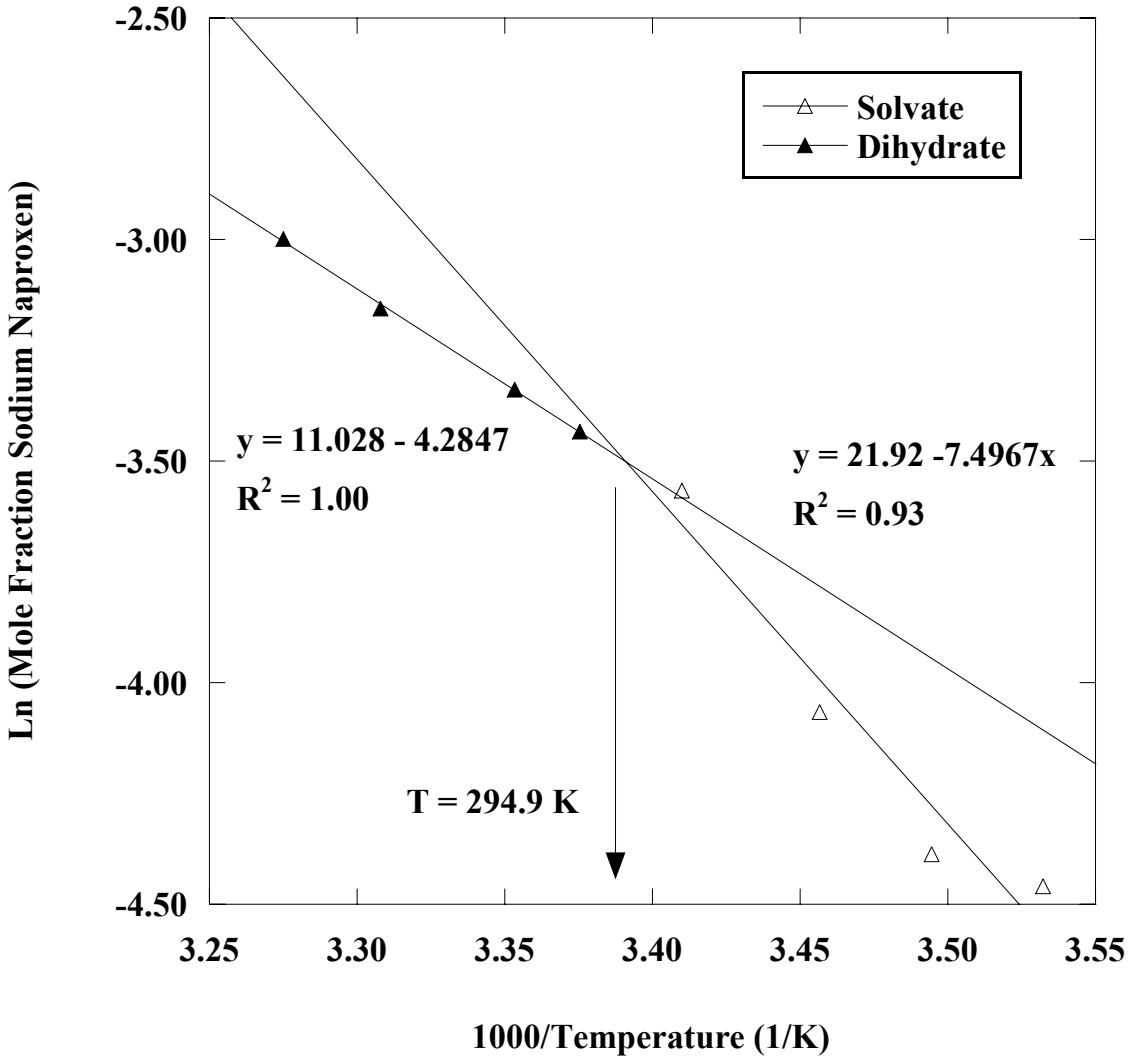

Figure 4.11. Van't Hoff plot of 14.5 mol % ethanol-in-water solvent.

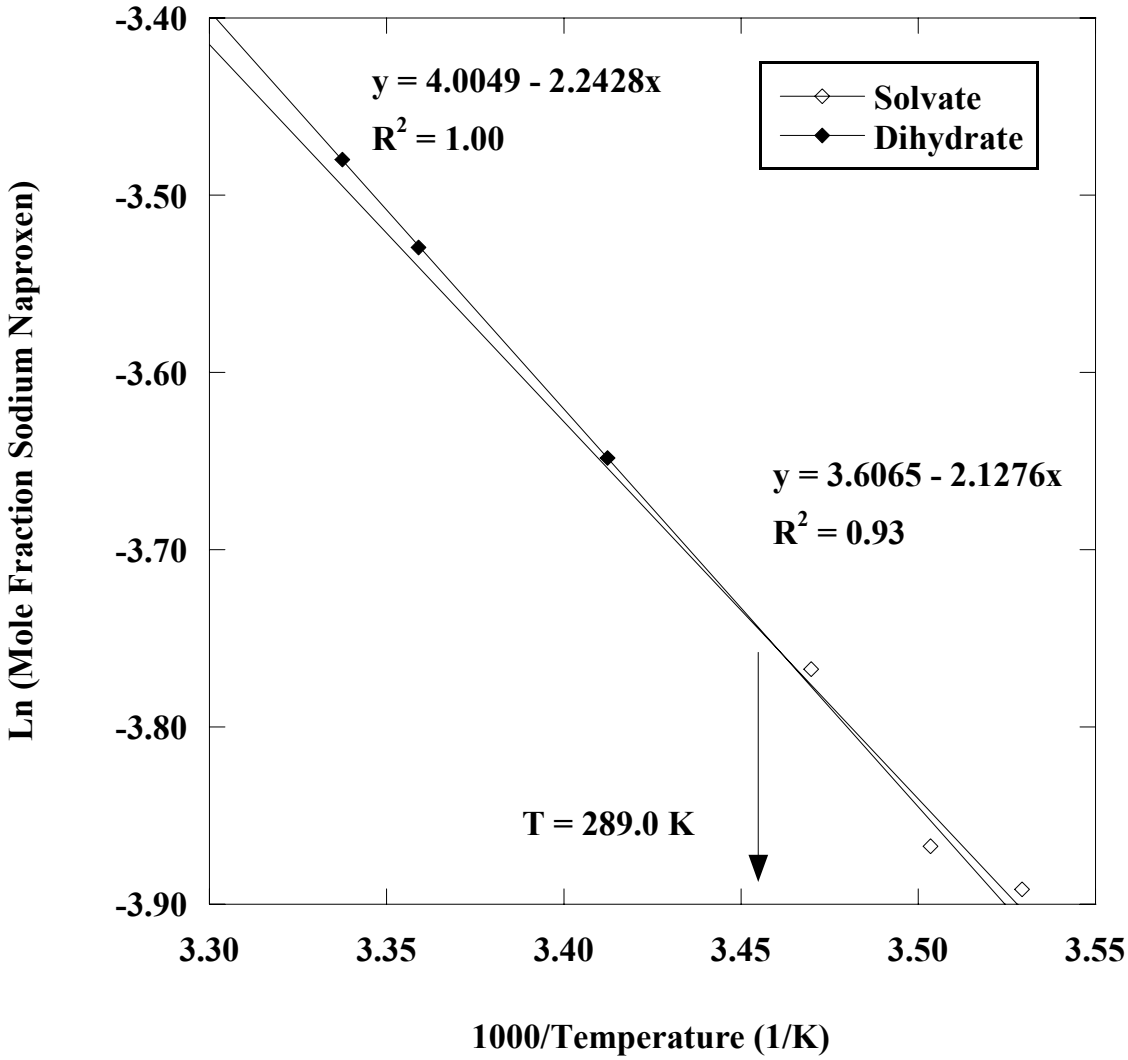

Figure 4.12. Van't Hoff plot of 44 mol % ethanol-in-water solvent.

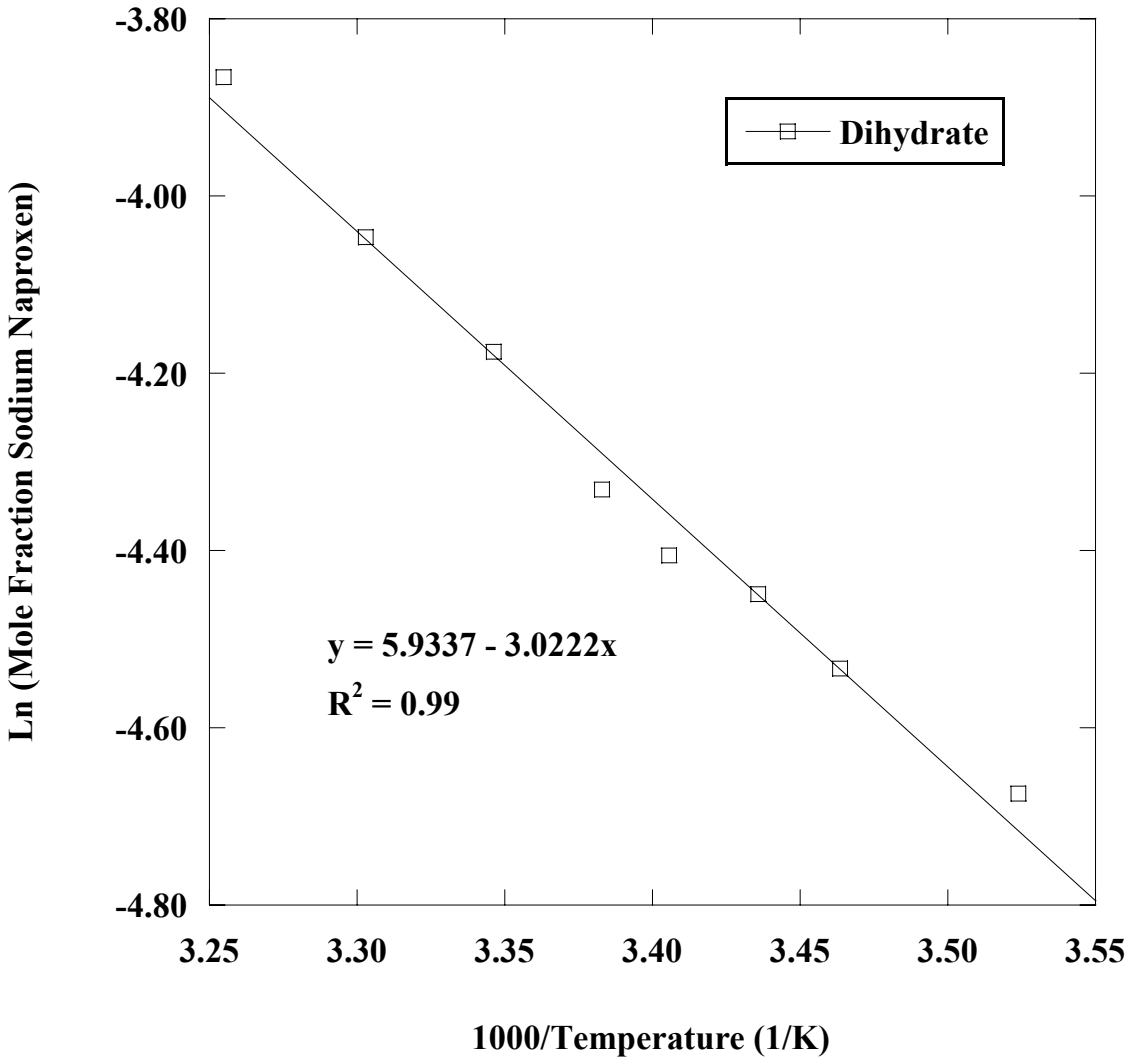

Figure 4.13. Van't Hoff plot of 67 mol % ethanol-in-water solvent.

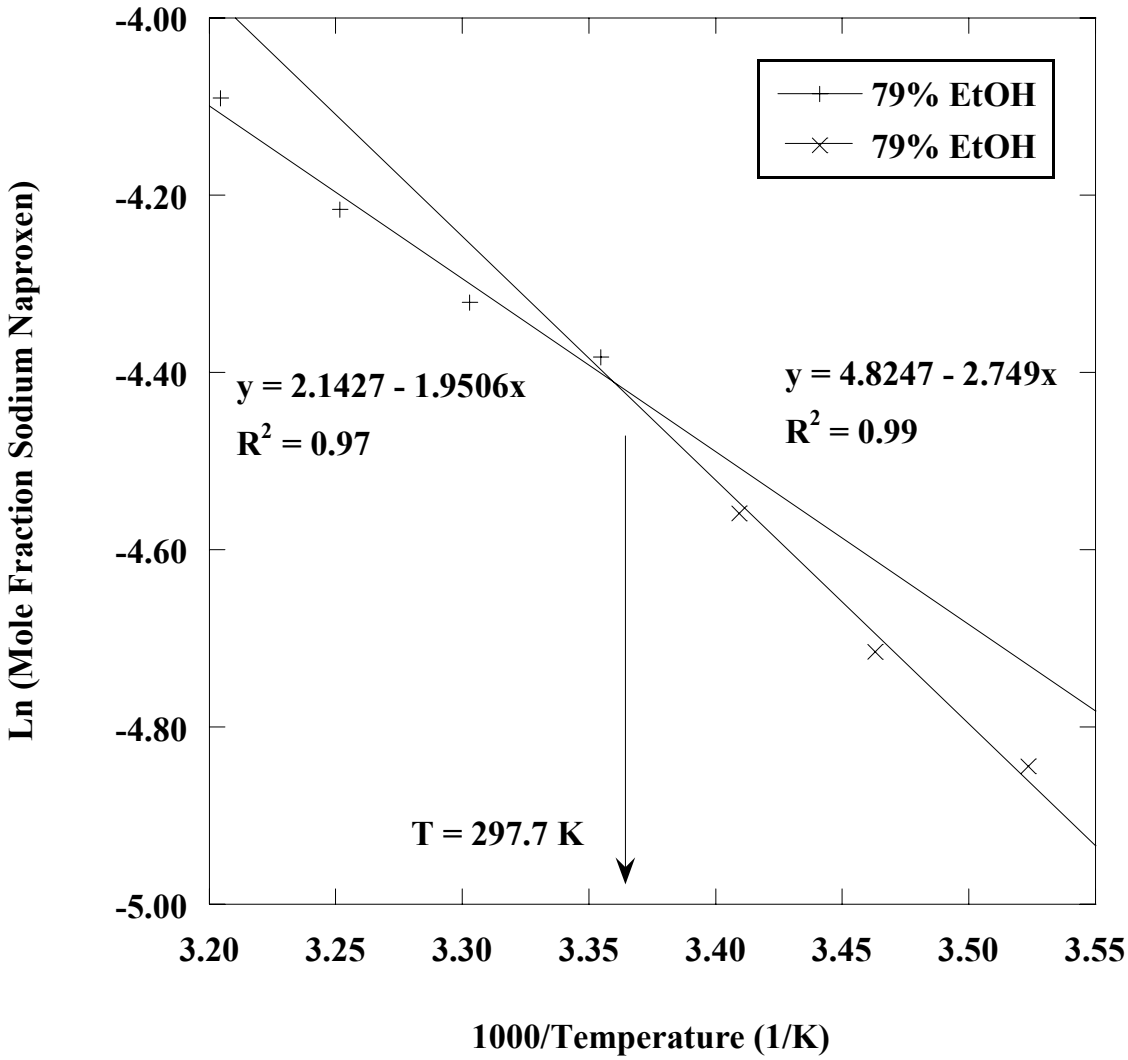

Figure 4.14. Van't Hoff plot of 79 mol % ethanol-in-water solvent.

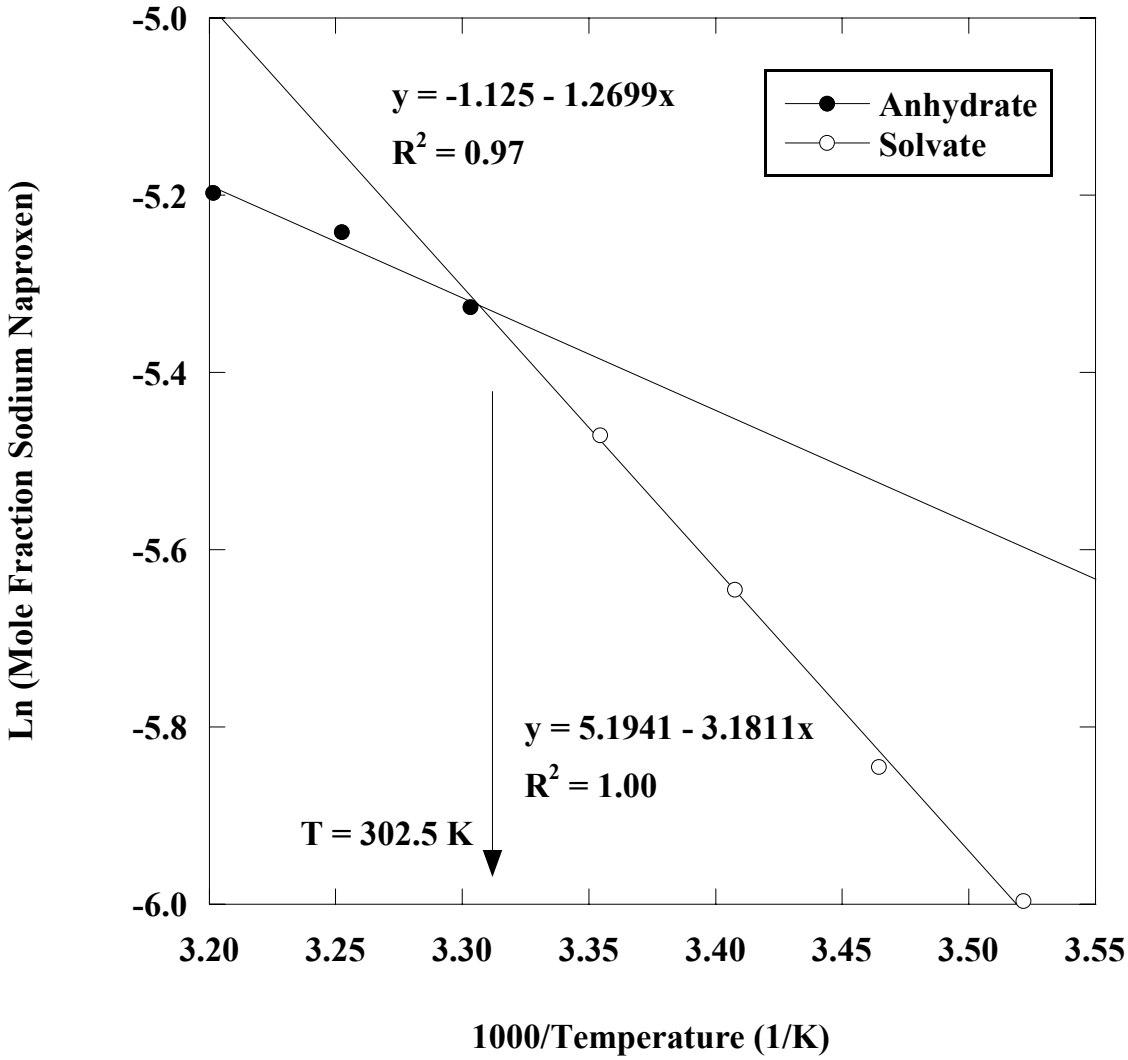

Figure 4.15. Van't Hoff plot of pure ethanol solvent.

The enthalpies and entropies of dissolution extracted from the slopes and intercepts of the best-fit linear regressions are listed in Table 4.3 and Table 4.4 for methanol-water and ethanol-water solvent mixtures.

Table 4.3. Enthalpy and entropy of dissolution of methanol-water mixed solvents from van't Hoff plots.

Methanol Concentration (mole %)	Solid State	Enthalpy of Dissolution (kJ/mol ASN)	Entropy of Dissolution (J/mol ASN)
10	Solvate	81.3	242.6
	Dihydrate	46.0	123.9
25	Solvate	63.2	452.9
	Dihydrate	22.4	188.3
47	Dihydrate	22.2	45.9
64	Dihydrate	27.9	68.3
	Monohydrate	13.4	20.7
100	Solvate	0.274	-1.53
	Anhydrate	7.63	-26.1

Table 4.4. Enthalpy and entropy of dissolution of ethanol-water mixed solvents from van't Hoff plots.

Ethanol Concentration (mole %)	Solid State	Enthalpy of Dissolution (kJ/mol ASN)	Entropy of Dissolution (J/mol ASN)
14.5	Solvate	62.3	182
	Dihydrate	35.6	91.7
44	Solvate	17.7	30.0
	Dihydrate	18.6	33.3
67	Dihydrate	25.1	49.3
79	Dihydrate	22.9	40.1
	Monohydrate	16.2	17.8
100	Solvate	26.4	43.2
	Anhydrate	10.6	-9.35

For the dihydrate and anhydrate in pure water the enthalpy of dissolution was 56.2 and 33.8 kJ/mol ASN, respectively (Kim, 2005). The enthalpy of dissolution decreased

for each pseudopolymorph as the concentration of the alcohol increased in the solvent. Dissolution can be viewed as occurring in three steps:

(1) breaking solute-solute attractions (endothermic)

(2) breaking solvent-solvent attractions (endothermic)

(3) Forming solvent-solute attractions (exothermic).

Since the enthalpy of dissolution seemed to decrease as the concentration of alcohol in the solvent increased, this would mean the breaking of solvent-solvent bonds was less endothermic and/or the forming of solvent-solute bonds was more exothermic. The heat of vaporization of water is high, signaling strong solvent-solvent interactions, as the amount of alcohol present in the solvent increased; these solvent-solvent interactions between water molecules would decrease. This meant a decrease in the endothermic nature of the solvent-solvent interactions pertaining to dissolution. Clearly, the decrease in enthalpies of dissolution was expected as the amount of alcohol increased in the solvent.

Pertaining to the differences in dissolution enthalpies for different pseudopolymorphs, Kim et al. (2005) were able to explain that in an enantiotropic system, a pseudopolymorph with a lower degree of hydration was more stable over a higher temperature range above the transition temperature, explained by the following equation:

$$\Delta\hat{H}_{\mathrm{sol},n} - \Delta\hat{H}_{\mathrm{sol},m} = \Delta\hat{H}_{\mathrm{d},n\to m} - (n-m)\Delta\hat{H}_{\mathrm{vap,H_2O}} + (n-m)\int_{\mathrm{T_d}}^{100} (C_{p_{\mathrm{H_2O_{(v)}}}} - C_{p_{\mathrm{H_2O_{(l)}}}})dT. \quad (4\text{-}1).$$

Where $\Delta\hat{H}_{\mathrm{sol}}$ is the heat of dissolution, $\Delta\hat{H}_{\mathrm{d}}$ is the heat of dehydration, $\Delta\hat{H}_{\mathrm{vap}}$ is the heat of vaporization, $\mathrm{T_d}$ is the dehydration temperature, C_p is the heat capacity, and m and n are degrees of hydration where $m<n$. The first term of the equation on the right hand side is always greater than the second, and the integral term is small; therefore, the right-hand side is always positive. Consequently, the heat of dissolution of hydration state m is always smaller than the heat of dissolution of hydration state n.

This can also be related back to the van't Hoff plots. If a system exhibits transitions according to the van't Hoff plot, the slope of the line must be smaller for the pseudopolymorph at the higher temperatures than that of the pseudopolymorphs at the lower temperatures, in order for the lines to cross. Since a smaller slope for the van't Hoff plot corresponds to less hydrated pseudopolymorph, this means that the less hydrated pseudopolymorph must be in equilibrium at the higher temperatures. Therefore, the dihydrate will exist at lower temperatures and the anhydrate at higher temperatures in pure water solvent systems. When considering a dihydrate to monohydrate transition, as in solutions of 64 mol% methanol and 79 mol% ethanol-in-water. The dihydrate will again be present at equilibrium at lower temperatures and have a larger enthalpy of dissolution than the monohydrate, which was present at higher temperatures. A similar analysis for solvate to dihydrate transitions is shown in chapter 5.

Table 4.5 and Table 4.6 are a summary of the figures presented above.

Table 4.5. Solid-state transitions and transition temperatures for methanol-water mixed solvents.

Methanol Concentration (mole %)	Solid State Transition (Lower T → Higher T)	Transition Temperature (K)
0	Dihydrate → Anhydrate	302
10	Solvate → Dihydrate	297
25	Solvate → Dihydrate	292
47	Dihydrate	---
64	Dihydrate → Monohydrate	293
100	Solvate → Anhydrate	300

Table 4.6. Solid-state transitions and transition temperatures for ethanol-water mixed solvents.

Ethanol Concentration (mole %)	Solid State Transition (Lower T → Higher T)	Transition Temperature (K)
0	Dihydrate → Anhydrate	302
14.5	Solvate → Dihydrate	295
44	Solvate → Dihydrate	289
67	Dihydrate	---
79	Dihydrate → Monohydrate	298
100	Solvate → Anhydrate	303

They list the solid state transitions that were observed and the temperatures at which theses transitions occurred according to the alcohol content of the mixed solvent. The transition in pure water is also listed (Kim, 2005).

As the fraction of alcohol in the solvent increased the transition temperature decreased, up to the point where no transition was observed. Then, as the fraction of alcohol in the solvent continued to increase, the transition temperature began to increase as well. These changes in transitions temperature can be better explained by looking at changes in water activity.

4.3 Role of Water Activity in Pseudopolymorphic Transitions

Khanhari and Grant (1995) postulated that the activity of water in a mixture plays an important role in determining the solubility and hydration state of a hydrate. In their analysis, formation of a hydrated crystal was represented by the following chemical equation:

$$A_{(solid)} + mH_2O \longleftrightarrow A \cdot mH_2O_{(solid)}.$$

The equilibrium constant, K_h, for the above process can be represented by

$$K_h = \frac{a[A \cdot mH_2O_{(solid)}]}{a[A_{(solid)}] * a[H_2O]^m} \tag{4-2}$$

Where $a[A \cdot mH_2O_{(solid)}]$, $a[A_{(solid)}]$, and $a[H_2O]$ are the activities of the hydrate crystal, anhydrate crystal, and water, respectively. If the standard states of the solids are assumed to be their pure phases and therefore exhibit an activity of 1, the above equation simplifies to

$$K_h = a[H_2O]^{-m} \tag{4-3}$$

where m is the number of moles in the stoichiometric equation that are taken up by one mole of the less hydrated species.

The same results can be obtained in a solvent-mediated transformation with the following chemical equation:

$$A_{(s)} + mH_2O_{(l)} \xrightleftharpoons{K_1} A_{(aq)} + mH_2O_{(l)} \xrightleftharpoons{K_2} A \cdot mH_2O_{(s)} \quad (4\text{-}4)$$

The equilibrium constants for the two steps are as follows:

$$K_1 = \frac{a[A_{(aq)}]}{a[A_{(s)}]} \quad (4\text{-}5)$$

$$K_2 = \frac{a[A \cdot mH_2O_{(s)}]}{a[A_{(aq)}] * a[H_2O]^m} \quad (4\text{-}6)$$

Where $a[A_{(s)}]$ is the activity of the solid in solution. The overall equilibrium constant was evaluated by multiplying Equation (4-4) with Equation (4-5) to arrive at the following equation

$$K_1 * K_2 = a[H_2O]^{-m} \quad (4\text{-}7),$$

which has the same implications as Equation (4-3).

The activity of water in the crystallization medium depends on the composition of the water / solvent mixture. Values of the water activity, a_w, can be calculated in such mixtures from literature values or thermodynamic approximations of the activity coefficient of water, γ_w, and the mole fraction of water, x_w, by

$$a_w = \gamma_w x_w \quad (4\text{-}8)$$

There then exists an equilibrium water activity where at higher levels one form of the hydrate crystal is stable and at water activities lower than the equilibrium water activity another form is more stable. Studies have shown that the hydration state of a stable crystal species depends on the water activity in the crystallization medium (Zhu et al., 1996; Zhu and Grant 1996; Qu et al., 2006). This method asserts that a_w in the mixture is the major variable determining the phase of the pseudopolymorph and that the

dissolved drug in the solvent mixture influences a_w to a smaller extent than the organic solvent.

In addition, Qu et al. (2006) have shown that the hydration state of a mixed hydrate formed from a water-ethanol solution is dependent on both the water activity and the temperature of the solution for carbamazepine. As the transition temperature increased, so did the equilibrium water activity where the transition from one hydrate species to the other was observed (see Figure 4.16). For the carbamazepine anhydrous(CBZA) / hydrate (CBZH) system in water-ethanol mixtures, the equilibrium water activity increased with increasing temperature.

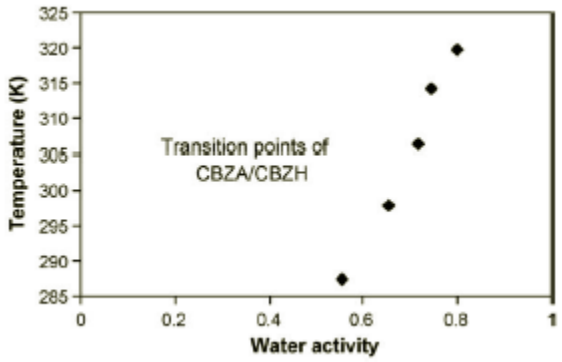

Figure 4.16. Transition points of CBZA/CBZH (Qu et al. 2006).

The activity of water was calculated at the transition point using the concentration of alcohol in the solvent and the transition temperature extracted from the van't Hoff plots. Assuming the solute did not affect the activity of water, a two-component Wilson equation was used to establish an activity coefficient, which was then substituted into Equation (4-8). The Wilson equation is given by

$$\ln \gamma_1 = 1 - \ln(x_1\Lambda_{11} + x_2\Lambda_{12}) - \left(\frac{x_1\Lambda_{11}}{x_1\Lambda_{11} + x_2\Lambda_{12}} + \frac{x_2\Lambda_{21}}{x_1\Lambda_{21} + x_2\Lambda_{22}} \right) \quad (4\text{- }9)$$

$$\ln \gamma_2 = 1 - \ln(x_2\Lambda_{22} + x_1\Lambda_{21}) - \left(\frac{x_2\Lambda_{22}}{x_2\Lambda_{22} + x_1\Lambda_{21}} + \frac{x_1\Lambda_{12}}{x_2\Lambda_{12} + x_1\Lambda_{11}} \right) \quad (4\text{- }10)$$

where water = 1 and methanol or ethanol = 2 and x_i is the mole fraction of species i, Λ_{11} and $\Lambda_{22} = 1$, and Λ_{12} and Λ_{21} are adjustable parameters defined as:

$$\Lambda_{12} \equiv \frac{\upsilon_2}{\upsilon_1} \exp\left(-\frac{\lambda_{12} - \lambda_{11}}{RT} \right) \quad (4\text{-}11)$$

$$\Lambda_{21} \equiv \frac{\upsilon_1}{\upsilon_2} \exp\left(-\frac{\lambda_{21} - \lambda_{22}}{RT} \right) \quad (4\text{-}12)$$

where υ_i the molar liquid volume of component i and the λ_{ij} are energies of interaction between the molecules designated in the subscripts. All values are known for methanol-water and ethanol-water systems (Smith and Van Ness, 1996). With γ_w and the concentration of alcohol in solution, a_w was calculated based on Equation (4-8). Figure 4.17 shows the activity of water at the transition points versus the mole percent of alcohol in the solvent.

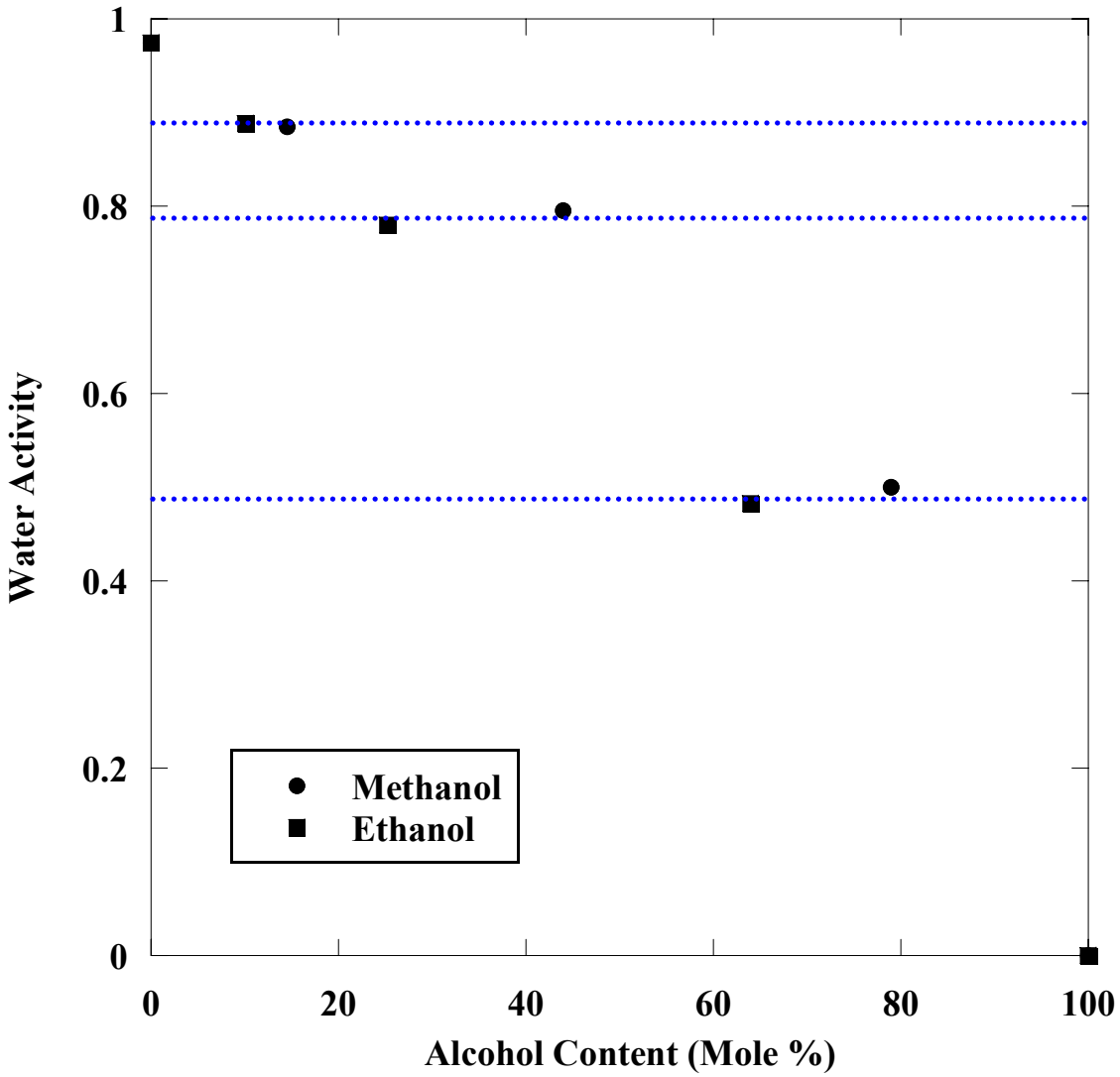

Figure 4.17. Water activity versus alcohol content for methanol-water and ethanol-water mixed solvent systems.

Note that the activities of water at which transitions occurred were the same irrespective of the alcohol in the solvent; i.e. transitions took place at water activities of 0.9, 0.8, and 0.5. Clearly, then, water activity is a controlling thermodynamic factor for pseudopolymorphic transitions.

It was interesting to note that the transitions with 10 mol% methanol and 14.5 mol% ethanol and with 25 mol% methanol and 44 mol% ethanol represented transitions from solvate to dihydrate but occurred at different water activities. Although the change in pseudopolymorphic form was the same at these points the water activity was actually different. This would suggest that there are preferential ranges of water activity for a certain transition, and within that range transitions will actually occur at specific points. For these transitions the equilibrium constant would depend both on the water activity and the alcohol activity of the solvent.

4.4 Role of Alcohol Activity in Pseudopolymorphic Transitions

On a similar note, the activities of alcohol in the solutions were also compared to see if alcohol activity had significance in terms of the transitions of pseudopolymorphic forms. As seen in Figure 4.18, there was no correspondence among alcohol activity and transitions of the pseudopolymorphs (transition pairs are circled). Water activity plays the dominant role in pseudopolymorphic transitions. This was most likely due to the fact that when a solvated form is present for a transition, the dihydrated form is also present so the chemical equation for transition is

$$\mathrm{A}\cdot m\mathrm{ROH} + 2\mathrm{H_2O} \leftrightarrow \mathrm{A}\cdot 2\mathrm{H_2O} + m\mathrm{ROH},$$

and the equilibrium constant is defined by the following equation:

$$K_h = a[\mathrm{ROH}]^m a[\mathrm{H_2O}]^{-2} \tag{4-13}$$

Since m is always less than 2 in the studies presented here, water activity will dominates the equilibrium constant so the alcohol activity is not expected to play as great a role as the water activity, across alcohol solvents.

Additionally, when comparing the methanol solvate-dihydrate transition with the ethanol solvate-dihydrate transition, the alcohol activities would not be expected to be the same since the transitions are actually different; an ethanol solvate would not form in methanol-water solutions. This would mean different equilibrium constants and although the water activities coincide because they were the dominate player in the equilibrium constant, the alcohol activities may not.

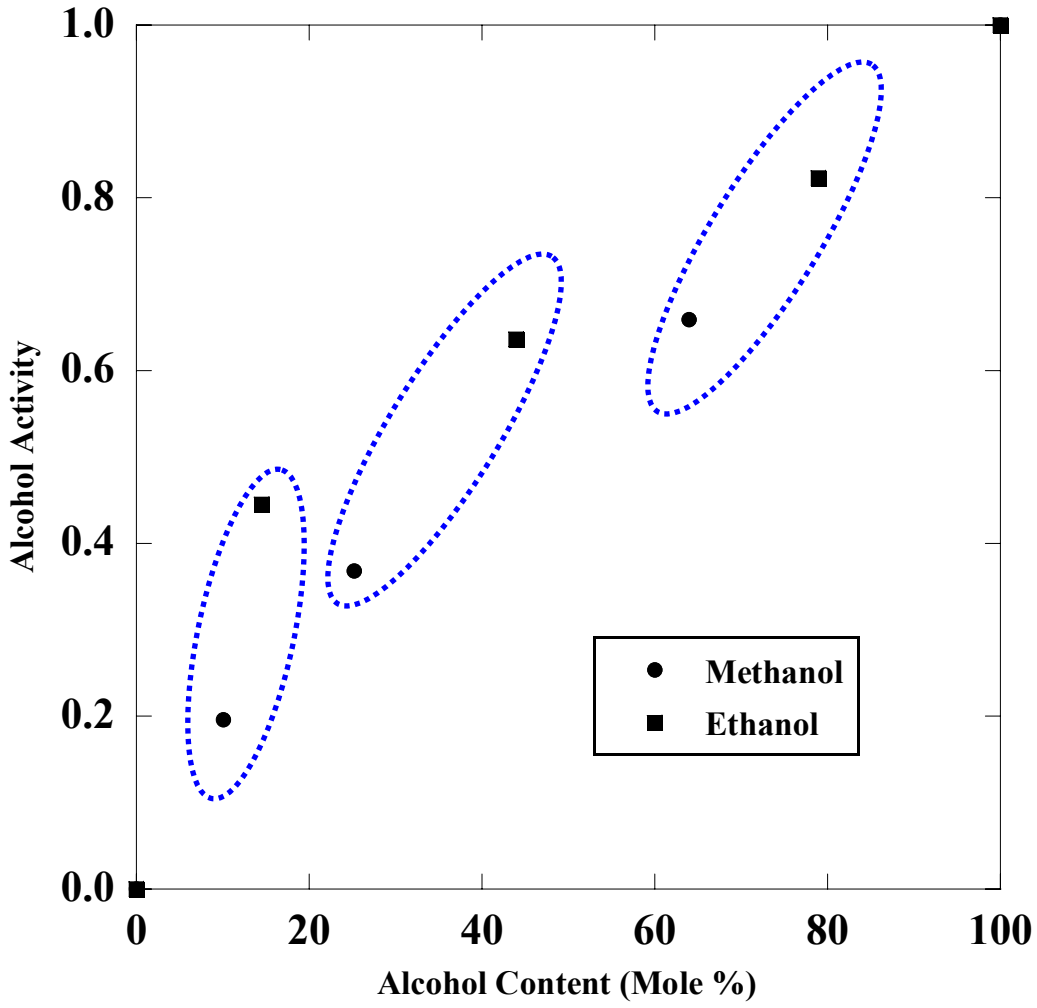

Figure 4.18. Alcohol activity versus alcohol content of methanol-water and ethanol-water mixed solvent systems.

4.5 Conclusions

The solubilities of sodium naproxen in methanol-water and ethanol-water mixtures, and in pure solvents of methanol and ethanol were measured. In general, methanol solutions exhibited a salting-in effect compared to pure water. For the ethanol solutions a salting-out effect was seen compared to the solubility of sodium naproxen in pure water. The following pseudopolymorphs were identified: anhydrate, monohydrate, dihydrate, methanol solvate, and ethanol solvate of sodium naproxen, existence of the alcohol solvates of sodium naproxen had not been previously reported.

By changing the alcohol content in the solvent solution, varying pseudopolymorphic forms of sodium naproxen were produced in equilibrium with the solution. This implies that solid-state formation of pseudopolymorphs and solubility can be controlled through solvent selection.

The transition temperatures from one pseudopolymorphic form to another for each of the solvent concentrations were determined and were distinct from each other. The transition temperatures initially decreased as the concentration of alcohol in the solvent increased, until there was no transition with the 47 mol% methanol solvent and the 67 mol% ethanol-in-water solvent. As the amount of alcohol increased past these points the transition temperatures began to increase.

Additionally, using the extracted transition temperatures and Wilson's equation to estimate the activity coefficient, the activities of water at the transition points was determined. It was shown that independent of the alcohol content, transitions occurred at the same water activity for corresponding alcohol concentrations, while correlations with alcohol activity was not apparent. This was explained by looking at the equation for the

equilibrium constant which was largely dependent on the water activity compared to the alcohol activity. It was interesting to note that at the 10 mol% methanol/ 14.5 mol% ethanol-in-water and 25 mol% methanol/ 44 mol% ethanol-in-water pairs, the same pseudopolymorphic transition occurred even though the water activities at these points were different. This would suggest that there was a range of water activities for pseudopolymorphic transition as opposed to one specific water activity when the transition would occur.

CHAPTER 5

STABILITY OF SOLVATE-HYDRATE SYSTEMS

In the previous chapter, a model by Kim et al. (2005) was used to explain pseudopolymorphic stability at high or lower temperatures based on the degree of solvation when the pseudopolymorphs only included anhydrate to hydrate transitions. A modified approach was required to examine transitions between hydrates and solvates. The modification, as described below, allowed determination of heats of solution.

5.1 Mixed-Solvent Thermodynamic Cycles

The following two chemical equations describe dihydrate and methanol solvate formations:

$$A \cdot 2H_2O \xrightarrow[MeOH]{\Delta H_{sol,A\cdot H_2O}} A_{(aq)} + 2H_2O_{(l)} \tag{5-1}$$

$$A \cdot MeOH \xrightarrow[H_2O]{\Delta H_{sol,A\cdot MeOH}} A_{(aq)} + MeOH_{(l)} \tag{5-2}$$

Using these equations, thermodynamic pathways shown in Figure 5.1 for Equation (5-1) and Figure 5.2 for Equation (5-2) were constructed, where T_s is the solution temperature and T_d is the dehydration temperature.

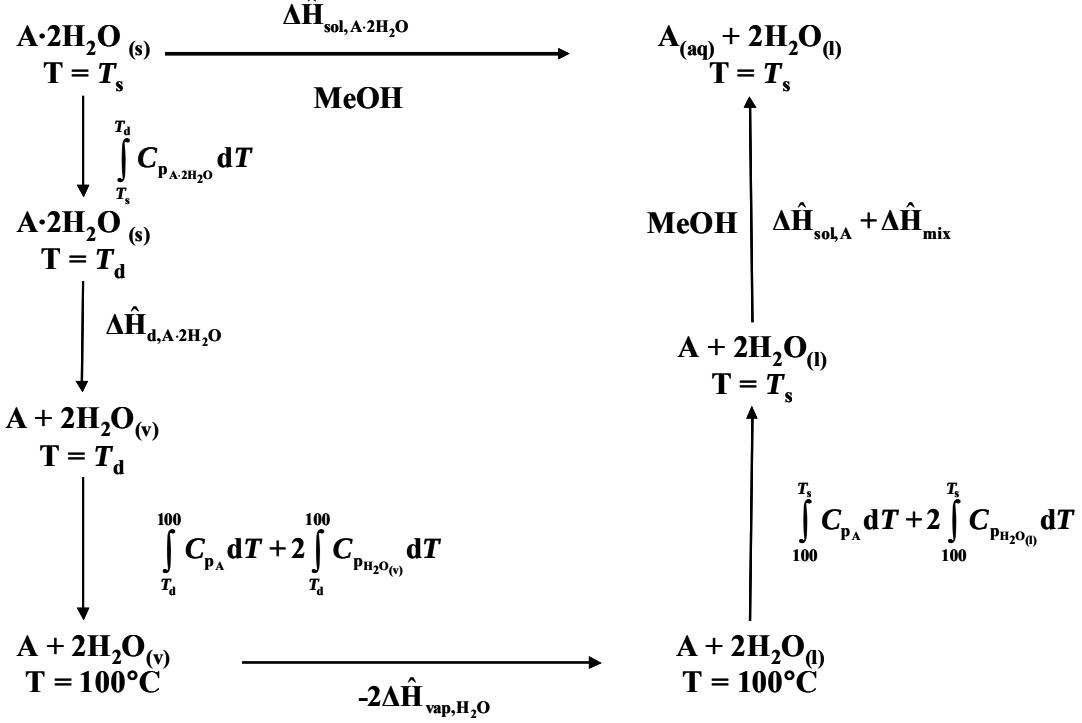

Figure 5.1. Thermodynamic cycle for dissolving dihydrate in methanol.

Based on this cycle the heat of solution was estimated by the following equation:

$$\begin{aligned}\Delta\hat{H}_{sol,A\cdot 2H_2O}[MeOH] = {} & \Delta\hat{H}_{d,A\cdot 2H_2O} - 2\Delta\hat{H}_{vap,H_2O} + \Delta\hat{H}_{sol,A}[MeOH] \\ & + \Delta\hat{H}_{mix}(2H_2O, MeOH) \\ & + 2\int_{T_d}^{100}[C_{p_{H_2O(v)}} - C_{p_{H_2O(l)}}]dT + \int_{T_d}^{100} C_{p_A}\,dT \\ & + \int_{T_s}^{T_d} C_{p_{A\cdot 2H_2O}}\,dT + \int_{100}^{T_s} C_{p_A}\,dT + 2\int_{T_d}^{T_s} C_{p_{H_2O(l)}}\,dT\end{aligned} \tag{5-3}$$

where $\Delta\hat{H}_{sol,i}[j]$ is the molar heat of solution of component i in solvent j, $\Delta\hat{H}_{d,i}$ is molar the heat of dehydration for component i, $\Delta\hat{H}_{vap,i}$ is the molar heat of vaporization of component i, $\Delta\hat{H}_{mix}(i,j)$ is the molar heat of mixing of components i and j, and C_{p_i} is the heat capacity of specie i. Assuming the heat capacity of the dihydrate was approximately equal to the sum of the heat capacity of anhydrate and two moles of water, as justified by Khankari et al. (1992), the following was true:

$$\int_{T_s}^{T_d} C_{p_{A\cdot 2H_2O}}\,dT \approx \int_{T_s}^{T_d} C_{p_A}\,dT + 2\int_{T_s}^{T_d} C_{p_{H_2O(l)}}\,dT \tag{5-4}$$

Equation (5-3) then became

$$\begin{aligned}\Delta\hat{H}_{sol,A\cdot 2H_2O}[MeOH] = {} & \Delta\hat{H}_{d,A\cdot 2H_2O} - 2\Delta\hat{H}_{vap,H_2O} + \Delta\hat{H}_{sol,A}[MeOH] \\ & + \Delta\hat{H}_{mix}(2H_2O, MeOH) \\ & + 2\int_{T_d}^{100}[C_{p_{H_2O(v)}} - C_{p_{H_2O(l)}}]dT\end{aligned} \tag{5-5}$$

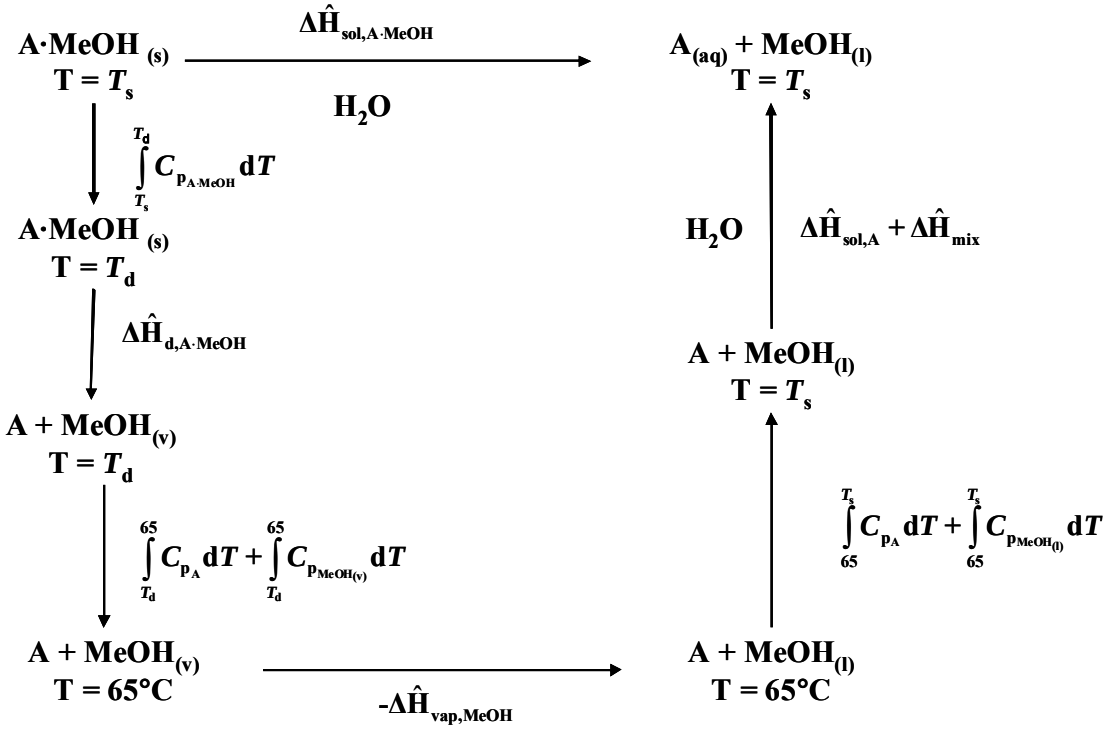

Figure 5.2. Thermodynamic cycle for the dissolution of methanol solvate in water.

Using the same approach as presented above the equation for the dissolution of a methanol solvate in water was

$$\begin{aligned}\Delta\hat{H}_{sol,A\cdot MeOH}[H_2O] = {} & \Delta\hat{H}_{d,A\cdot MeOH} - \Delta\hat{H}_{vap,MeOH} + \Delta\hat{H}_{sol,A}[H_2O] \\ & + \Delta\hat{H}_{mix}(H_2O, MeOH) \\ & + \int_{T_d}^{65}[C_{p_{MeOH(v)}} - C_{p_{MeOH(l)}}]dT + \int_{T_d}^{65} C_{p_A}\,dT \\ & + \int_{T_s}^{T_d} C_{p_{A\cdot MeOH}}\,dT + \int_{T_d}^{T_s} C_{p_A}\,dT + 2\int_{T_d}^{T_s} C_{p_{MeOH(l)}}\,dT\end{aligned} \tag{5-6}$$

Again assuming that the methanol was present in liquid-like structure of the solvated species

$$\int_{T_s}^{T_d} C_{p_{A\cdot MeOH}}\,dT \approx \int_{T_s}^{T_d} C_{p_A}\,dT + 2\int_{T_s}^{T_d} C_{p_{MeOH(l)}}\,dT \tag{5-7}$$

equation (5-6) became

$$\begin{aligned}\Delta\hat{H}_{sol,A\cdot MeOH}[H_2O] = {} & \Delta\hat{H}_{d,A\cdot MeOH} - \Delta\hat{H}_{vap,MeOH} + \Delta\hat{H}_{sol,A}[H_2O] \\ & + \Delta\hat{H}_{mix}(H_2O, MeOH) \\ & + \int_{T_d}^{65}[C_{p_{MeOH(v)}} - C_{p_{MeOH(l)}}]dT\end{aligned} \tag{5-8}$$

All of the values on the right hand sides of Equations (5-5) and (5-8) were known or could be estimated. Using these equations, the heats of solution of the dihydrated species in methanol and of the methanol solvate in water could be estimated. But more importantly, the stability of one pseudopolymorph compared to the other can be determined.

By subtracting Equation (5-2) from Equation (5-1), the following chemical equilibrium equation resulted:

$$A \cdot 2H_2O + MeOH_{(l)} \xrightarrow[H_2O,MeOH]{\Delta H_{sol,A\cdot H_2O} - \Delta H_{sol,A\cdot MeOH}} A \cdot MeOH + 2H_2O_{(l)} \qquad (5\text{-}9)$$

This represents the transition from the dihydrated species to the methanol solvate and the following mathematical equations resulted from the thermodynamic cycles:

$$\begin{aligned}\Delta\hat{H}_{sol,A\cdot 2H_2O}[MeOH] - \Delta\hat{H}_{sol,A\cdot MeOH}[H_2O] = {} & \Delta\hat{H}_{d,A\cdot 2H_2O} - \Delta\hat{H}_{d,A\cdot MeOH} \\ & - 2\Delta\hat{H}_{vap,H_2O} + \Delta\hat{H}_{vap,MeOH} \\ & + \Delta\hat{H}_{sol,A}[MeOH] - \Delta\hat{H}_{sol,A}[H_2O] \\ & + \Delta\hat{H}_{mix}(2H_2O, MeOH) \\ & - \Delta\hat{H}_{mix}(H_2O, MeOH) \\ & + 2\int_{T_d}^{100}[C_{p_{H_2O(v)}} - C_{p_{H_2O(l)}}]dT \\ & - \int_{T_d}^{65}[C_{p_{MeOH(v)}} - C_{p_{MeOH(l)}}]dT\end{aligned} \qquad (5\text{-}10)$$

From DSC data, the heat of dehydration of dihydrated sodium naproxen was 108.6 kJ/mol and the heat of desolvation of the methanol solvated sodium naproxen was 57.9 kJ/mol. The heat of vaporization of water was 40.7 kJ/mol (Stark and Wallace, 1976) and the heat of vaporization of methanol was 34.5 kJ/mol (Yaws, 2003). The heats of dissolution in pure solvents of the anhydrous form of sodium naproxen can be taken from previous van't Hoff plots of solubility; $\Delta\hat{H}_{sol,A}[MeOH] = 0.274\,{}^{kJ}\!/_{mol}$ and $\Delta\hat{H}_{sol,A}[H_2O] = 33.8\,{}^{kJ}\!/_{mol}$. The heat capacity of water in the liquid state was 4.186 J/g°C and in the vapor state was 2.009 J/g°C. The heat capacities of methanol in its liquid and vapor states were 79.5 $J\cdot K^{-1}\cdot mol^{-1}$ and 52.3 $J\cdot K^{-1}\cdot mol^{-1}$, respectively (Yaws, 2003). The heat of mixing for methanol and water was small compared to the other values, but could be determined from literature values or from approximations. Additionally the heat of mixings needed here would be similar in value so both terms can

be neglected. Substituting these values into Equation (5-10), $\Delta\hat{H}_{\text{sol,A}\cdot 2\text{H}_2\text{O}} - \Delta\hat{H}_{\text{sol,A}\cdot\text{MeOH}} = -26.9\,{}^{\text{kJ}}\!/_{\text{mol}}$. A negative value on the right-hand side of the equation meant the heat of dissolution of the dihydrated from of sodium naproxen was smaller than the heat of dissolution of the methanol solvated form of sodium naproxen. The smaller heat of solution meant a lower slope for the van't Hoff plot which would correspond to the higher temperature range. Therefore the dihydrated form was more stable at the higher equilibrium temperature than the alcohol solvated form. The same analysis would apply to the ethanol solvated form of sodium naproxen and its transformation to the dihydrated sodium naproxen form, showing that the ethanol solvate form was more stable at lower temperatures than the dihydrate form.

Based on Equation (5-10), there was also a point when the heat of solution of the dihydrated species would be greater than that of the alcohol solvated form as the size of the alcohol solvent increases. The terms relating to the dehydration of dihydrate, vaporization of water and the heat of dissolution of the anhydrous form in water remained the same. The heat of solution of the anhydrate in the alcohol was small and had little effect on the overall sign of the equation. The only two remaining terms of interest were the heat of desolvation of the alcohol and the heat of vaporization of the alcohol. As will be seen in chapter 8, the heat of desolvation had small changes in terms of mole of the solvate as the size of the alcohol solvent increase. But with increasing size of the alcohol solvent or an increase in the carbon chain of the solvent, the heat of vaporization of the alcohol also increased. Therefore, the heat of vaporization of the alcohol present in the solvated form played a large role in determining the differences in the heat of solutions of the dihydrated versus solvated form. This implied that the dihydrated species was be

stable across a larger temperature range as the size of the alcohol solvent increased. More importantly it implied that the solvated form was less stable as the size of the alcohol solvent present in the crystal structure increased.

5.2 Conclusions

It was shown using thermodynamic cycles that based on the heats of solution of the dihydrated and alcohol solvated forms of sodium naproxen, the dihydrate was stable at higher temperatures while the alcohol solvate was stable at lower temperatures. This supported the data presented in chapter 4 related to the transitions of pseudopolymorphic forms of sodium naproxen in mixed alcohol-water systems.

Additionally, this approach gave insight into the stability of other alcohol solvates of sodium naproxen and other pseudopolymorphs. It showed that as the size of the alcohol increased its likelihood to form stabile alcohol solvates decreased as the stability of the dihydrated form of sodium naproxen dominated across a wider temperature range. This will be explored in later chapters of this work.

CHAPTER 6

CHARACTERIZATION OF A NOVEL METHANOL SOLVATE

Sodium naproxen is a non-steroidal, anti-inflammatory drug that has been shown to exhibit four pseudopolymorphic forms (anhydrous, monohydrated, dihydrated, and tetrahydrated). These anhydrate and hydrated species have been thoroughly characterized in the literature as shown in Chapter 2, but a recently discovered solvated, non-hydrated form of sodium naproxen has not yet been explored. Characterization of the solvate, including determination of the crystal structure and the interaction between the solvent and non-solvated crystal molecules, is important for understanding, explaining, and predicting the behavior of the solvate during processing.

Although methanol is not used in the production of sodium naproxen, the use of an inert aromatic hydrocarbon solvent, specifically toluene, has been documented to produce a more pure chiral product (Phan and Robert, 1997). No solvate formation is seen with the toluene solvent, but understanding solvate formation with other solvents could aid in the selection of suitable solvents for various processing aspects.

Using a batch cooling crystallization process with anhydrous sodium naproxen dissolved in methanol solutions, a solvated form was produced. The present study examined this novel methanol solvate of sodium naproxen using powder X-ray diffraction, thermogravimetric analysis, differential scanning calorimetry, and nuclear magnetic resonance for characterization. These methods can be used to determine key characteristics, such as dehydration enthalpies. A thorough understanding of the

characteristics of the methanol solvate of sodium naproxen will aid in understanding and predicting the behavior of sodium naproxen in mixed solvent systems with methanol.

6.1 Experimental Section

6.1.1 Materials

The sodium naproxen used in the experiments was provided by Albemarle Corp., and was used without further processing or purification. The methanol solvate crystals were produced through batch cooling crystallization; approximately 5 g of sodium naproxen was dissolved in approximately 15 g of pure methanol at 10°C, ensuring that crystals were still present in the solution. The solution was placed in an equilibrium cell as described in Chapter 3. The HPLC-grade methanol (purchased from Fisher Scientific) was dried overnight using molecular sieves. The solution was then heated to 55°C, thereby dissolving the crystals and forming an unsaturated solution. The solution was then cooled to 10°C, at an approximate cooling rate of 0.6°C per minute, for the crystallization of the methanol solvate of sodium naproxen to occur. Upon crystallization the, solution remained at 10°C for at least 18 hours to ensure equilibrium was reached. The slurry mixture was then vacuum filtered and the crystals allowed to dry overnight to ensure excess solvent on the surface of the crystals was removed. The resulting crystals used for further analysis after being finely ground using a mortar and pestle.

6.1.2 Thermogravimetric Analysis (TGA)

Mass loss of the methanol solvate of sodium naproxen was measured using a TG/DTA 320 instrument manufactured by Seiko Instrument Inc. Crystal samples of 10 to 15 mg were heated from 22°C to 130°C in aluminum pans that were 5 mm in diameter.

A ramping rate of 10°C/min was used with a nitrogen purge rate of 90 mL/min. As recommended by Di Martino et al (2001), all TGA runs were carried out with open pans to ensure proper desolvation of the crystals.

6.1.3 Differential Scanning Calorimetry (DSC)

Desolvation endotherms were measured using a DSC 220C instrument (Seiko Instrument Inc.) The temperature range of the experiments was 22 to 290°C with a heating rate of 10°C/min and a nitrogen purge rate of 90 mL/min. Crystal samples of 10 to 15 mg were placed in open aluminum pans with a diameter of 7 mm. The use of open aluminum pans was necessary to obtain quantitative evaluations of the desolvation energy (DiMartino et al., 2001).

6.1.4 Polarized Light Microscopy (PLM)

Analysis of crystal samples was performed under a Leica DM LM microscope equipped with a Sony DKS-5000 digital camera and an objective lens of 20X. The microscope was equipped with a Sony DKC-5000 digital camera that converted the focused light into a digital signal, which was then visualized by Image-Pro Plus version 4.5.

6.1.5 Nuclear Magnetic Resonance (NMR)

Crystal samples were dissolved in deuterated water and the liquid sample was analyzed using ^{1}H-NMR at 400 MHz and room temperature. A Varian Mercury Vx 400 with a 5 mm broadband probe head with ^{1}H decoupling was used to obtain the NMR analysis with an acquisition time of 2 seconds and a total run time of 50 seconds.

6.1.6 Powder X-ray Diffraction (PXRD)

Crystals of solvated sodium naproxen were analyzed using PXRD analysis. A PANanlystical X-Pert Pro Alpha-1 diffractometer with copper Kα1 radiation was used in conjunction with the X'Celerator detector. Crystal samples were gently ground to a fine powder prior to analysis. The PXRD pattern was made over a diffraction-angle (2θ) range of 10° to 80°, with a step size of 0.02° and a counting time of 1 second per step.

6.1.7 Fourier Transfer Infrared Spectroscopy (FTIR)

Fourier Transfer Infrared spectroscopy was performed on a Nicolet Company 4700 FT-IR Diamond with an optical resolution of 0.4 cm^{-1} using solid crystal samples after drying. The wavenumber range for sample collection was approximately 4000 to 400 cm^{-1}. Data acquisition and processing was performed using a computer with Analytical OMNIC software.

6.2 Results and Discussion

6.2.1 Thermal and Chemical Analysis of the Samples

The theoretical solvent content of the methanol solvate form of sodium naproxen was 11.258 wt%. Analysis of TGA data provided results that were close to the expected value: 11.240 ± 1.715 (mean ± SD) wt%, based on four runs. Typical data are shown in Figure 6.1. The measured weight loss was similar to that of water loss from dihydrated sodium naproxen, 12.499 wt%, but upon further analysis of the TGA curves a difference in the dehydration process was observed. As illustrated the dehydration of dihydrated sodium naproxen gave two observable dehydration steps in the TGA curves (Kim and Rousseau, 2004), which are Figure 6.1, thought to correspond to the release of two water

molecules per mole of sodium naproxen. In contrast, only one step was observable in the derivative of the TGA curve (dTGA) for the methanol solvate form, and this step corresponds to the release of the single methanol molecule.

Note that the mass loss from the methanol solvated form began at approximately 40°C and then started to diminish at approximately 90°C. This is in contrast to the onset of mass loss for the hydrated forms of sodium naproxen, which began almost immediately at room temperature (Kim and Rousseau, 2004).

This analysis was what first led to the discovery of the methanol solvate form. Since a solvated form of sodium naproxen had not been previously observed, it was initially suspected that the form was merely a dihydrated sodium naproxen due to the similar overall mass loss. Upon further examination of the thermogram the mechanism for release of the solvent, a one step solvent loss versus a two step loss, led to further analysis.

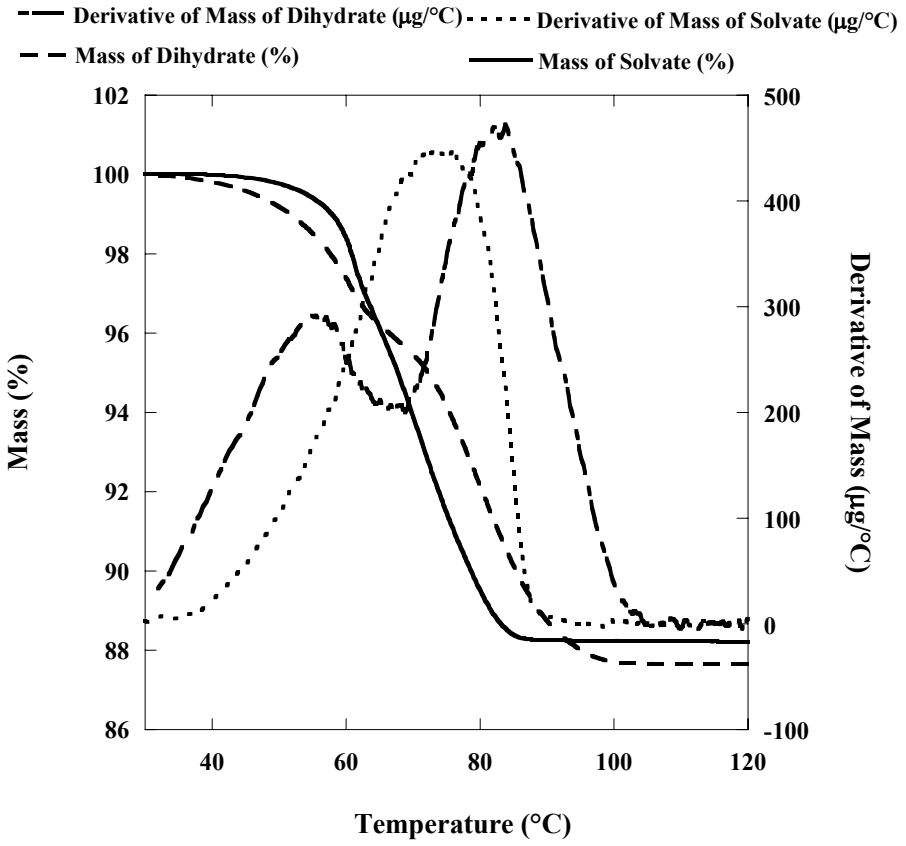

Figure 6.1. Thermogravimetic analysis curves and derivatives of the thermogravimetric analysis curves of mass loss of methanol solvate and dihydrated sodium naproxen.

The DSC analysis was carried out in open pans to avoid any limitations in evaporation due to the cover lid (DiMartino et al., 2001). The results gave a heat of desolvation, based on the initial mass of the sample, of 203.6 ± 1.4 J/g for three runs. This value was similar to the reported heat of dehydration of the monohydrated sodium naproxen, 207.3 J/g; however, it was significantly lower than the heat of dehydration of the dihydrated sodium naproxen, 376.8 J/g (Kim and Rousseau, 2004). If the anhydrous species was used as the basis for desolvation and dehydration, the heat of desolvation became 229.5 J/g for the solvate. The heat of dehydration for the monohydrate based on the anhydrate was 220.5 J/g. Assuming this value of the heat of dehydration for the monohydrate was equal to that for the second water leaving the dihydrate, it can be subtracted from the total heat of dehydration of the dihydrate to determine the heat of dehydration required for the removal of the first water molecule. This would mean the heat of dehydration for the first water molecule based on the mass of the anhydrate was 207.1 J/g (Kim and Rousseau, 2004). While a summary of the heats of desolvation/dehydration is given in Table 6.1, we note that the dehydration energies of tetrahydrated sodium naproxen have not been reported (DiMartino et al., 2007).

There was less than a 10% difference between the heats of dehydration and the heat for methanol removal, which implied that the interactions between the molecules of the water atoms with the surrounding atoms are energetically similar to the interactions of the methanol atom with the surrounding atoms. The reason for the slightly greater heat of solvation was possibly due to the size of the methanol molecule in comparison to that of a water molecule. It has been shown that the dehydration of sodium naproxen occurs through channels (Kim and Rousseau, 2004); hence, it would require more energy for a

larger molecule, such as methanol, to move through the channels than a smaller molecule, compared to water.

Table 6.1. Comparison of heats of desolvation/dehydration of solvate, monohydrate, and dihydrate.

Compound	Heat of Desolvation (J/g sample)	Heat of Desolvation (J/g Anhydrate)	Heat of Desolvation of First Molecule (J/g Anhydrate)	Heat of Desolvation of Second Molecule (J/g Anhydrate)
Solvate	203.6	229.5	229.5	---
Monohydrate	207.3	220.5	220.5	---
Dihydrate	376.8	427.6	207.1	220.5
Tetrahydrate	---	---	---	---

The heat of desolvation can also be expressed as 1802 J/g methanol. One can then compare this value with the heat of vaporization for methanol, 1096 J/g methanol, (Yaws, 2003) at 65°C where the desolvation endotherms reaches its maximum. With a difference of 706 J/g solvent, it was apparent that the methanol was not merely evaporating from the crystal structure and there was some molecular interactions of the methanol with the sodium naproxen. The difference in energy between vaporization and desolvation for the methanol solvated form was similar to that of water for the monohydrate form 764 J/g solvent. This could have been another indication that the interactions of the methanol molecule with sodium naproxen in the alcohol solvated form were similar to that of the water molecule in the monohydrate form of sodium naproxen.

Because the mass loss of the methanol solvate of sodium naproxen was approximately that of the dihydrated sodium naproxen, solution ^{1}H-NMR was performed to ensure that methanol was present in the solid samples and that water from the

atmosphere or other extraneous source was not adsorbing onto the crystal. The resulting spectra are given in Figure 6.2 and Figure 6.3. The upper spectrum was of a sample prepared with the methanol solvate of sodium naproxen, and it shows a methanol peak at approximately 3.2 ppm. Each of the remaining peaks are labeled according to the chemical structure present in the figure. The peak at 5.67 ppm was that of the solvent.

In order to ensure that methanol was present in the crystal structure and not merely on the surfaces of the crystal, a similar ^{1}H-NMR analysis was performed on a solution prepared with sodium naproxen crystals prepared in methanol, but at an equilibrium temperature where the solvate was not formed. (Using the previously described procedure, non-solvated crystals have been found to result if the equilibrium crystallization temperature was greater than 40°C.) As can be seen in Figure 6.2 and Figure 6.3, the NMR spectrum of the non-methanol solvate form was identical to that of the methanol solvate of sodium naproxen except for the absence of the methanol peak. This showed that any residual methanol that remained on the surface of the crystals after filtration was insufficient to show up in the NMR spectrum, which provides further evidence that methanol in the methanol solvate crystal, was indeed part of the crystal structure.

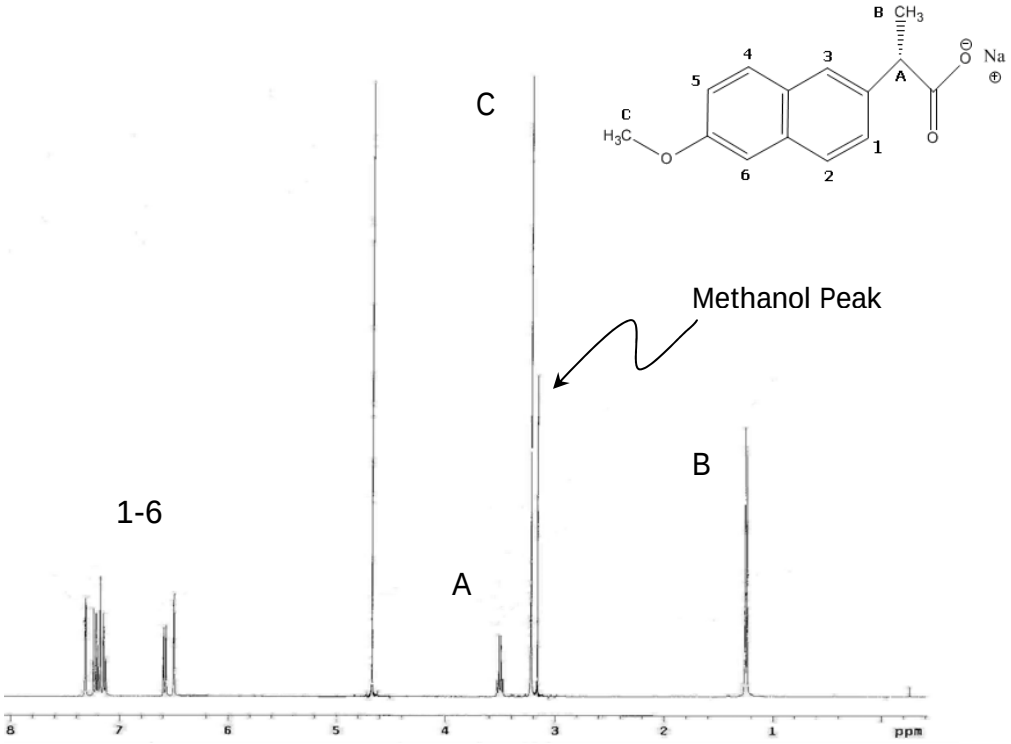

Figure 6.2. [1]H-nuclear magnetic resonance spectrum of the methanol solvate of sodium naproxen.

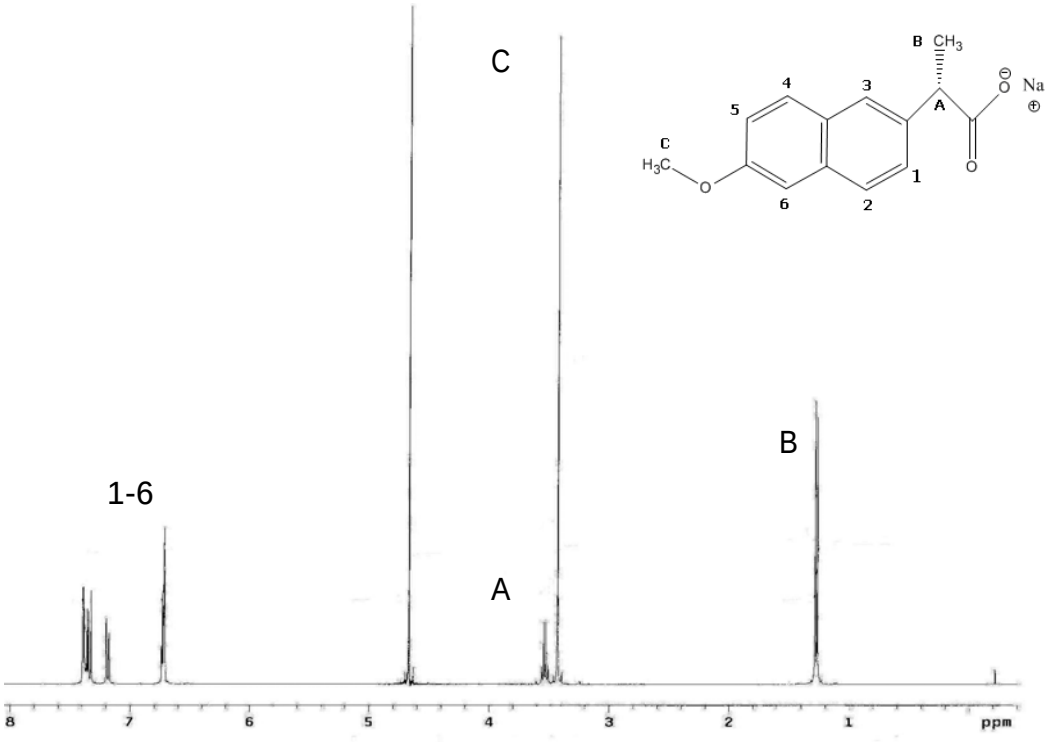

Figure 6.3. ^{1}H-nuclear magnetic resonance spectrum of anhydrous sodium naproxen.

The PXRD pattern of the methanol solvate of sodium naproxen is shown in Figure 6.4. This spectrum differed in peak positions and intensities from the PXRD patterns of the previously known pseudopolymorphs of sodium naproxen (anhydrate, monohydrate, and dihydrate) reported in literature (DiMartino et al., 2007; Kim and Rousseau, 2004), confirming that this novel pseudopolymorph was a distinct crystalline species. Comparison to the tetrahydrated form of sodium naproxen was not possible, since the PXRD pattern was not available in the literature.

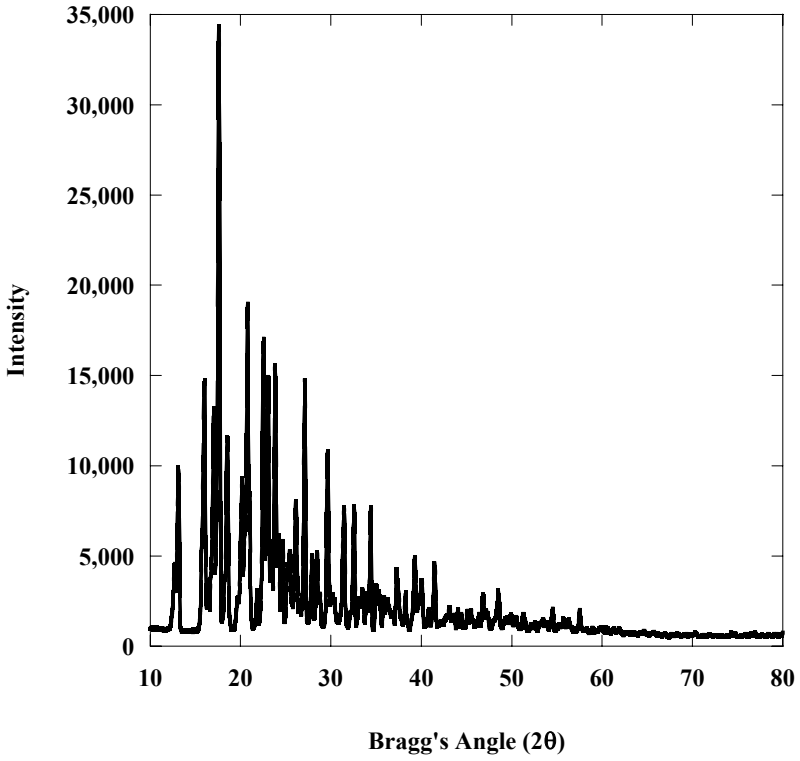

Figure 6.4. Powder x-ray diffraction pattern of the methanol solvate of sodium naproxen.

FTIR results can be seen in Figure 6.5. A broad stretch was seen at a wavenumber of 3348.6 cm^{-1}. Typically stretches between 3600-3200 cm^{-1} are associated with an O-H from alcohols. More specifically, a sharp, weak stretch from 3600-3500 cm^{-1} is indicative of a "free" or unassociated O-H group, while broad stretches in the 3400-3200 cm^{-1} range indicate hydrogen bonding from associated O-H groups. Based on the FTIR spectrum it was clear that there was some interaction of the methanol in the solvated crystal structure, since hydrogen bonding was apparent.

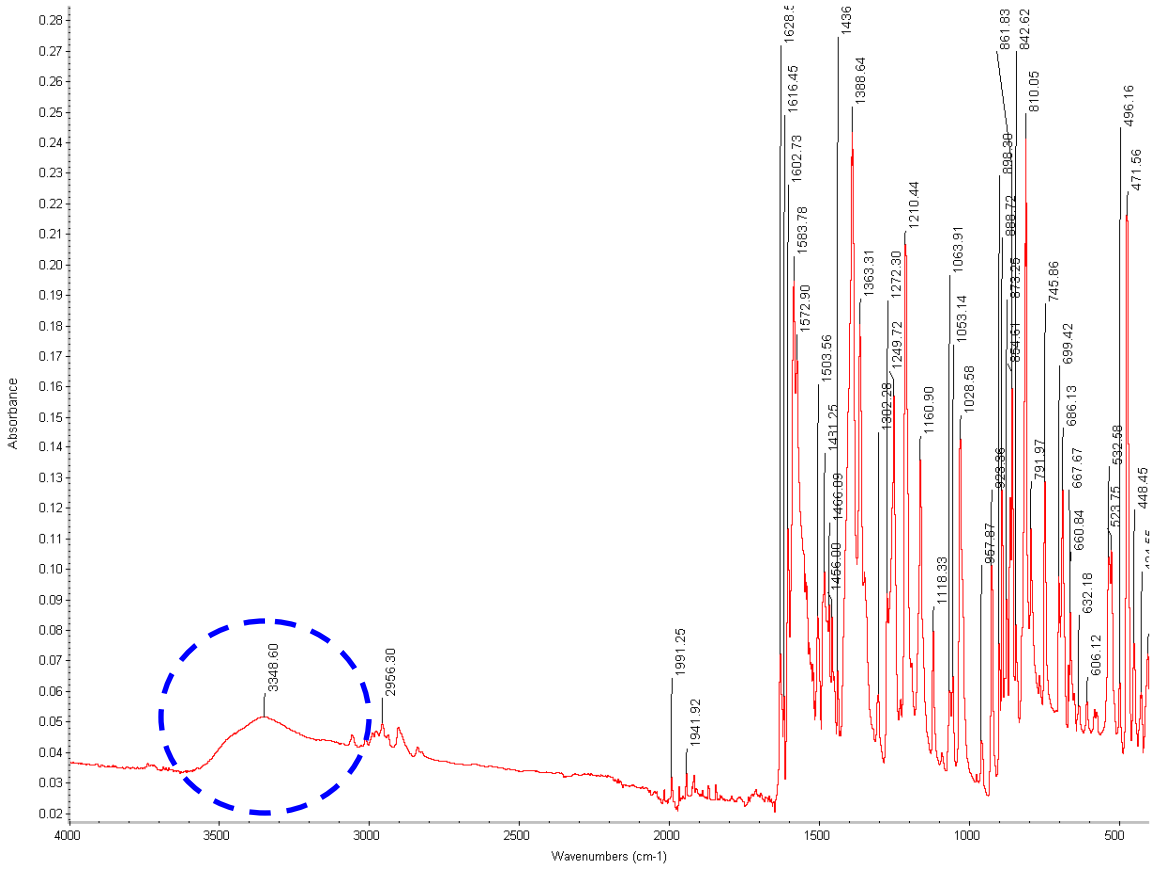

Figure 6.5. FTIR spectrum of methanol solvated form of sodium naproxen.

6.2.2 Crystal Habit

The crystal habits of the anhydrate, monohydrate, and dihydrate of sodium naproxen have been investigated previously (Kim and Rousseau, 2004; DiMartino et al., 2001) and are shown in Figure 6.6 along with crystals of the methanol solvate of sodium naproxen. The shape of the tetrahydrated form of sodium naproxen has not been reported and thus was not presented here.

Anhydrous sodium naproxen exhibited a needle-like shape that was similar to that of the dihydrated pseudopolymorph. The needle-like crystals of the dihydrated sodium naproxen were thinner and smaller than the anhydrate crystals. Monohydrated crystals were less needle-like and formed plate-like crystal structures that were also considerably larger than crystals of the anyhydrate and dihydrate of sodium naproxen. The precise shape of the methanol solvate of sodium naproxen was difficult to characterize; the edges of the crystals were not well defined in the photomicrographs that were taken, and the solvated crystals were smaller than the anhydrous and hydrated forms of sodium naproxen.

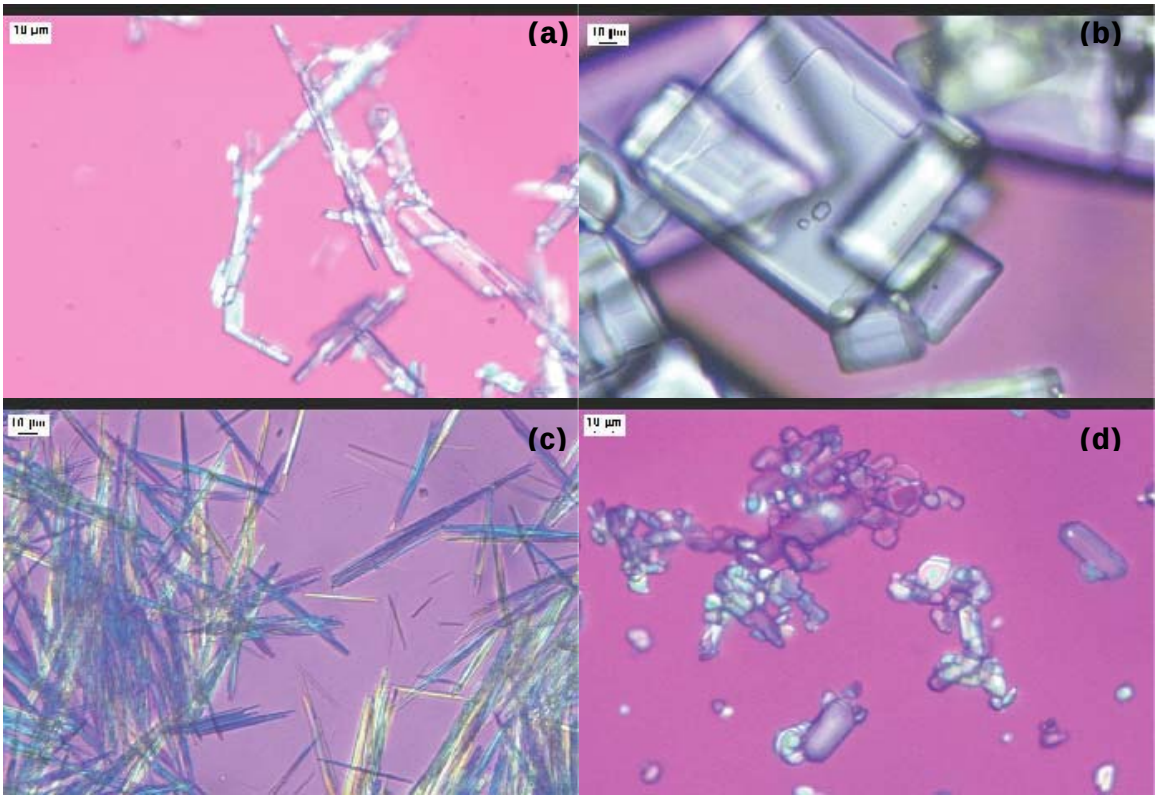

Figure 6.6. Photomicrographs of (a) anyhydrate, (b) monohydrate, (c) dihydrate, and (d) methanol solvate of sodium naproxen.

6.3 Conclusions

Further characterization of the methanol solvated form of sodium naproxen was presented is this chapter. While the methanol solvated form showed similar mass loss to the dihydrated form of sodium naproxen, it was shown to desolvate in one step as opposed to two, which initially led to its discovery. Further analysis by ^{1}H-NMR showed that methanol was indeed in the crystal structure due to that fact that a methanol peak was observed when a methanol solvated form is grown from equilibrium conditions at 10°C in pure methanol, while no methanol peak it observed for anhydrate sodium naproxen crystals grown through the same procedure at 40°C. Characterization of the methanol solvated form of sodium naproxen additionally showed that the energy of desolvation for the methanol solvated form was slightly greater than that of the monohydrate in terms of J/g anhydrate. The energy of desolvation also showed that methanol was indeed in the crystal structure since the desolvation endotherm in terms of moles of alcohol was greater than the heat of vaporization of pure methanol at the desolvation temperature, so the methanol was not merely on the surface of the crystal.

Additionally, the PXRD pattern of the methanol solvated sodium naproxen was distinct from the other report PXRD patterns, showing it was a discrete crystal species. Finally the crystal habit of sodium naproxen was compared to that of the anhydrate, monohydrate, and dihydrate forms through PLM imaging. Methanol solvated crystals of sodium naproxen appear to be prism-like in shape, and are small compared to the sizes of the other pseudopolymorphs of sodium naproxen. In conclusion, a novel pseudopolymorphic form of sodium naproxen was discovered and characterized by TGA, DSC, ^{1}H-NMR, PXRD and PLM.

6.4 Acknowledgments

The author would like to acknowledge Vittoria Blasucci for her assistant with the performing ^{1}H-NMR and IR spectrums. Also, acknowledgments are extended to Dr. Pamela Pollet for aiding in the analysis of the ^{1}H-NMR spectra.

CHAPTER 7

CRYSTAL STRUCTURE OF A METHANOL SOLVATE OF SODIUM NAPROXEN

Crystal structures provide important information needed to understand the chemical and physical properties of organic compounds. When hydrates and solvates are formed, the crystal structures provide insight into the differences between pseudopolymorphic states that can result from processing steps, such as crystallization, lyophilization, wet granulation, spray-drying, or storage in humid environments (Khankari and Grant, 1995). Knowing crystal structures can help prevent or predict possible transformations of pseudopolymorphic forms.

The structures of naproxen (Ravikumar et al., 1985) and sodium naproxen (Kim et al, 2004) have been determined, as well as the structure of the monohydrated form (Kim et al., 1990). The present work was done to (a) determine the structure of the methanol solvated form of sodium naproxen and (b) how it relates to other known pseudopolymorphic forms.

7.1 Crystal Growth

Sodium naproxen supplied by Albemarle Corp. was used without further purification to obtain the crystals studied. Single crystals of the methanol solvate from of sodium naproxen were prepared by slow evaporation of a saturated solution of sodium naproxen in methanol at 4°C as shown in the Figure 7.1. The apparatus was placed in an enclosure containing desiccants, but was also open to the atmosphere using parafilm with

small holes to allow evaporation. The desiccants were used to prevent water from absorbing onto the single crystal.

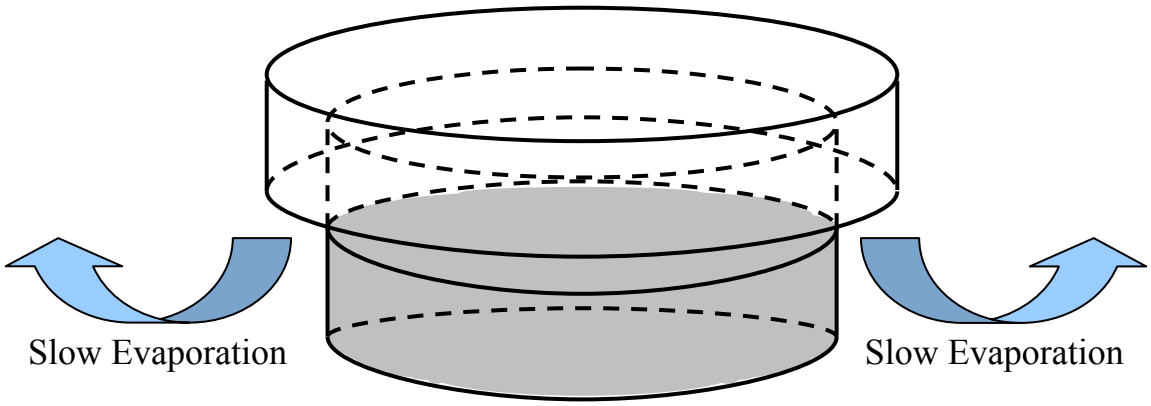

Figure 7.1. Slow Evaporation Apparatus.

7.2 Equipment

7.2.1 Single Crystal X-Ray Diffraction

The crystal was analyzed using a single crystal Bruker APEX II CCD diffractometer. The instrument has a sealed Copper x-ray tube with an Oxford Cryostream low temperature system and was controlled by PC's running the Bruker APEX2 suite of programs. The instrument used a Monocap X-ray beam intensifier.

7.2.2 Software

Visualization of the packing in the methanol solvate crystal was done using the Mercury® CSD 2.2 for Windows®. This software was also used to compute a powder x-ray diffraction pattern using the single crystal structure.

7.3 Results and Discussion

The asymmetric unit of methanol solvated sodium contained two independent sodium naproxen molecules and 3 independent methanol molecules as shown in Figure 7.2. These data conflicted with the data presented in the previous chapter which seemed to show a one-to-one ratio of anhydrous sodium naproxen to methanol in the solvated crystals, possibly due to the differences in temperature for the formation of the crystals.

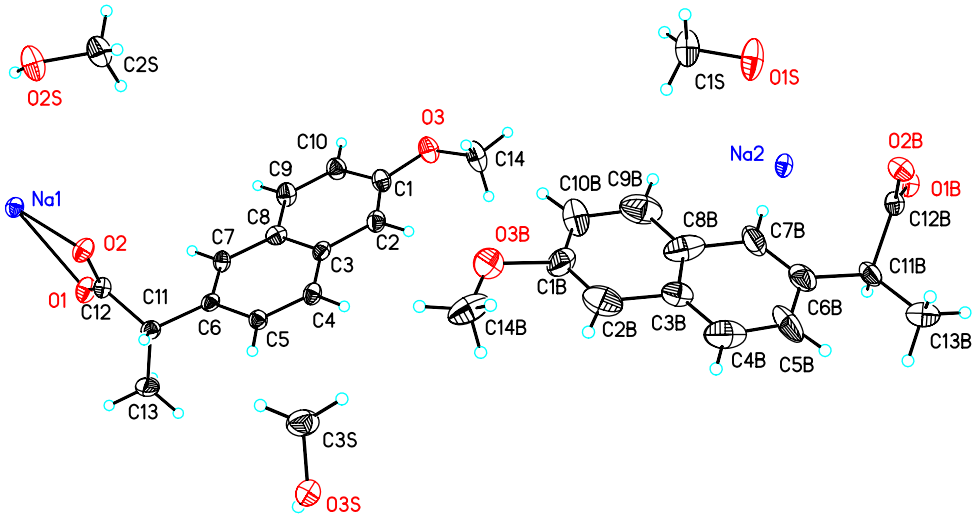

Figure 7.2. A perspective drawing of methanol solvated sodium naproxen with 3 methanol molecules (1S, 2S, and 3S) and two sodium naproxen molecules (- and B).

7.3.1 Single Crystal Analysis

There was some disorder in the second molecule (B) as evidenced by the enlarged thermal ellipsoids shown in Figure 7.2. The crystal structure provided no obvious explanation for this.

There were three single bonds in each of the two sodium naproxen molecules present in the methanol solvated form of sodium naproxen, C1-O3, C6-C11, and C11-C12 in the first molecule and C1B-O3B, C6B-C11B, and C11B-C12B for the second molecule. Newman projections around these three bonds are shown in Figure 7.3. Little differences were seen along the C1-O3 bonds between the two molecules, but large differences were apparent along the other bonds between the respective pairs of molecules. Significant differences between the torsion angles C7-C6-C11-C12 (-29.5(6)°) and C7B-C6B-C11B-C12-B (172.7(6)°) were seen as shown in Figure 7.3 (c) and Figure 7.3 (d), respectively. The same was true for the torsion angles C13-C11-C12-O1 (-30.5(7)°) and C13B-C11B-C12B-O1B (112.2(6)°), which can be seen in Figure 7.3 (e) and Figure 7.3 (f),respectively. The differences in the torsions angles were most likely due to the interactions between the carboxyl oxygen and sodium, which interactied with the oxygen on the methanol group.

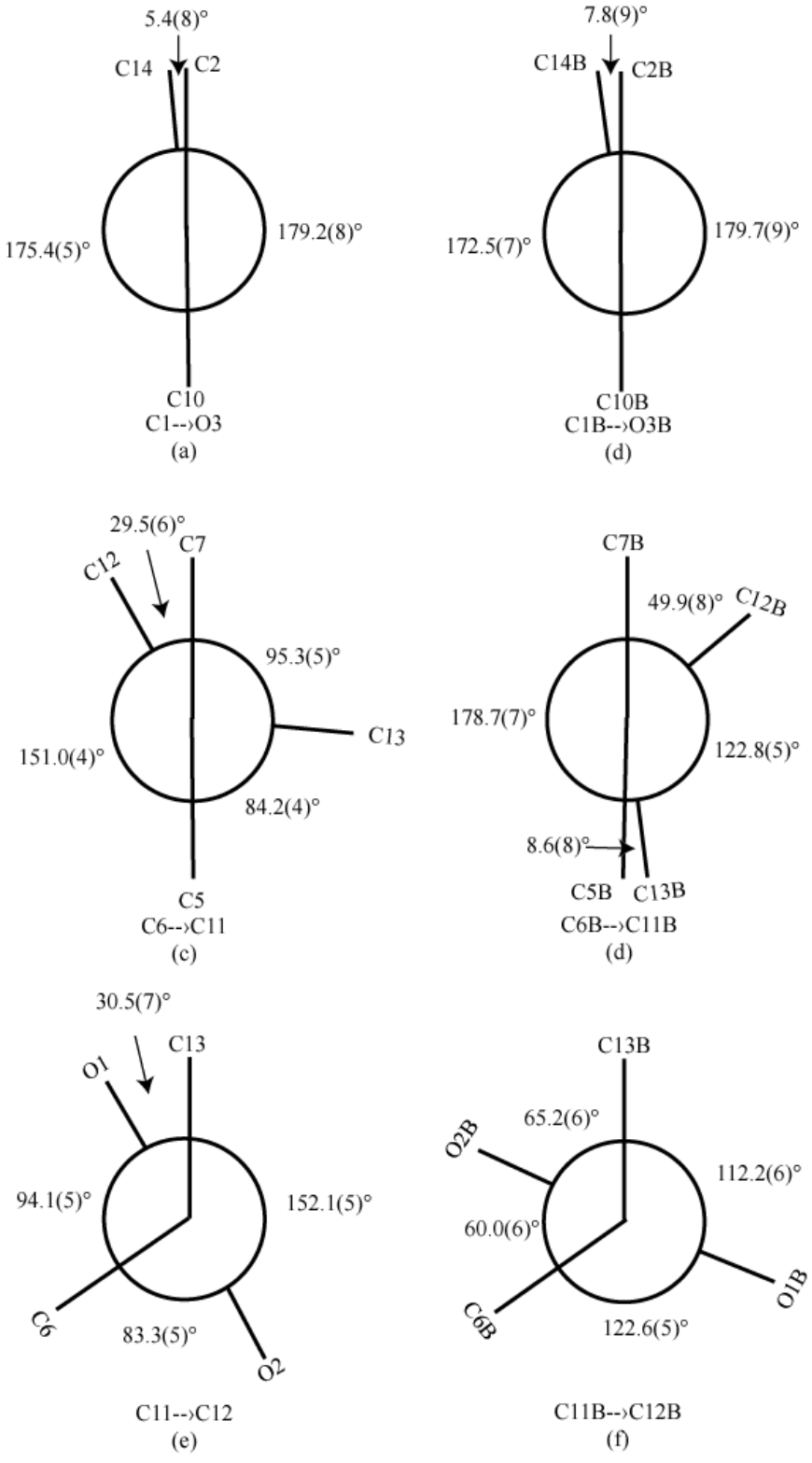

Figure 7.3. Newman projections of methanol solvated sodium naproxen along the bond of (a) C1-C11, (b) C1B-C11B, (c)C6-C11, (d)C6B-C11B, (e) C11-C12, and (f) C11B-C12B.

The methoxy groups in each of the molecules was essentially coplanar with the naphthyl ring which gave rise to a narrowing of the O3-C1-C10 and O3B-C1B-C10B, angles and an enlargement of the C2-C1-O3 and C2B-C1B-O3B angles. Domaino et al. (1979) previously reported a similar effect and attributed it to some degree of conjugation between the oxygen in the methoxy group and the benzene ring, which also gave rise to shortening of the C-O bond.

Table 7.1. Selected geometric angles for methanol solvate of sodium naproxen.

Atoms	Angle (°)
O3-C1-C10	114.9(4)
C2-C1-O3	125.0(4)
O3B-C1B-C10B	110.7(5)
C2B-C1B-O3B	121.7(7)

The molecular geometry of the methanol solvate of sodium naproxen can be compared to that of both the anhydrous material (Kim et al., 2004) and the monohydrate material (Kim et al., 1990). The bond lengths and angles of the methoxy group of the methanol solvated form were similar to those in the monohydrate and anhydrate form. But when looking at the torsion angles, there were small differences. Surprisingly, the torsion angle for the methoxy group in the solvated species (C2-O3-C1-C14 = -5.4(8)°, C2B-O3B-C1B-C14B = -7.8(9)°) was similar to that of the anhydrous material (-7.4(5)° and -5.2(5)°) and slightly larger than that of the monohydrate material (-4.1°).

The anhydrous, monohydrated, and methanol solvated salts crystallized in space group $P2_1$. In order to compare to the crystal volumes, the volume of the monohydrate was doubled since $Z' = 2$ for this material, while $Z' = 4$ for the anhydrous material and the

methanol solvated material. The unit volume of the methanol solvated salt was 28.1% larger than the anhydrate material, and 15.8% larger than double the unit volume of the monohydrate material. Changes in packing and crystal volume, from the methanol solvate to the anhydrous form, are attributed to the removal of the solvent from the crystal structure and the subsequent rearrangement to form sodium coordination. The increased size of the methanol solvate compared to the monohydrate was attributed to the size difference of the solvent molecules, methanol versus water.

Three-dimensional packing diagrams along the three axes of the crystal structure are shown in Figure 7.4. Hydrogen bonding is shown in dotted red lines in Figure 7.4. It was these hydrogen bonds that provide stability for the solvated crystal, just as they were the dominating force for stability in the monohydrated crystal. Additionally, the oxygen atoms from the methanol solvent in the crystal structures coordinated around the sodium ions of the sodium naproxen. The sodium atom from the first sodium naproxen molecule coordinated with seven oxygen atoms either from the carboxyl groups or from the solvent; O1, O2, two $O1B^{i,\ ii}$, $O2B^{ii}$, $O2S^{iii}$, and $O3S^{iv}$. The second sodium atom coordinated with only six oxygen atoms; $O1^{v}$, $O1B^{vi}$, $O2B^{iii}$, $O1S^{iii}$, $O2S^{i}$ and $O3S^{vii}$. These coordinations are presented in an enlarged view of the packing diagram shown in Figure 7.5. These interactions were compared to similar Na-O interactions presents in the anhydrous and monohydrate from of sodium naproxen in Table 7.2. This coordination was similar to the coordination seen in monohydrates sodium naproxen as shown by Kim et al. (2004) with an additional coordination on the first sodium atom.

Symmetry codes: (i) -x+1, y+1, z-1, (ii) x-1, y-1, z+1, (iii) x, y-1, z, (iv) x-1, y-1, z, (v) –x+1, y+1/2, -z+1, (vi) –x+2, y-1/2, -z, (vii) x, y-1, z-1

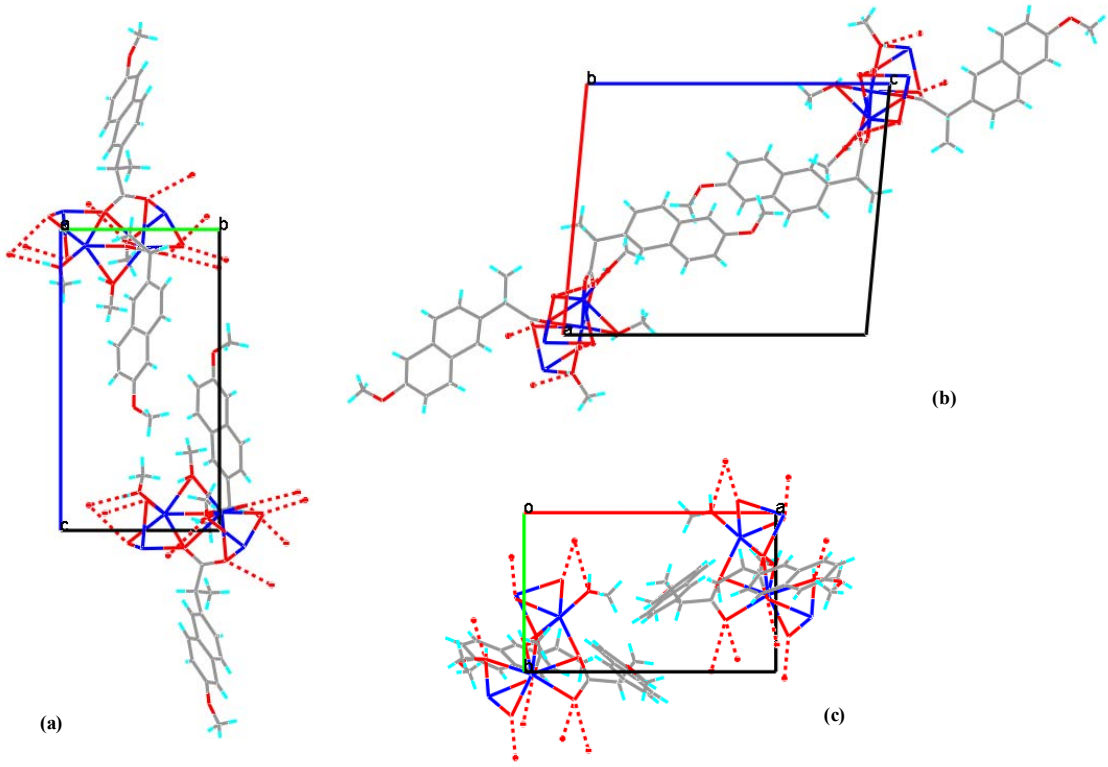

Figure 7.4. Packing diagrams along (a) the a-axis, (b) the b-axis, and (c) the c-axis of the methanol solvate of sodium naproxen. Sodium atoms are depicted in blue, oxygen atoms in red, carbon atoms in gray, and hydrogen atoms in light blue.

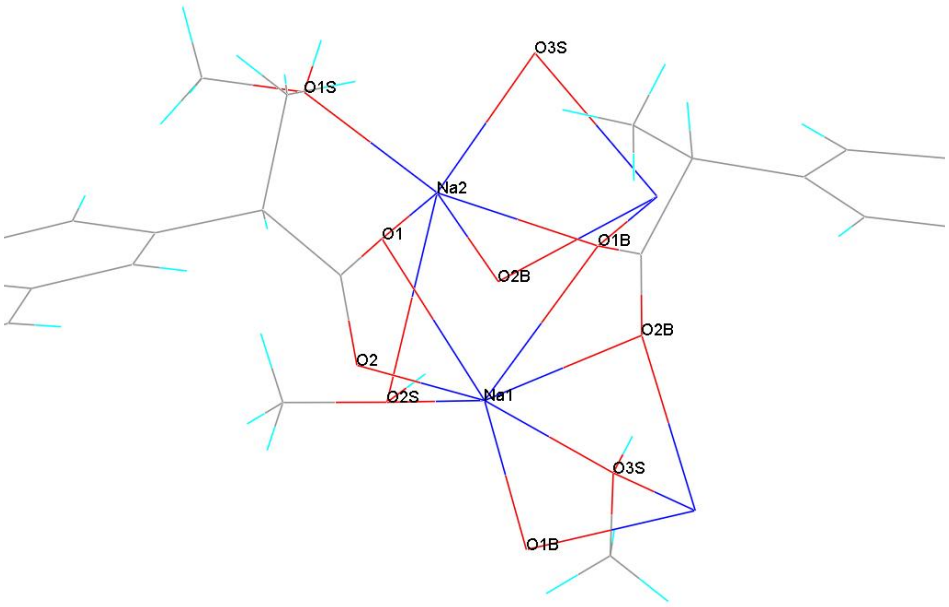

Figure 7.5. Enlarged figure showing sodium coordination in methanol solvate.

Table 7.2. Comparison of distances between Na and O by Na-O interactions of anhydrous (Kim et al., 2004), monohydrate (Kim et al., 1990) and methanol solvate of sodium naproxen.

Pseudopolymorphs	Anhydrate		Monohydrate	Methanol Solvate	
	1[a]	2[a]		1[a]	2[a]
Distance	2.259(2)	2.276(2)	2.272[b]	2.346(3)[b]	2.237(4)[b]
	2.279(2)	2.291(2)	2.328[b]	2.471(4)[b]	2.371(4)[b]
	2.290(2)	2.328(2)	2.375[b]	2.544(4)[b]	2.460(4)[b]
	2.394(2)	2.341(2)	2.690[b]	2.562(4)[b]	2.302(4)[c]
				2.606(4)[b]	
			2.273[c]	2.371(4)[c]	2.394(4)[c]
			3.210[c]	2.496(4)[c]	2.842(5)[c]

[a]The anhydrate and methanol solvate have two independent sodium atoms in each unit cell.
[b]Bond Distances are between a sodium cation and oxygen atoms in three different carboxyl groups.
[c]Bond distances are between a sodium cation and the oxygen in the solvent.

Table 7.3 shows a summary of the crystallographic data and structure refinements for the methanol solvate of sodium naproxen.

7.3.2 Comparison of Crystals made by Cooling versus Slow Evaporation

Analysis of the single crystal prepared by slow evaporation illustrated a 2:3 sodium naproxen to methanol ratio, or a 1.5 solvate, while that of the powder samples, prepared by slow cooling crystallization, had a 1:1 ratio of sodium naproxen to methanol under TGA analysis. In order to determine if the crystals were distinct, a powder x-ray diffraction pattern was simulated from the single crystal data, and measured from crystals prepared through slow evaporation Figure 7.6 shows the simulated PXRD pattern compared to the PXRD pattern from the crystals prepared according to chapter 6 and those seen in the solubility experiments, as well as a PXRD pattern of crystals prepared by slow evaporation and then ground into a fine powder. The two measured patterns, Figure 7.6 (b) and (c), which are shown as mirror-images for comparison reasons, appeared to be similar, with only small differences in peaks and peak intensities, which were most likely due to differences in packing of the samples. The samples were top-packed and were prepared by different users. Additionally needle-like crystals, like the ones studied here, had some affinity for alignment, which could have distorted PXRD patterns which assume a random orientation of crystals. The simulated single crystal PXRD (Figure 7.6 (a)) indicated peaks around a Bragg's angle of 14° which were not apparent in the PXRD taken from the other samples. This indicated that a significant amount of the 2:3 ratio solvate was not present in the powder sample. Additionally, the absence of peaks around 22° for the simulated pattern, indicate that the two samples were distinct.

Table 7.3. Crystal data and structure refinements.

Empirical Formula	$C_{15.5}H_{19}NaO_{4.5}$
Formula Weight	300.30
Temperature	173(2) K
Wavelength	1.54178 Å
Crystal System	Monoclinic
Space Group	P2(1)
Unit Cell Dimensions	a = 12.7203(3) Å b = 7.9897(2) Å c = 15.2523(4) Å α = 90° β = 95.3740(10)° γ = 90°
Volume	1543.30(7) $Å^3$
Z'	4
Density (calculated)	1.292 $Mg.m^3$
Absorption Coefficient	1.014 mm^{-1}
F(000)	636
Crystal Size	0.22 x 0.21 x 0.16 mm^3
θ Range for Data Collection	2.91 to 66.64°
Index Range	-14 <=h<=15, -9<=k<=8, -16<=l<=16
Reflections Collected	11006
Independent Reflections	4203 [R(int) = 0.0223]
Completemess to θ = 66.64°	88.1%
Absorption Correction	Semi-Empirical from Equivalents
Max. And Min. Transmissions	0.8545 and 0.8076
Refinement Method	Full-Matrix Least-Squares on F^2
Data/Restraint/Parameters	4203/26/386
Goodness-of-Fit- on F^2	1.047
Final R Indices [I>2σ(I)]	R1 = 0.0627, wR2 = 0.1687
R Indices (All Data)	R1 = 0.0661, wR2 = 0.1731
Absolute Structure Parameters	0.19(12)
Largest Diff. Peak and Hole	0.843 and -0.399 $eÅ^{-3}$

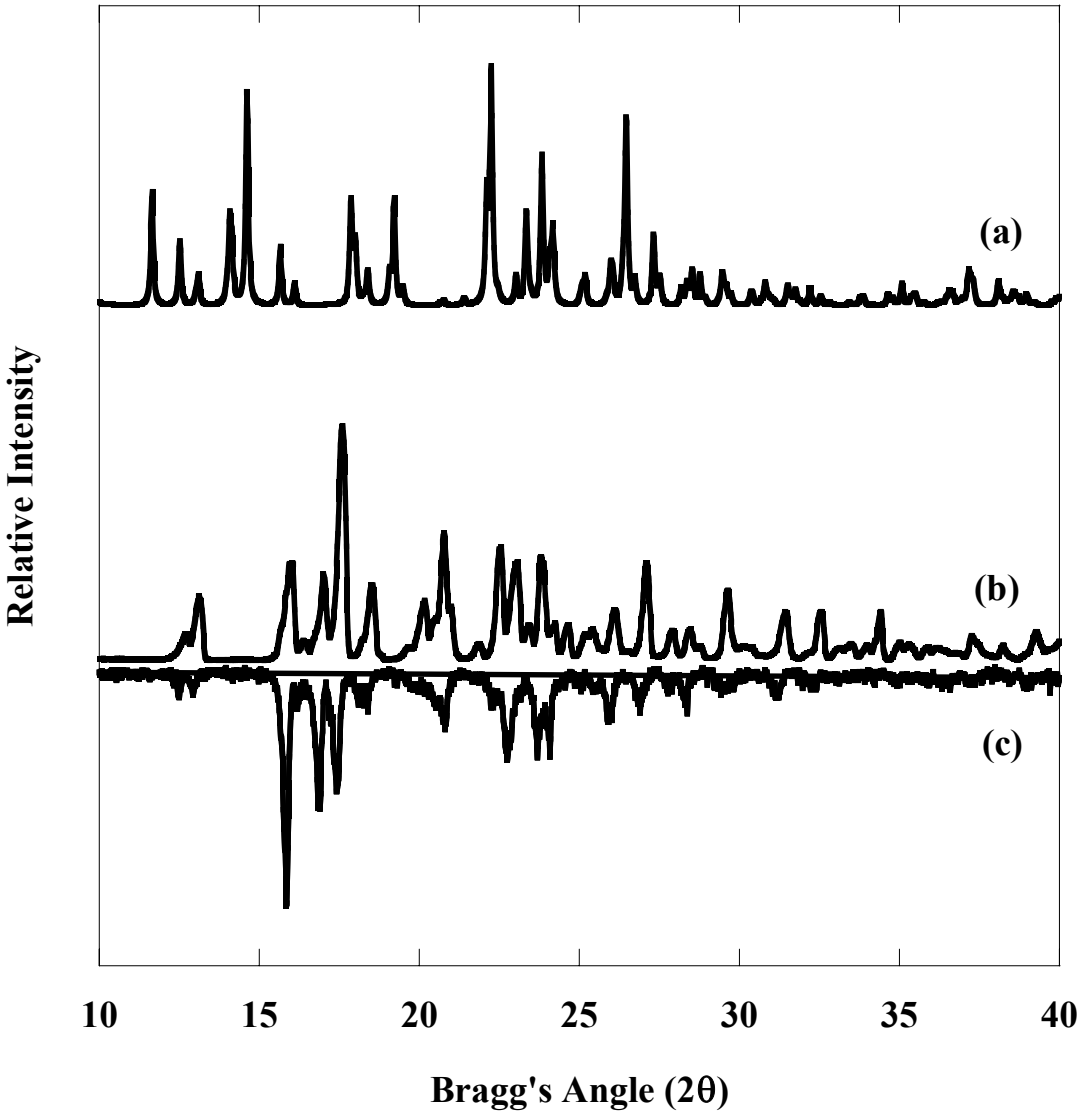

Figure 7.6. (a) Simulated PXRD pattern from single crystal with 2:3 ratio of sodium naproxen to methanol, (b) measured PXRD pattern of 1:1 sodium naproxen to methanol from cooling crystallization, (c) measured PXRD pattern from slow evaporation crystallization .

Based on this analysis, it was assumed that the 1.5 solvate, as measured by single crystal x-ray diffraction, was not a true representation of the sample. Selection of the crystal was not based on how well it represented the overall sample, but on how well a single crystal XRD pattern can be obtained. It was possible that the crystal selected was merely one of a few present in the sample which contained a majority of $C_{14}H_{13}NaO_3$-$\cdot CH_3OH$ solvates.

Although the crystals were different, analysis of the $C_{14}H_{13}NaO_3 \cdot 1.5CH_3OH$ single crystal structure and packing arrangement can give insight to how methanol molecules are arranged and bonded in the $C_{14}H_{13}NaO_3 \cdot CH_3OH$ molecule. Similar hydrogen bonding and Na-O coordination would be expected in the 1:1 ratio methanol solvate compared to those present in the 2:3 ratio methanol solvate. Comparisons can also be made to known structures of anhydrous sodium naproxen and monohydrated sodium naproxen. For example the 1:1 methanol solvate would be expected to have a larger unit volume than the monohydrate due to the size of the methanol solvent.

7.4 Conclusions

A single crystal of a methanol solvate of sodium naproxen was characterized using x-ray diffraction. This solvate had a chemical formula of $C_{14}H_{13}NaO_3 \cdot 1.5CH_3OH$, which was not the expected 1:1 ratio of sodium naproxen to methanol as indicted by previous results from slow cooling crystallization. Although different from the expected crystal, the structure of the 1.5 solvate gave insight into bonding and coordination in a possible $C_{14}H_{13}NaO_3 \cdot CH_3OH$ solvate. The 1.5 solvate showed similar hydrogen boding and Na-O coordination to the monohydrate species, with hydrogen bonding being the

dominate force in solvate formation. An increase in unit volume was also observed most likely due to the inclusion of a larger number of solvent molecules in the crystal structure.

7.5 Acknowledgments

The author would like to acknowledge Dr. Kenneth Hardcastle with the Chemistry Department at Emory University for performing the single-crystal x-ray diffraction.

CHAPTER 8

ORGANIC ALCOHOL SOLVATES OF SODIUM NAPROXEN

Growing organic crystals from solution can allow incorporation of the solvent into the crystal lattice. Inclusion of this solvent has three functions: (1) participating in hydrogen-bonding networks, (2) filling space in the unit cell, with no strong interactions between solute and solvent molecules, and (3) facilitating closest packing arrangements. (Görbitz and Hersleth, 2000; Myrdal and Jozwiakowski, 2000). Whether a solvent exhibits one or all of these functions, its incorporation into the crystal structure is important for determining the physical properties of the solvate.

Identification of structures with organic solvent molecules incorporated in the crystal lattice is steadily increasing. A search of the Cambridge Structural Database in November 2006 revealed that there are 85,316 compounds that are known to form solvates (including hydrates) with the 51 most common solvents, (van de Streek, 2007). Clearly it is important to consider the possibilities of solvent inclusion in crystallization experiments. Additionally, for many compounds the presence of solvents is needed for successful crystallization outcomes. For example, structures with cavities or empty channels are generally unstable and occasionally crystals may not be obtained if the structure of solute molecules is not supported by carefully selected solvent molecules (Kitaigorodski, 1961).

Previous studies of sodium naproxen have focused on hydrate formations and the solid-state transformations associated with them, but none have looked at the ability to

form alcohol solvates (DiMartino et al., 2007; DiMartino et al., 2001; Kim and Rousseau, 2004; Kim et al., 1990). In this chapter, the role of organic alcohol solvents and their ability to form solvates with sodium naproxen under batch cooling crystallization was examined. The study analyzed these novel organic alcohol solvates of sodium naproxen using thermogravimetric analysis, differential scanning calorimetry, polarized light microscopy, ^{1}H-nuclear magnetic resonance, and powder X-ray diffraction for characterization. Moving beyond the fact that these solvates exist, the work provided insight to the role size and shape of alcohol molecules play in the ability of sodium naproxen to solvate.

8.1 Experimental Section

8.1.1 Materials

Sodium naproxen was provided by Albemarle Corp., and was used without further processing or purification. The following alcohols were purchased from VWR Inc.: low-water 2-propanol, ACS Grade 99.5% 1-propanol, 99.4% min. 1-butanol, and HPLC grade isobutanol. Each alcohol was dried overnight using 3Å molecular sieves to remove water. The solvated crystals were produced through batch cooling crystallization; approximately 5 g of sodium naproxen was dissolved in approximately 15 g of alcohol at 10°C in an equilibrium cell. Approximately 2 g of sodium naproxen was added until a slurry solution was achieved and sodium naproxen no longer dissolved. The solution was then heated until all the crystals dissolved as determined by visible inspection. The solution was then cooled to 10°C, at an approximate rate of 0.6°C per minute, for the crystallization of solvated sodium naproxen species to occur. After

allowing the solution to reach equilibrium, as described in Chapter 3, the slurry mixture was vacuum filtered and the resulting crystals used for analysis.

8.1.2 Thermogravimetric Analysis (TGA)

Mass loss of the sodium naproxen samples was measured using a TG/DTA 320 instrument manufactured by Seiko Instrument Inc. Crystal samples of 10 to 15 mg were heated from 22°C to 130°C in aluminum pans that were 5 mm in diameter. A ramping rate of 10°C/min was used with a nitrogen purge rate of 90 mL/min. As recommended by Di Martino et al, all TGA runs were carried out with open pans (2001).

8.1.3 Differential Scanning Calorimetry (DSC)

Desolvation endotherms were measured using a DSC 220C instrument (Seiko Instrument Inc.) The temperature range of the experiments was 22 to 290°C with a heating rate of 10°C/min and a nitrogen purge rate of 90 mL/min. Crystal samples of 10 to 15 mg were placed in open aluminum pans with a diameter of 7 mm. The use of open aluminum pans was necessary to obtain quantitative evaluations of the desolvation energy (DiMartino et al., 2001).

8.1.4 Polarized Light Microscopy (PLM)

Analysis of crystal samples was performed under a Leica DM LM microscope equipped with a Sony DKS-5000 digital camera and an objective lens of 20X. The microscope was equipped with a Sony DKC-5000 digital camera that converted the focused light into a digital signal, which was then visualized by Image-Pro Plus version 4.5.

8.1.5 Nuclear Magnetic Resonance (NMR)

To determine the solvent in the crystal structures, crystal samples were dissolved in deuterated water and the solution samples were analyzed using ^{1}H-NMR at 400 MHz and room temperature. A Varian Mercury Vx 400 with a 5 mm broadband probe head with ^{1}H decoupling was used to obtain the NMR analysis with an acquisition time of 2 seconds and a total run time of 50 seconds.

8.1.6 Powder X-ray Diffraction (PXRD)

Crystals of the solvated sodium naproxen were analyzed using PXRD analysis. A PANanlystical X-Pert Pro Alpha-1 diffractometer with copper Kα1 radiation was used in conjunction with the X'Celerator detector. Crystal samples were gently ground to a fine powder prior to analysis. The PXRD pattern was made over a diffraction-angle (2θ) range of 10° to 80°, with a step size of 0.02° and a counting time of 1 second per step.

8.2 Results and Discussion

8.2.1 Thermal Analysis

An example of a typical TGA and DSC for 2-propanol solvate is shown in Figure 8.1. This figure is representative of TGA and DSC thermograms for all of the alcohol solvates with changes only seen in the final % mass. Mass loss prior to the melting point of sodium naproxen (250°C) was assumed to be a result of desolvation; i.e. removal of the solvent from the crystal.

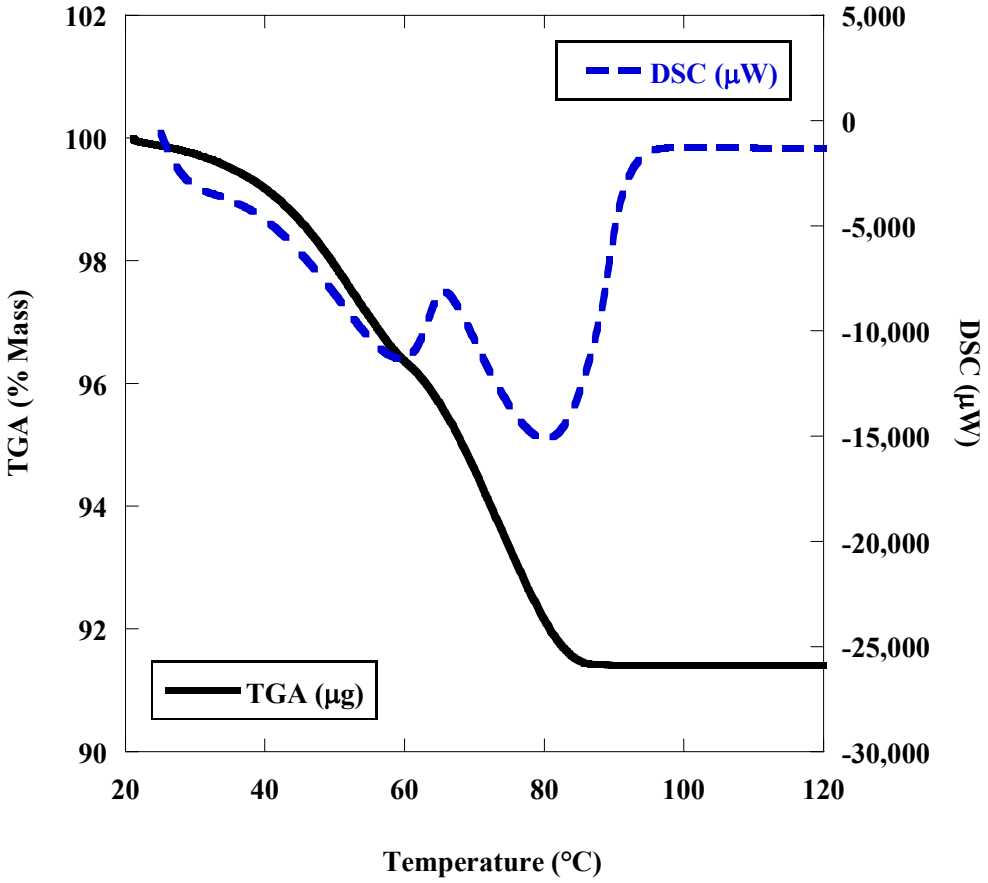

Figure 8.1. Representation of TGA and DSC traces of alcohol solvates.

Based on complete solvent removal mass loss, and the molecular weight of the alcohol, a molar ratio of alcohol to sodium naproxen can be determined as follows:

$$\% \text{ Mass Loss} = \frac{\text{Molar Ratio} * \text{Alcohol MW}}{\text{Molar Ratio} * \text{Alcohol MW} + \text{Sodium Naproxen MW}} \quad (8\text{-}1)$$

Table 8.1 shows the percent mass loss (± one standard deviation, based on 3-4 independent experiments) and equivalent molar ratio of alcohol to one mole of sodium naproxen for each of the alcohol solvents as determined by the TGA:

Table 8.1. TGA mass loss of alcohol solvates.

Alcohol	Ethanol	1-Propanol	2-Propanol	1-Butanol	Isobutanol
% Mass Loss	13.5 ± 0.4	10.4 ± 2	9.0 ± 0.8	9.5 ± 0.7	7.3 ± 0.7
Molar Ratio	0.86	0.49	0.42	0.36	0.27

These percent mass losses may seem small but when compared to mass loss for an anhydrated form of sodium naproxen prepared from similar methods, which had less than about a 1% mass loss, these amounts were statistically significant based on standard deviations. These results clearly showed that each of the solvents has been incorporated into sodium naproxen crystals.

As the size of the alcohol increased, the amount of alcohol present in the crystal structure, as represented by the TGA data, decreased on a molar basis. Additionally, the

branched alcohols were present in the crystal at smaller molar amounts than the unbranched alcohols. Using the compounds' densities and molecular weights, their molar densities can be calculated and are listed in Table 8.2.

Table 8.2. Molar Densities of Alcohols.

Alcohol	Ethanol	1-Propanol	2-Propanol	1-Butanol	Isobutanol
Molar Density (mole/L)	17.1	13.4	13.1	10.9	10.8

The molar densities followed the same pattern as the molar amount of alcohol present in the solvate structure. Since molar densities also take into account the structure of the molecule, these results indicated that both the length of the carbon chain present in the alcohol and the branching of the alcohol affected its ability to solvate with sodium naproxen. Bulkier alcohol molecules would have more difficulty in creating the hydrogen bonds necessary to form solvates with sodium naproxen. Since hydrogen bonding has been shown to be the predominate attraction in the hydrates (Kim et al., 2004) and methanol solvate of sodium naproxen, bulkier molecules would be limited in their ability to form similar solvates. Hence the pattern of decreased alcohol present in the solvates as the length of the hydrocarbon chain and branching increases.

DSC data were used to show how strongly each solvent is bound in the crystal structure and to show that such solvents were not merely on the surface of the crystals. Table 8.3 shows the average endotherm values for each of the alcohol solvates during the desolvation step.

Table 8.3. DSC desolvation energies (± one standard deviation) of alcohol solvates.

Alcohol	Ethanol	1-Propanol	2-Propanol	1-Butanol	Isobutanol
Desolvation Energy (J/g solvated sodium naproxen)	217 ± 17	210 ± 29	195 ± 22	238 ± 5	208 ± 19
Desolvation Energy (J/g anhydrous sodium naproxen	251	234	214	263	224

In order to compare the values across alcohol solvates, the desolvation energies were converted to J/g of anhydrous sodium naproxen using the molar ratios determined by the TGA and are also listed in the table.

In addition, desolvation values were also be converted to J/ g alcohol in the solvate and compared to the latent heat of vaporization of the alcohol at a particular temperature. Table 8.4 shows the converted values compared to the latent heat of vaporization at 65°C (Yaws, 2003). This temperature was chosen since it falls approximately in the center of the range of temperatures where desolvation occurs.

Table 8.4. Comparison of desolvation energies and latent heats of vaporization.

Alcohol	Ethanol	1-Propanol	2-Propanol	1-Butanol	Isobutanol
Desolvation Energy (kJ/mole alcohol)	74	121	130	186	211
Heat of Vaporization at 65°C (kJ/mole alcohol)	39.64	44.82	46.40	47.07	49.67
Desolvation Energy – Heat of Vaporization (kJ/mole alcohol)	35	77	84	139	162

The heat of desolvation was greater than the latent heat of vaporization indicating that the alcohol was not merely on the surface of the crystal and evaporating. Additionally, the difference in desolvation energy and heat of vaporization followed the reverse pattern to the TGA data presented earlier. As the number of carbons in the organic alcohol increased and the amount of branching increased, the energy required to remove the solvent from the crystal structure also increased.

Hydrates have been classified in three ways (Kim and Rousseau, 2004): (1) isolated-site hydrates, which show sharp narrow TGA mass losses and DSC endotherms upon dehydration, (2) ion-associated hydrates, which display strong metal-water interactions and higher dehydration temperatures and molar heats of dehydration, and (3) channel hydrates, which have early onset temperatures of dehydration and broader TGA and DSC traces. Both monohydrated (Kim and Rousseau, 2004) and dihydrated (Kim et al., 1990) sodium naproxen have been shown to lose water by diffusion through channels in the crystal. Figure 8.1 indicates the solvated forms were channel solvates due to both the early onset of desolvation with temperature and the broader TGA and DSC traces.

The channels would make it more difficult for larger or branched species to incorporate into the crystal structure, since larger channels are needed and could cause instability. This explains why as the size of the alcohol increased, the amount of alcohol in the solvate decreased. Additionally, since less alcohol was present the ratio of oxygen from the alcohol to sodium from the sodium naproxen was smaller, meaning the Na-O coordination would be stronger. For every oxygen molecule present in the solvate there were more sodium molecules available for coordination/bonding. This would make the

bonds stronger. These stronger bonds clearly illustrate why there was an increase in the energy necessary to remove the solvent from the solvated species per mole of alcohol.

8.2.2 Crystal Shapes

Figure 8.2 shows photomicrographs which were taken of each of the solvated crystals of sodium naproxen. The solvated crystals of propanol and butanol solvents had a needle-like shape similar to that of the anhydrated species, while the ethanol solvated species was larger and seemed to have a plate-like shape. The edges of the ethanol crystals were not sharp most likely due to their instability (they began to dissolve into solution as the photomicrographs are being taken). A similar shape was seen with the methanol solvated form of sodium naproxen (Chavez and Rousseau, 2008).

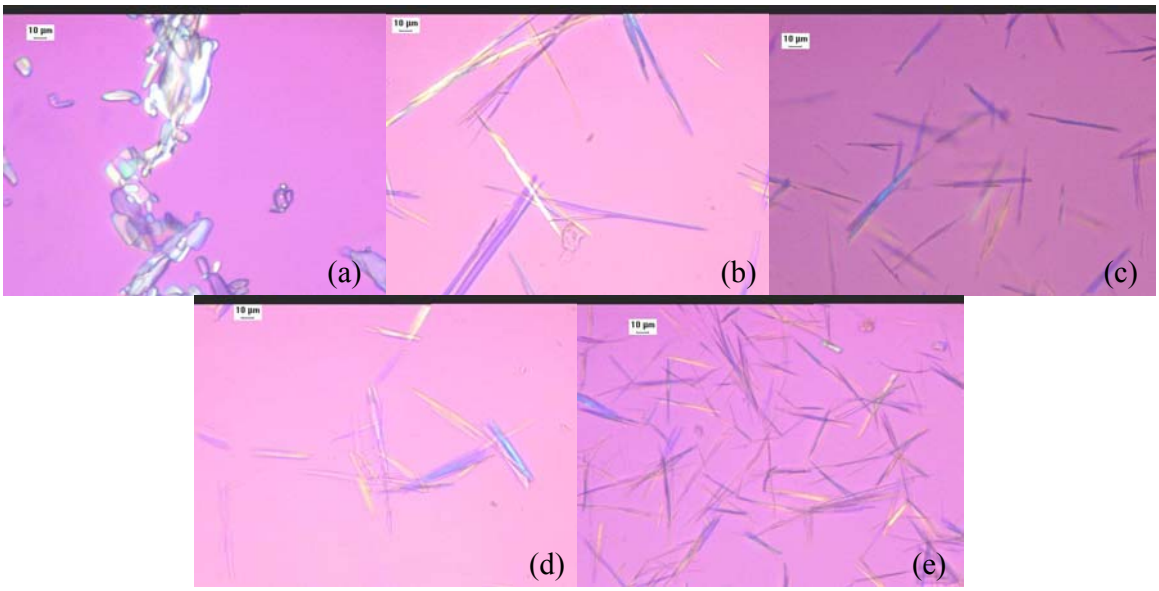

Figure 8.2.. Photomicrographs of (a) ethanol, (b) propanol, (c) 2-propanol, (d) butanol, and (e) isobutanol solvated crystals of sodium naproxen.

According to the photomicrographs, the overall crystal shape was not affected when larger solvent molecules were used for cooling crystallization possibly due to the fact that a significant amount of the alcohol solvent was not present in the crystal structure. But when smaller molecules were used there was a significant effect on the overall crystal shape observed using photomicroscopy.

8.2.3 Nuclear Magnetic Resonance

^{1}H-NMR was used to show if the solvent present in the crystals was indeed the alcohol. This method was used previously with the methanol solvated form of sodium naproxen (Chavez and Rousseau, 2008) and an additional methanol peak was seen along with the peaks associated with sodium naproxen. But for the current alcohol solvates being explored there was no presence of additional peaks corresponding to the alcohol solvent, as seen in Figure 8.3-Figure 8.8. This is most likely due to the concentration of the alcohols present in the solution. Ideally for NMR spectroscopy a solution of a concentration range between 5-10 mg/mL is needed. (Jacobsen, 2007) Due to the low solubility of the solvated forms in D_2O and the small of amount of alcohol present in the crystal as shown through TGA data, there was not enough alcohol present in the ^{1}H-NMR sample to be properly detected. Interesting to note though was the apparent slight rearrangement of some the peaks compared to the ^{1}H-NMR spectrum of anhydrous sodium naproxen. This would indicate slight variations in the chemical environments between the anhydrated form of sodium naproxen and the solvated forms studied here, showing the alcohol does have some effect on the final crystal produced via cooling crystallization.

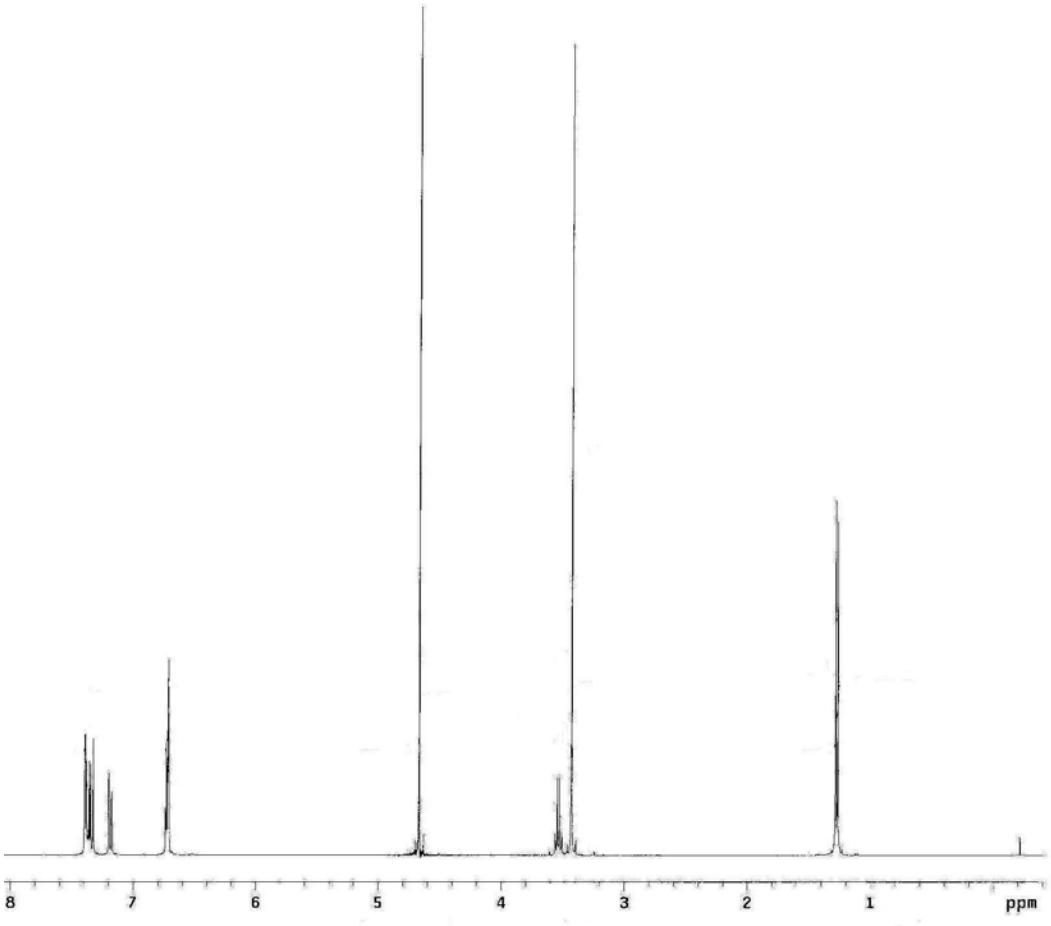

Figure 8.3. ^{1}H-NMR for anhydrous sodium naproxen.

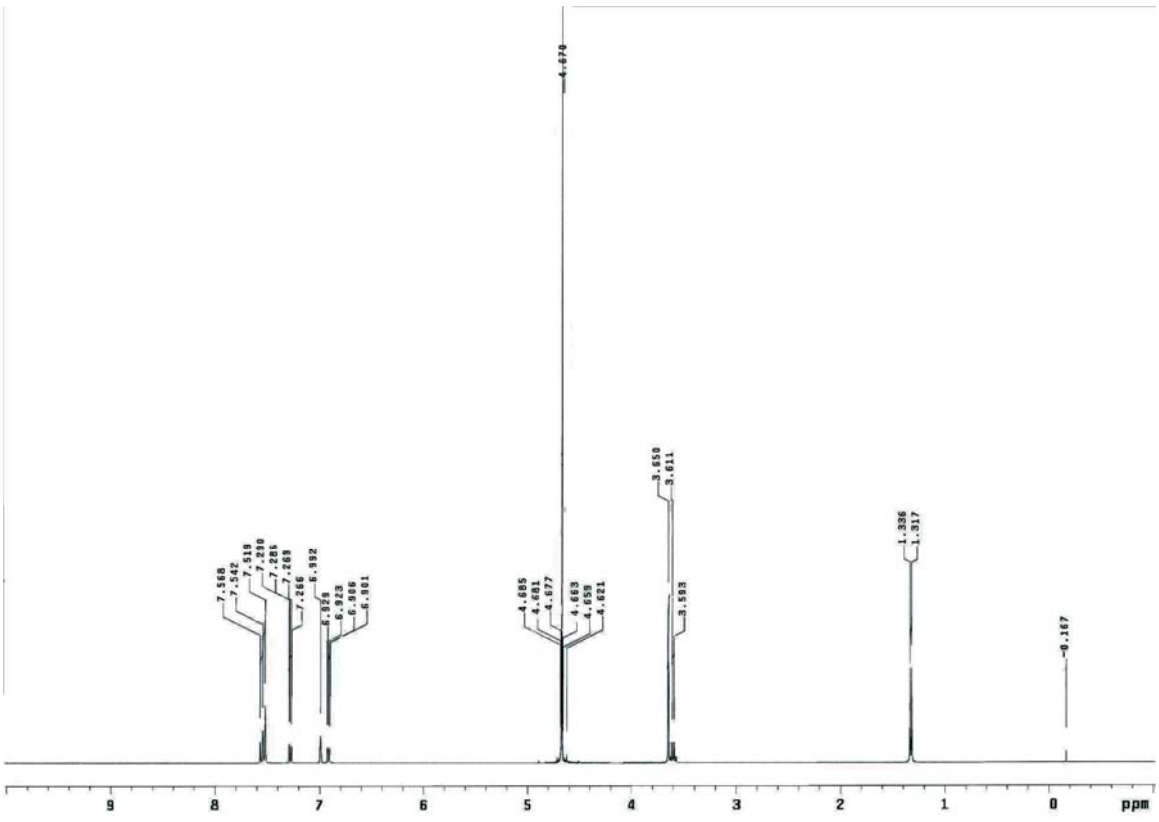

Figure 8.4. ^{1}H-NMR spectrum for ethanol solvate of sodium naproxen.

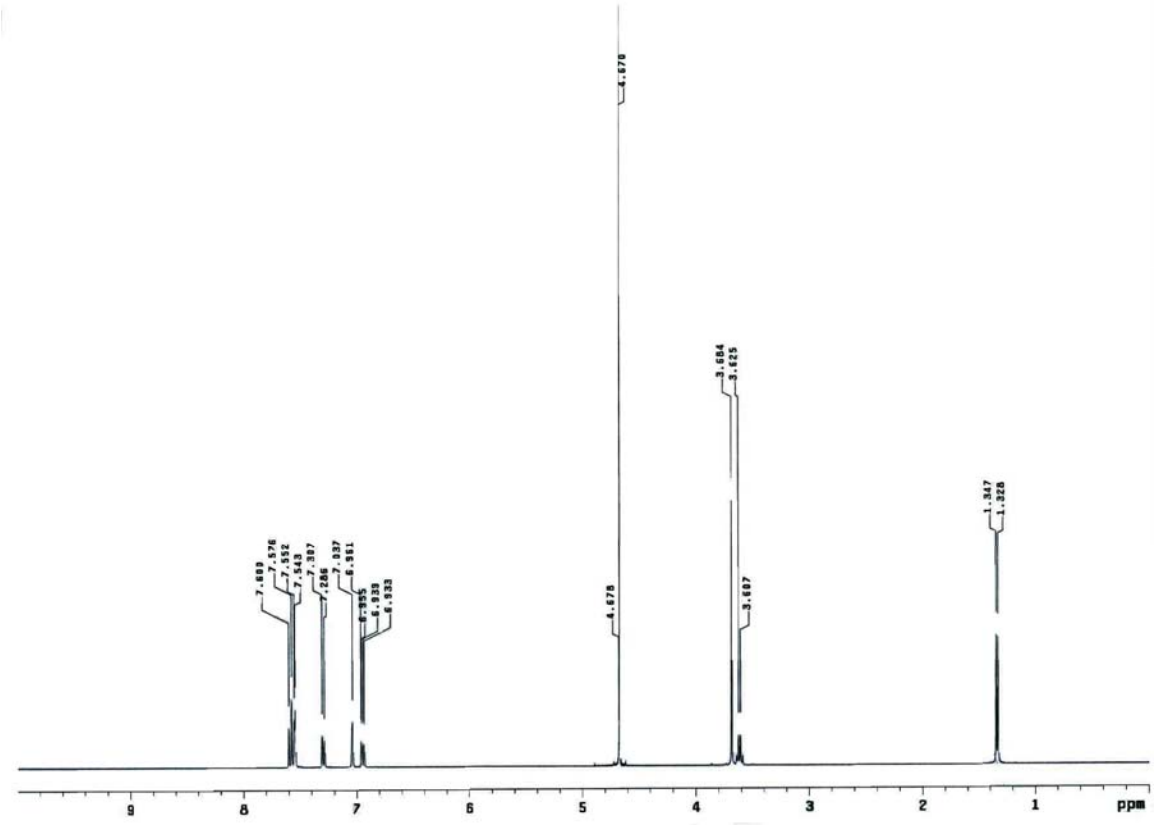

Figure 8.5. [1]H-NMR spectrum for 1-propanol solvate of sodium naproxen.

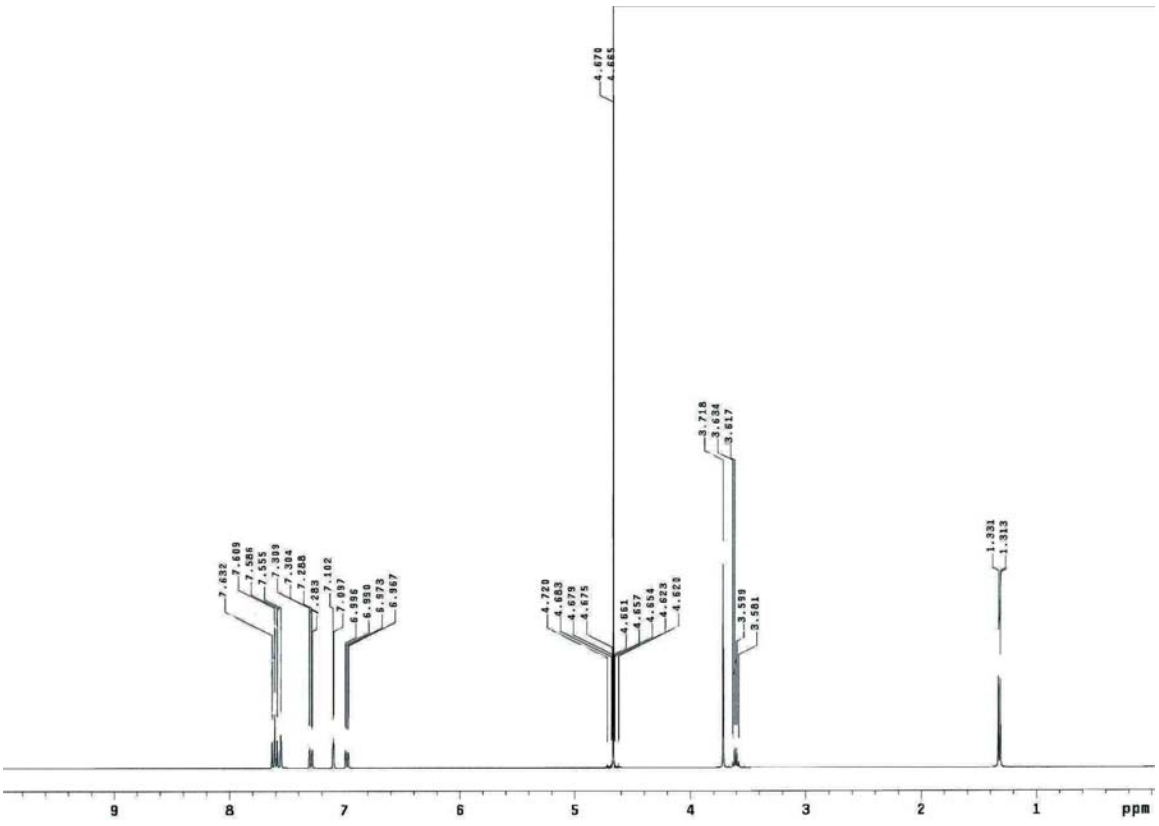

Figure 8.6. ^{1}H-NMR spectrum for 2-propanol solvate of sodium naproxen.

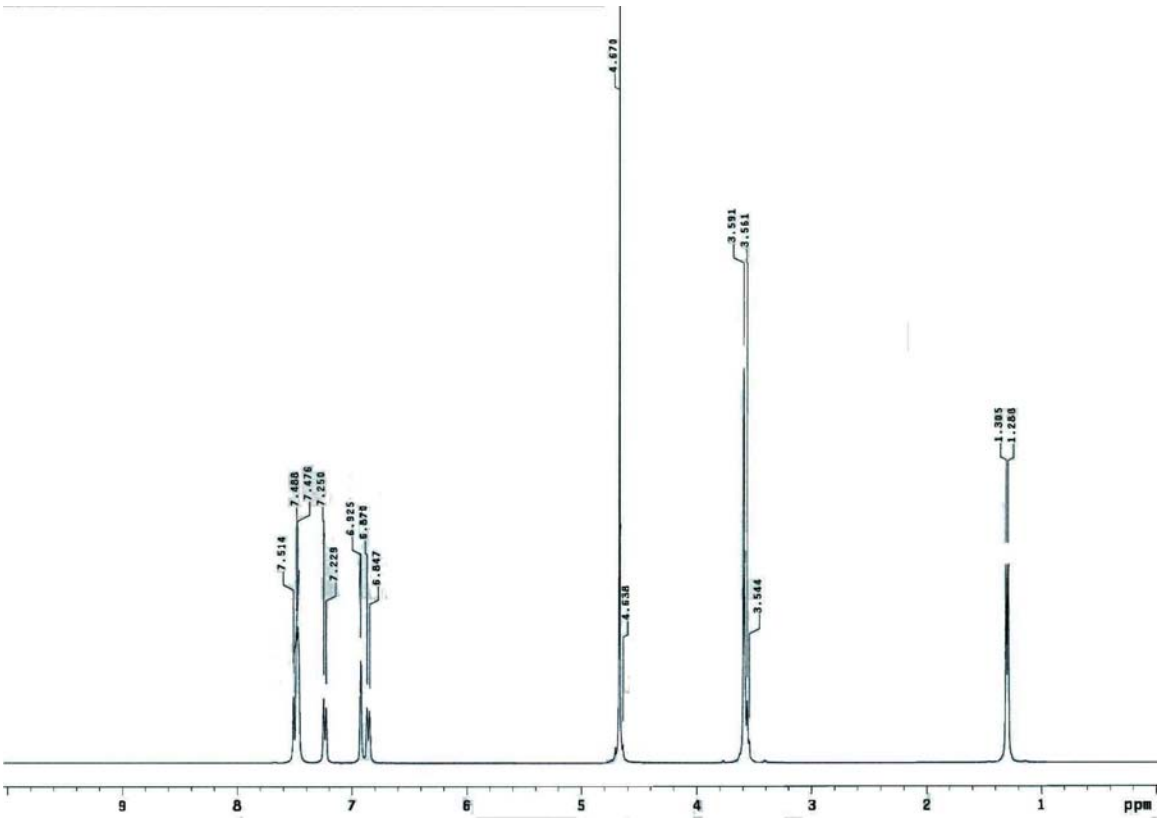

Figure 8.7. ^{1}H-NMR spectrum for 1-butanol solvate of sodium naproxen.

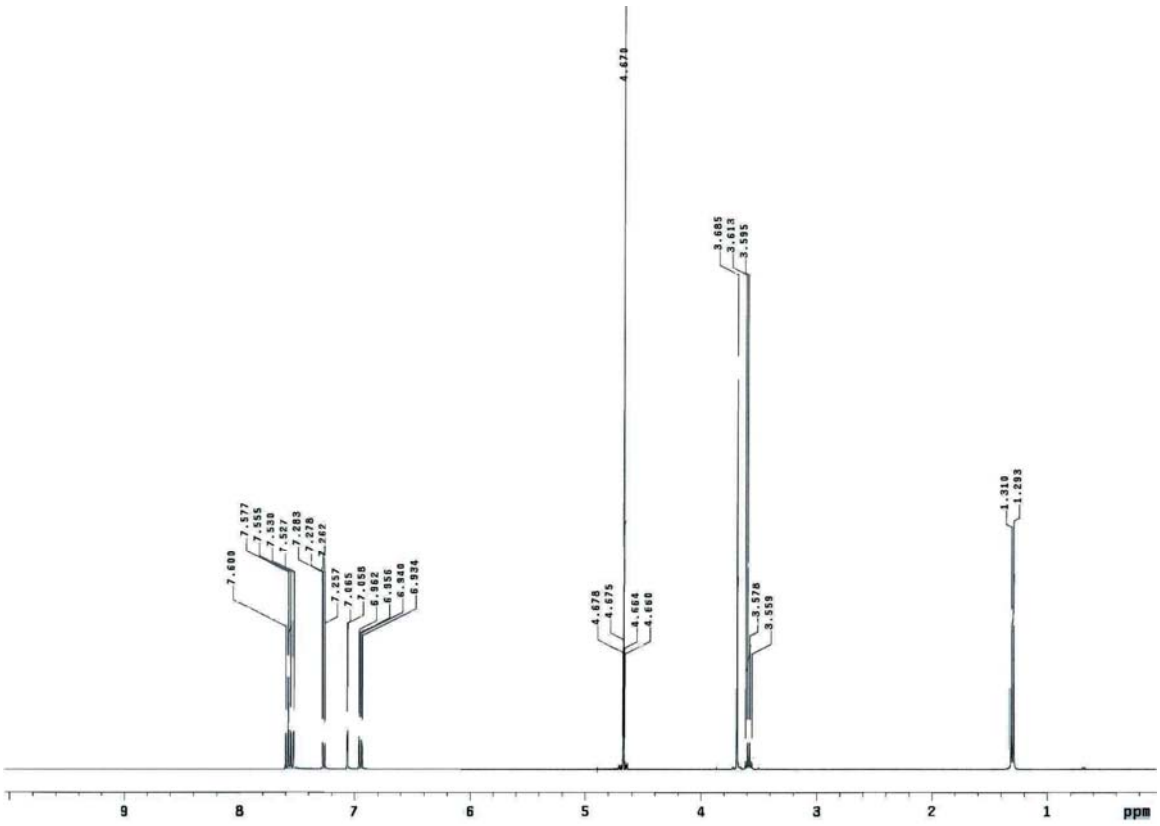

Figure 8.8. ^{1}H-NMR spectrum for isobutanol solvate of sodium naproxen.

8.2.4 Powder X-Ray Diffraction

PXRD was used to determine if the solvated crystals had distinct crystal structures and how these structures compared. As shown in Figure 8.9, the diffractograms were similar and only had slight differences with respect to the anhydrous PXRD pattern. The methanol, ethanol, 1-propanol and isobutanol solvated forms exhibited a complete absence of the anhydrous peak seen at a 2θ of 13.2°, which was a result from diffraction of the (003) plane (Kim et al., 2004). This showed that no anhydrous material was present in these solvated forms. The 2-propanol and 1-butanol had a peak at 13.0°, which was similar to the anhydrous peak, but did not give a clear indication that a mixture was present. A clearer indication of the absence of a mixture can be explained by the absence of peaks for the 2-propanol and 1-butanol solvates at a Bragg's angle of 20.0°, which was present in the anhydrous PXRD pattern. Additional peaks at 12.5°, 12.0°, 11.9°, 12.0°, and 12.4° were seen in the ethanol, 1-propanol, 2-propanol, 1-butanol, and isobutanol solvated forms, respectively. An additional peak was also visible around a Bragg's angle of 15.8° for all of the solvated crystals. This peak was not present in the diffractogram of the anhydrous crystals. Also not present in the anhydrous PXRD scan was a peak at 16.9°, which was seen in both the methanol and ethanol patterns.

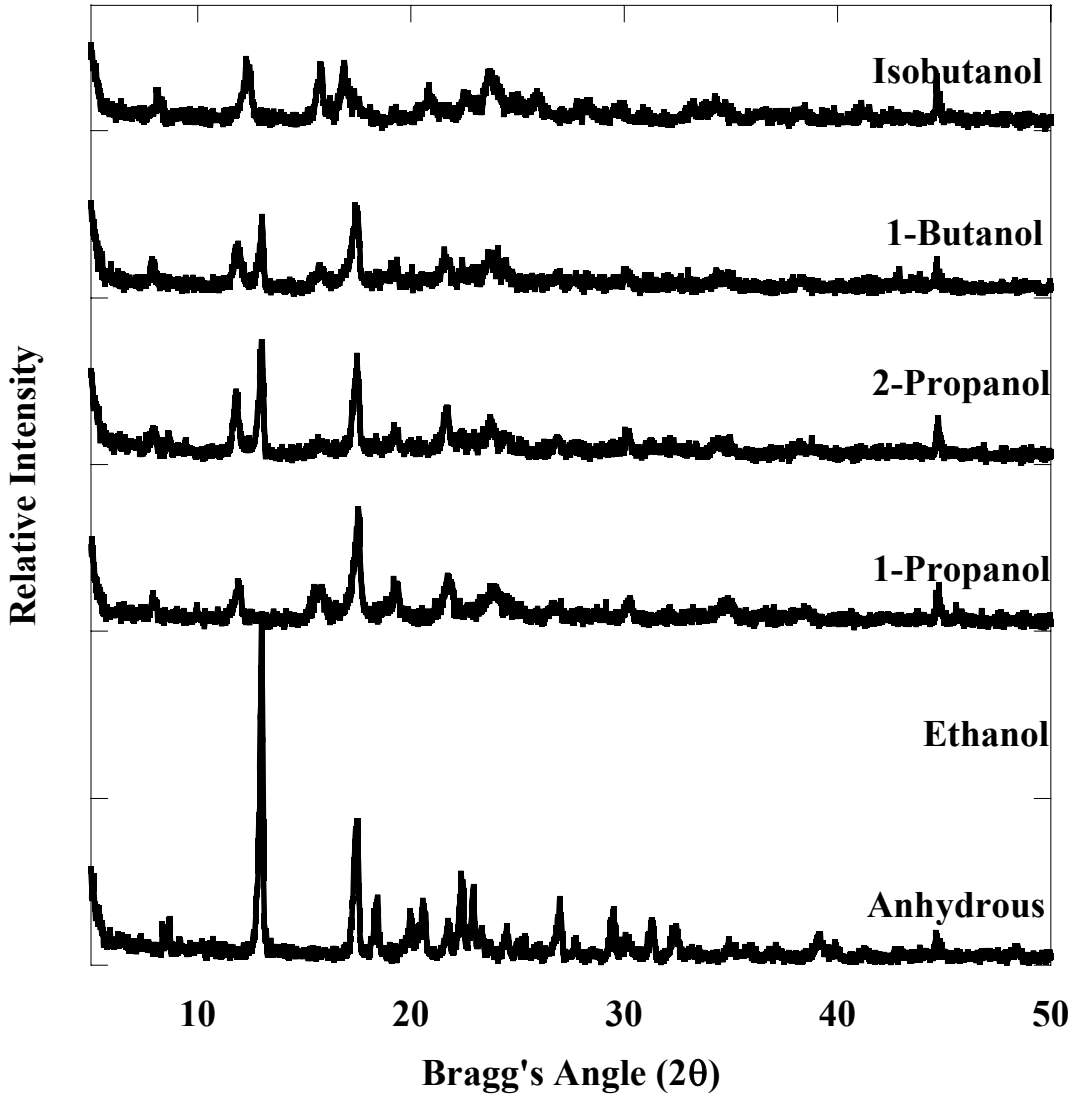

Figure 8.9. PXRD data for solvated crystals of sodium naproxen.

These differences showed that the solvent does have an effect on the crystal structure, even if only slightly, and they were distinct crystals. Some of these differences could be seen in the photomicrographs of the various solvated crystals as presented earlier.

8.3 Conclusions

The ability of alcohol solvents to form solvates with sodium naproxen was discussed in terms of their size and shape. Each of the solvates was analyzed using TGA, DSC, photomicroscopy, ^{1}H-NMR, and PXRD. Results showed that each of the crystals obtained from cooling crystallization in the pure solvents were distinct and some inclusion of the solvent was observed for all of the organic solvents tested. Additionally larger amounts of solvent affected crystal shape, as seen with the ethanol solvated forms.

The findings presented here mostly impact the solvate formation of channel-type solvates, similar to that of sodium naproxen. The ability of the organic solvents to create these channels and be removed from them has a large influence of the data presented here relating to the solvents chain length and branching.

Examining how the size and shape of a solvent can influence crystal growth and shape can aid in the understanding of the ability of compounds to form solvates. And with the increasing number of solvates being discovered, this understanding can be useful for solvent selection.

CHAPTER 9

CONCLUSIONS AND RECOMMENDATIONS

9.1 Conclusions

Solubilities of sodium naproxen over an approximate temperature range of 10°C to 40°C was measured using high performance liquid chromatography in solutions of 10 mol%, 25 mol%, 47 mol% methanol-in-water and pure methanol, as well as 14.5 mol%, 44 mol%, 67 mol%, 79 mol% ethanol-in-water and pure ethanol. Addition of the organic alcohols caused both salting-out and salting-in effects. At lower concentrations of methanol a salting-in effect was observed, while at higher concentrations and with ethanol a salting-out effect was evident. In terms of temperatures, concentration increased as temperature increased. It should be noted that solvent concentration played a larger role than temperature in affecting solubilities. Changes in pseudopolymorphic forms were also evident based on solid-state analysis. The following pseudopolymorphic forms were present in the solution and temperature ranges studied in these systems: anhydrate, monohydrate, dihydrate, methanol solvate, and ethanol solvate.

These changes in pseudopolymorphic form were further analyzed using van't Hoff plots (logarithm of solubility versus inverse temperature) to determine the transition temperature between the two stable pseudopolymorphs. Extracting the transition temperature, and using the known solvent concentration, the activity of water at the transition point was determined. Using the activity of water at the transition point, it was seen that independent of the alcohol concentration, water activity was the same for methanol and ethanol solutions at the transition point. It should be noted that the

transition from an alcohol solvated form of sodium naproxen to the dihydrated form was evident at two independent water activities. This work suggested that there are a range of water activities where a specific transition will occur, as opposed to only one specific water activity.

Additionally, novel organic alcohol solvates of sodium naproxen were explored. The alcohol solvated forms of sodium naproxen, which included a methanol, ethanol, 1-propanol, 2-propanol, 1-butanol, and isobutanol solvated forms, were characterized using a variety of techniques including TGA, DSC, PXRD, ^{1}H-NMR, and PLM imaging. It was shown that the recrystallization of anhydrous sodium naproxen in pure alcohol solvents at low temperatures gave rise to solvated crystals. This was apparent in ^{1}H-NMR data where there were clear changes in the spectrum compared to the anhydrous form. This indicated some change in atomic interactions. Furthermore, these techniques generally indicated that as the size of the alcohol increased its ability to be included in the crystal decreased, as indicated by the TGA studies. This was due to the bonding ability of solvents in sodium naproxen and how these solvents are included in the crystal structure. The channel-like locations of solvents make it difficult for larger molecules to allow a stable crystal structure since they inhibit the hydrogen bonding and sodium-oxygen interactions. This explanation can be extended to the results from the DSC studies. More energy was required to remove larger molecules from the crystal structure than smaller molecules. Both size and shape of the solvents played a role in its ability to form pseudopolymorphs of sodium naproxen.

The methanol solvated form of sodium naproxen was the most thoroughly explored pseudopolymorph in this work. Additional studies on the methanol solvate of sodium naproxen included IR and, most importantly, a single crystal XRD.

9.2 Recommendations

Recommendations for future work are listed as follows: (1) follow-up study on organic alcohol solvates of sodium naproxen, (2) mechanism for transitions of pseudopolymorphs, (3) predictions of pseudopolymorphic transitions.

(1) A number of organic alcohol solvates were briefly studied in this thesis. A more thorough analysis of these organic solvates is possible. This would include the stability and dissolution studies of these organic solvates and comparisons to structural similarities of other pseudopolymorphic forms of sodium naproxen. The ethanol solvated form showed smaller crystal size than other pseudopolymorphs of sodium naproxen, which would mean faster dissolution and could have some pharmaceutical applications. Smaller, stable crystals can have better packing features and dissolution in patients. Understanding how simple recrystallization in an ethanol solvent could help obtain such crystals would be useful. These solvated forms also provide a possible simulation study on the crystal structures of the solvates in terms of stabilization forces.

(2) In industrial settings, sudden appearances of unknown pseudopolymorphs or polymorphs are important because it often attributes to loss of time and money. To understand the microscopic mechanism of transformation would

provide insight into the stability of the polymorphic and pseudopolymorphic forms. Three pseudopolymorphic transitions are seen with sodium naproxen: anhydrate to dihydrate, dihydrate to solvate, and dihydrate to monohydrate. The study of the microscopic mechanisms of these transitions would be a good place to start in studying transitions.

(3) Initially, this work was carried out in hopes of developing a predictive model for pseudopolymorphic transitions. Due the discovery of solvated forms of sodium naproxen, which was a more interesting study, this section was not developed. Having a model to predict the transitions of pseudopolymorphs would be very useful in industrial settings for helping to avoid or force transitions when it is so desired. A predictive model, on when pseudopolymorphic changes would occur, has not yet been realized but would have a large impact on the understanding and possible discovery of pseudopolymorphic forms. More precise modeling of the activity coefficients, including that of the dissolved solute, would be an appropriate place to initiate the work.

APPENDIX A:

HPLC CALIBRATIONS

This appendix contains all of the calibration curves from the HPLC experiments that were conducted in support of the solubility of sodium naproxen in various solvents. Depending on the time the experiments took for a specific concentration, multiple calibration curves may have been needed for the same solvent concentration.

A.1 Pure Water

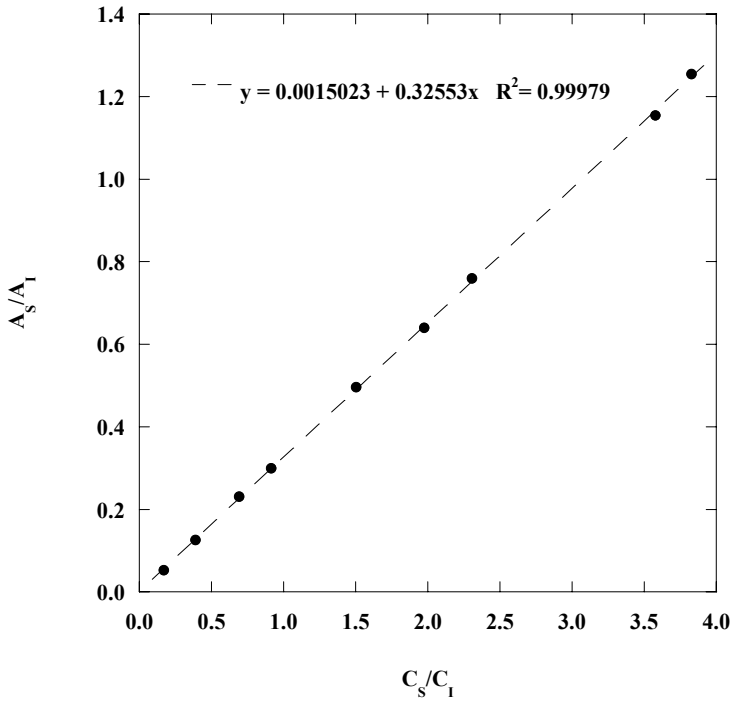

Figure A.1. Calibration curve for pure water made on July 6, 2006.

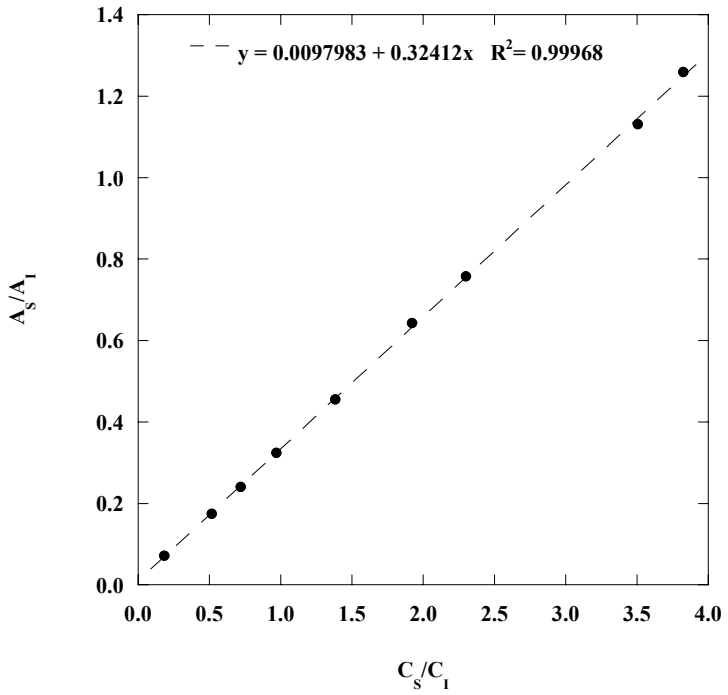

Figure A.2. Calibration curve for pure water Made on August 2, 2006.

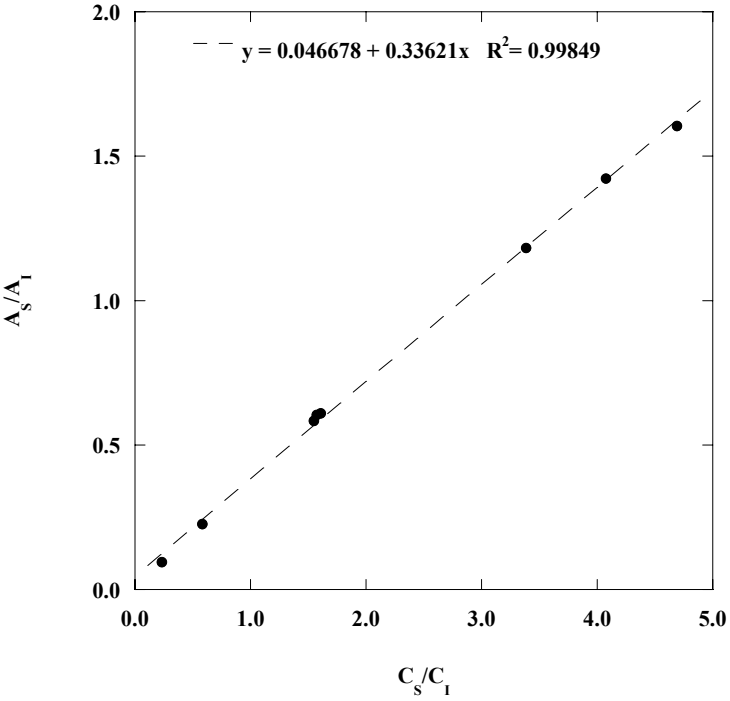

Figure A.3. Calibration curve for pure water Made on August 14, 2006.

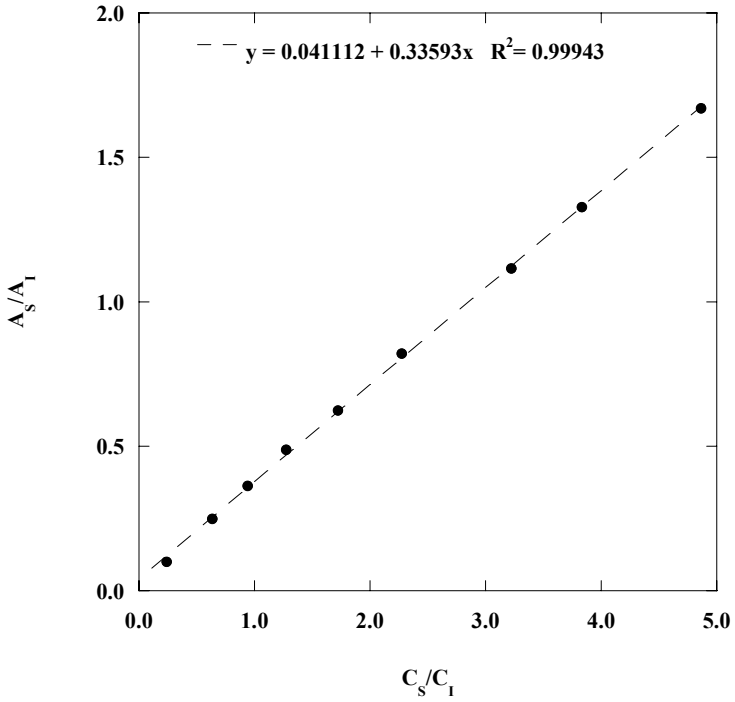

Figure A.4. Calibration curve for pure water made on October 6, 2006.

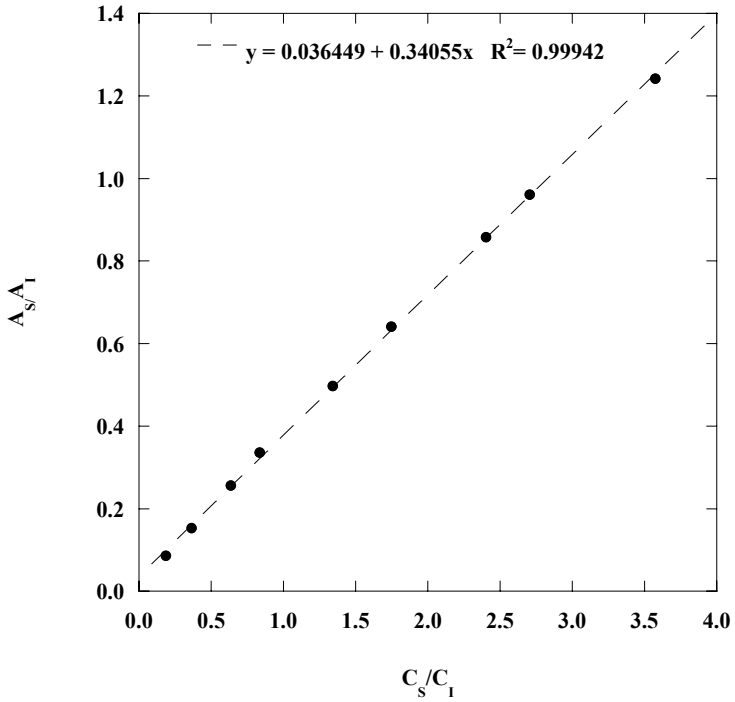

Figure A.5. Calibration curve for pure water made on October 30, 2006.

A.2 10 mol% Methanol-in-Water

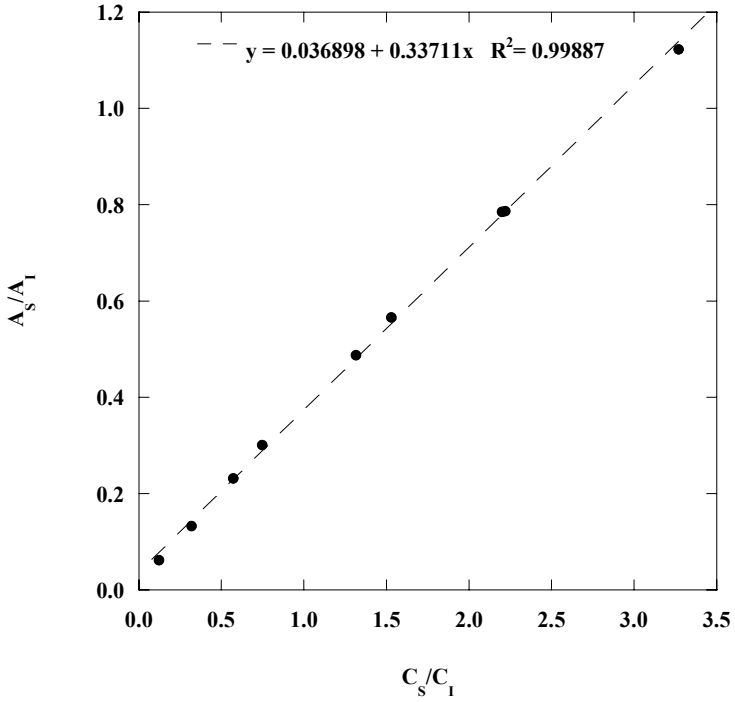

Figure A.6. Calibration curve for 10 mol% methanol-in-water made on November 2, 2006.

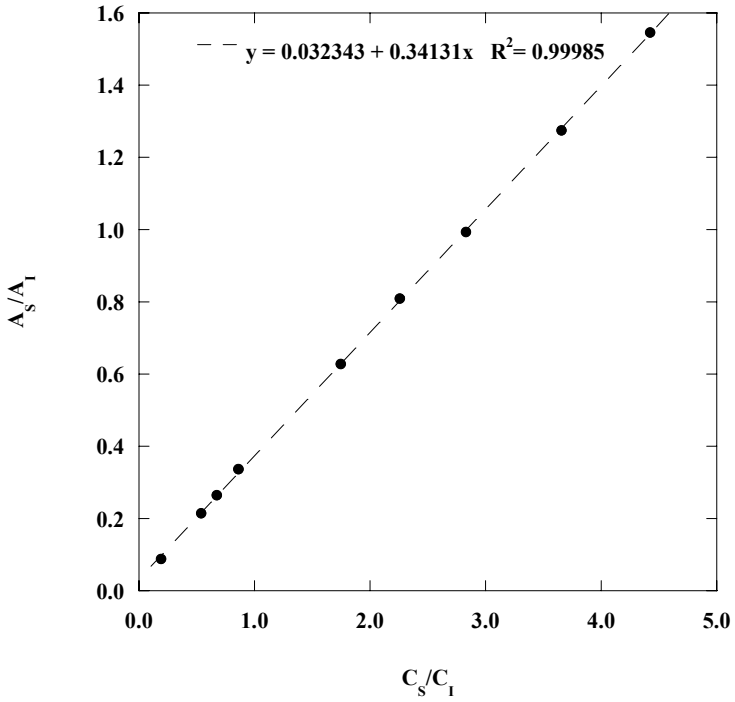

Figure A.7. Calibration curve for 10 mol% methanol-in-water made on November 28, 2006.

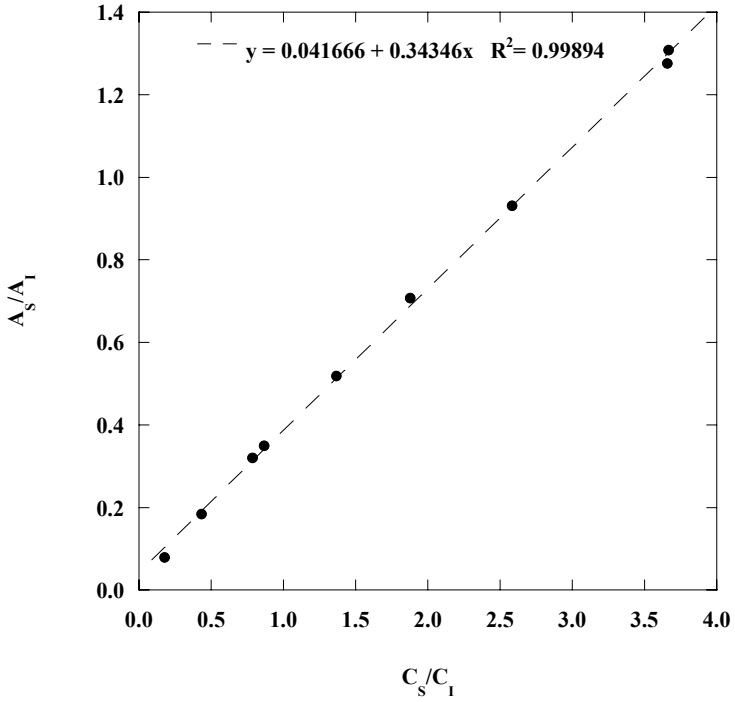

Figure A.8. Calibration curve for 10 mol% methanol-in-water made on January 2, 2007.

A.3 25 mol% Methanol-in-Water

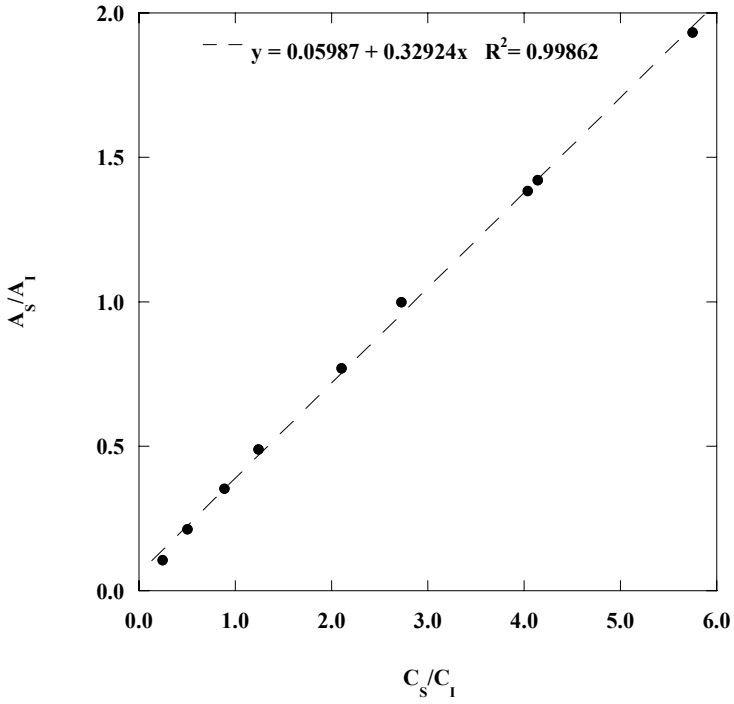

Figure A.9. Calibration curve for 25 mol% methanol made on January 31, 2007.

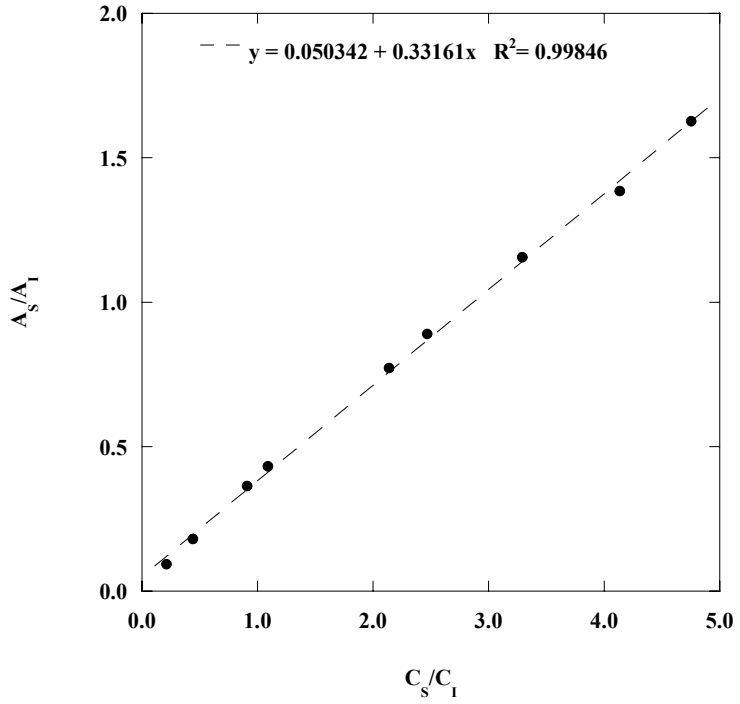

Figure A.10. Calibration curve for 25 mol% methanol-in-water made on February 27, 2007.

A.4 47 mol% Methanol-in-Water

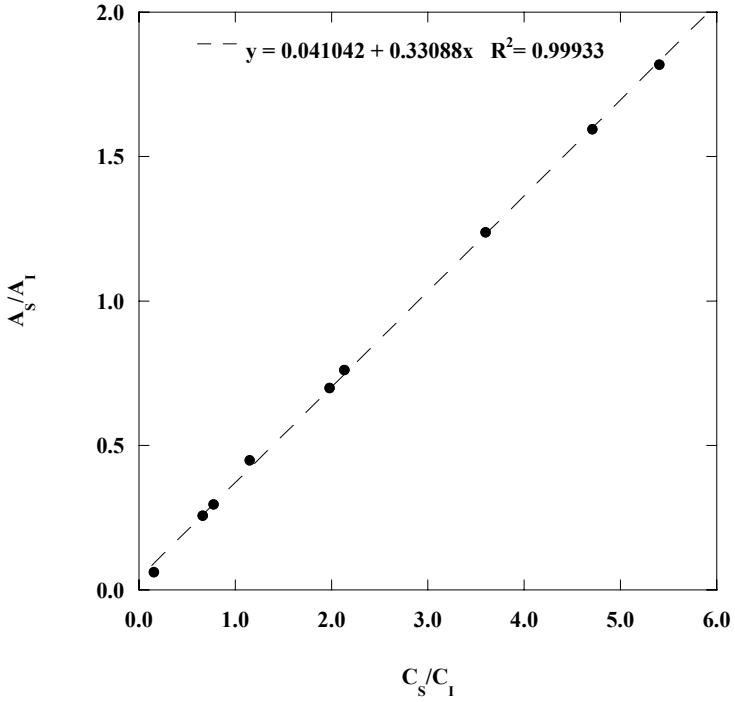

Figure A.11. Calibration curve for 46 mol% methanol-in-water made on March, 27, 2007.

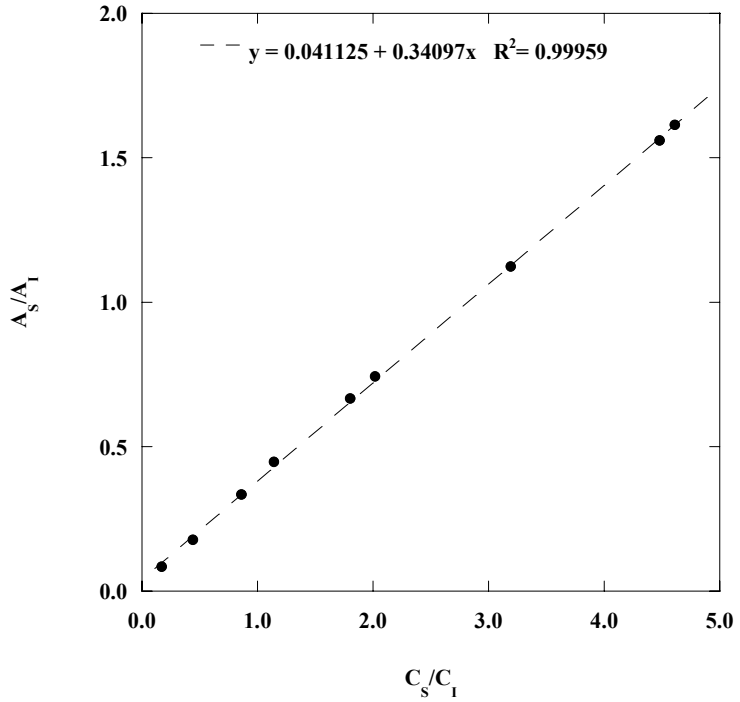

Figure A.12. Calibration curve for 47 mol% methanol-in-water made on April 24, 2007.

A.5 Pure Methanol

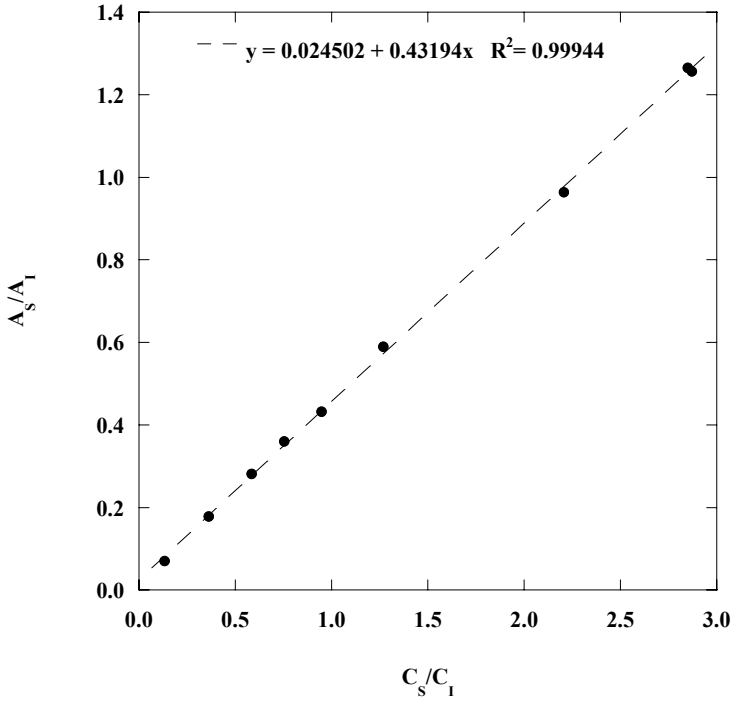

Figure A.13. Calibration curve for pure methanol.

A.6 14.5 mol% Ethanol-in-Water

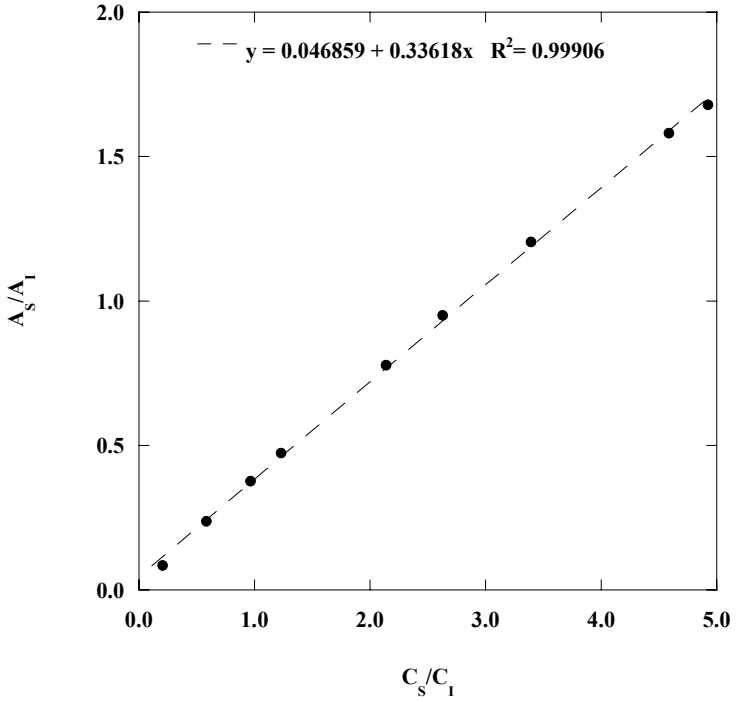

Figure A.14. Calibration curve of 14.5 mol% ethanol-in-water.

A.7 44 mol% Ethanol-in-Water

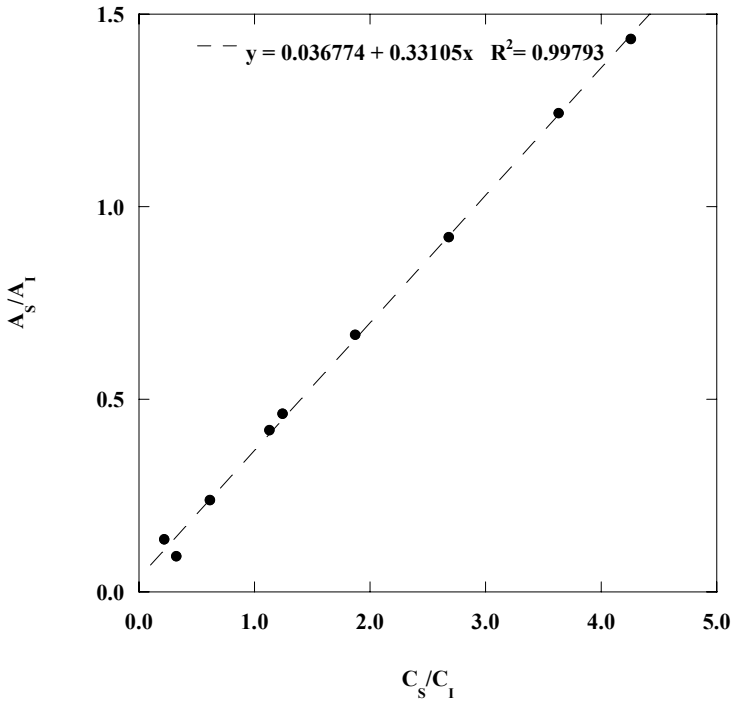

Figure A.15. Calibration curve for 44 mol% ethanol-in-water.

A.8 67 mol% Ethanol-in-Water

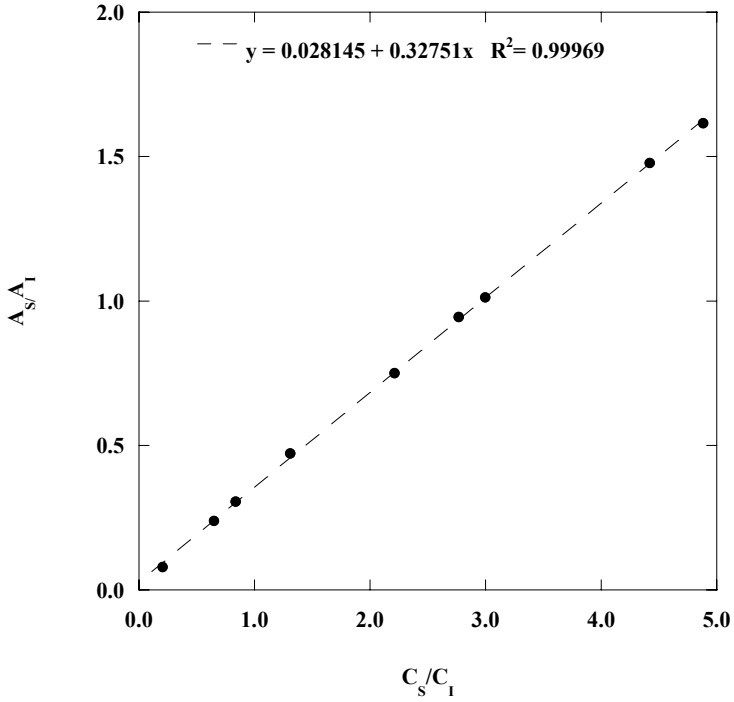

Figure A.16. Calibration curve for 67 mol% ethanol-in-water.

A.9 79 mol% Ethanol-in-Water

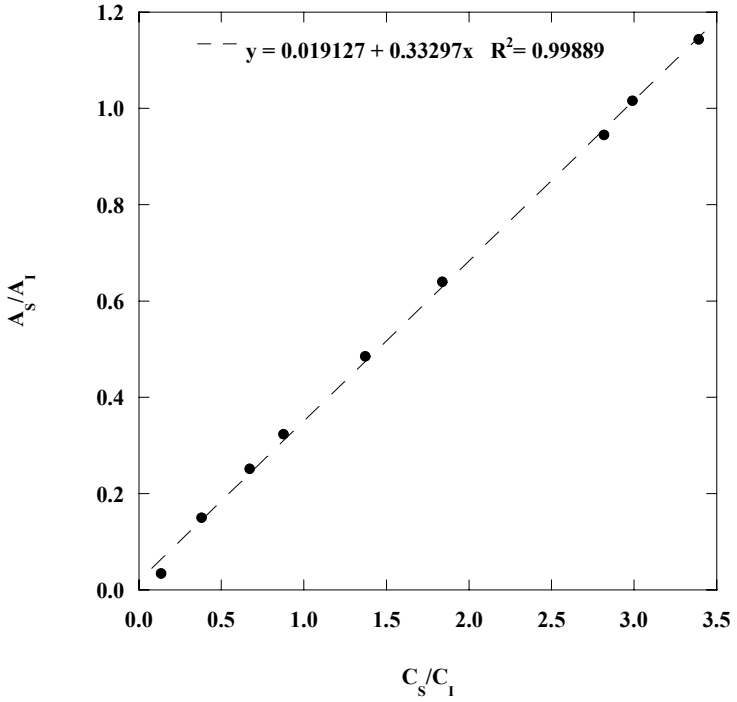

Figure A.17. Calibration curve for 79 mol% ethanol-in-water.

A.10 Pure Ethanol

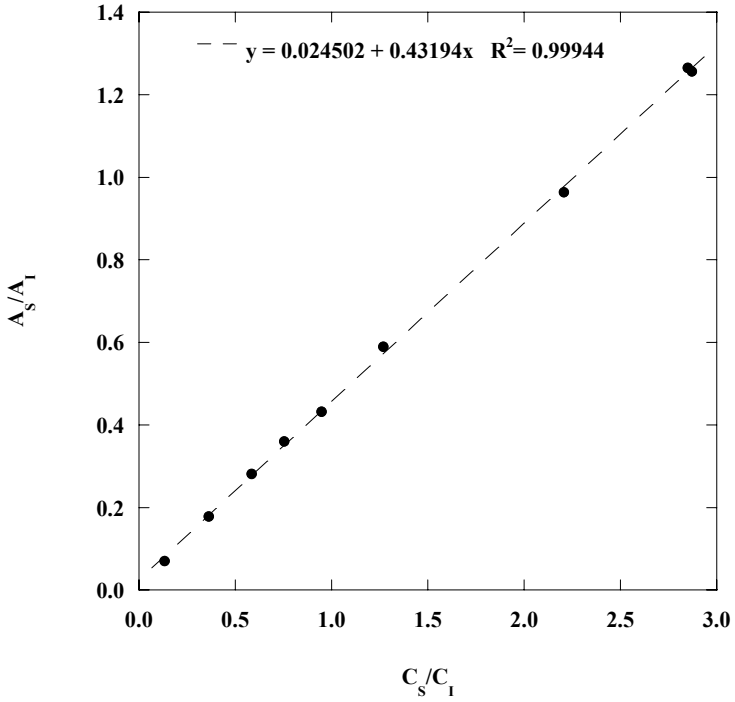

Figure A.18. Calibration curve for pure ethanol made May 22, 2008.

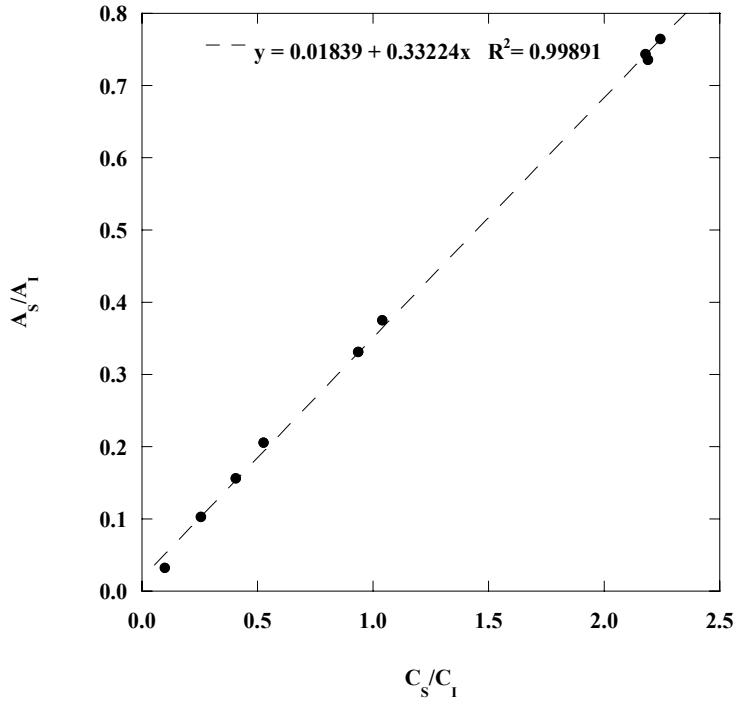

Figure A.19. Calibration curve for pure ethanol made on June 4, 2008.

APPENDIX B:

CRYSTALOGRAPHY DATA OF METHANOL SOLVATE OF SODIUM NAPROXEN

Table B.1. Atomic coordinates ($x10^4$) and equivalent isotropic displacement parameters ($Åx10^3$) for methanol solvate of sodium naproxen. U(eq) defined as one third of the trace of the orthogonalized U^{ij} tensor.

	x	y	z	U(eq)
C(1)	4000(4)	-374(6)	4973(3)	39(1)
C(2)	4659(4)	466(6)	5570(3)	39(1)
C(3)	4479(3)	465(6)	6495(3)	33(1)
C(4)	5112(3)	1336(6)	7125(3)	35(1)
C(5)	4887(3)	1357(6)	7986(3)	32(1)
C(6)	3998(3)	522(5)	8269(3)	30(1)
C(7)	3394(3)	-390(6)	7650(3)	33(1)
C(8)	3610(3)	-473(6)	6752(3)	37(1)
C(9)	2976(4)	-1381(7)	6111(3)	43(1)
C(10)	3166(4)	-1339(7)	5253(3)	43(1)
C(11)	3754(3)	646(6)	9213(3)	34(1)
C(12)	2566(3)	480(5)	9290(3)	29(1)
C(13)	4390(4)	-652(9)	9794(4)	58(2)
C(14)	4856(5)	658(8)	3752(4)	63(2)
C(1B)	8065(4)	9188(9)	5029(5)	73(2)
C(2B)	9007(6)	9845(9)	5081(5)	82(2)
C(3B)	9640(4)	9558(7)	4265(4)	52(1)
C(4B)	10630(5)	10120(10)	4273(5)	87(2)
C(5B)	11109(6)	9795(9)	3523(4)	78(2)
C(6B)	10652(5)	8860(8)	2785(4)	61(2)
C(7B)	9671(6)	8294(10)	2800(4)	79(2)
C(8B)	9081(5)	8650(8)	3621(5)	75(2)
C(9B)	8094(6)	8035(10)	3570(5)	92(3)

Table B.1. *Continued*

	x	y	z	U(eq)
C(10B)	7563(6)	8294(10)	4333(5)	77(2)
C(11B)	11280(4)	8500(7)	2018(3)	43(1)
C(12B)	10647(3)	8922(6)	1137(3)	32(1)
C(13B)	12325(5)	9435(11)	2072(4)	74(2)
C(14B)	7815(5)	9971(10)	6445(6)	85(2)
C(1S)	6667(5)	10178(7)	1836(4)	58(2)
C(2S)	514(5)	8157(8)	7409(4)	52(1)
C(3S)	7550(4)	9160(9)	8993(4)	64(2)
Na(1)	311(1)	151(2)	9396(1)	33(1)
Na(2)	8583(1)	1561(2)	547(1)	36(1)
O(1)	2197(3)	-929(4)	9442(2)	44(1)
O(2)	2002(2)	1767(4)	9163(2)	41(1)
O(3)	4078(3)	-393(5)	4087(2)	51(1)
O(1B)	10500(2)	7784(4)	575(2)	37(1)
O(2B)	10341(3)	10413(4)	1012(2)	37(1)
O(3B)	7376(4)	9342(7)	5758(3)	77(1)
O(1S)	7438(3)	9942(4)	1268(3)	66(1)
O(2S)	40(3)	8289(4)	8185(3)	54(1)
O(3S)	8473(3)	9206(5)	9573(3)	37(1)

Table B.2. Bond lengthes (Å) and angles (°) for methanol solvated form of sodium naproxen.

C(1)-C(2)	1.356(7)	C(1B)-C(2B)	1.304(9)
C(1)-O(3)	1.364(6)	C(1B)-C(10B)	1.385(10)
C(1)-C(10)	1.410(7)	C(1B)-O(3B)	1.484(8)
C(2)-C(3)	1.450(7)	C(2B)-C(3B)	1.561(9)
C(2)-H(2A)	0.9500	C(2B)-H(2B)	0.9500
C(3)-C(4)	1.383(6)	C(3B)-C(4B)	1.335(8)
C(3)-C(8)	1.422(6)	C(3B)-C(8B)	1.366(8)
C(4)-C(5)	1.369(6)	C(4B)-C(5B)	1.370(9)
C(4)-H(4A)	0.9500	C(4B)-H(4BA)	0.9500
C(5)-C(6)	1.415(6)	C(5B)-C(6B)	1.429(9)
C(5)-H(5A)	0.9500	C(5B)-H(5BA)	0.9500
C(6)-C(7)	1.370(6)	C(6B)-C(7B)	1.329(9)
C(6)-C(11)	1.505(7)	C(6B)-C(11B)	1.505(8)
C(7)-C(8)	1.424(7)	C(7B)-C(8B)	1.546(9)
C(7)-H(7A)	0.9500	C(7B)-H(7BA)	0.9500
C(8)-C(9)	1.408(7)	C(8B)-C(9B)	1.344(9)
C(9)-C(10)	1.353(7)	C(9B)-C(10B)	1.414(10)
C(9)-H(9A)	0.9500	C(9B)-H(9BA)	0.9500
C(10)-H(10A)	0.9500	C(10B)-H(10B)	0.9500
C(11)-C(12)	1.532(6)	C(11B)-C(13B)	1.520(9)
C(11)-C(13)	1.543(7)	C(11B)-C(12B)	1.538(7)
C(11)-H(11A)	1.0000	C(11B)-H(11B)	1.0000
C(12)-O(1)	1.250(5)	C(12B)-O(1B)	1.251(6)
C(12)-O(2)	1.258(5)	C(12B)-O(2B)	1.262(5)
C(12)-Na(1)	2.899(4)	C(12B)-Na(1)#1	2.826(5)
C(13)-H(13A)	0.9800	C(13B)-H(13D)	0.9800
C(13)-H(13B)	0.9800	C(13B)-H(13E)	0.9800
C(13)-H(13C)	0.9800	C(13B)-H(13F)	0.9800
C(14)-O(3)	1.429(7)	C(14B)-O(3B)	1.247(9)
C(14)-H(14A)	0.9800	C(14B)-H(14D)	0.9800
C(14)-H(14B)	0.9800	C(14B)-H(14E)	0.9800
C(14)-H(14C)	0.9800	C(14B)-H(14F)	0.9800

Table B.2. *Continued.*

C(1S)-O(1S)	1.381(6)	C(1S)-H(1S1)	0.9800
C(1S)-H(1S2)	0.9800	O(2B)-Na(2)#12	2.460(4)
C(1S)-H(1S3)	0.9800	O(2B)-Na(1)#1	2.471(4)
C(2S)-O(2S)	1.381(7)	O(1S)-Na(2)#12	2.302(4)
C(2S)-H(2S1)	0.9800		
C(2S)-H(2S2)	0.9800	O(1S)-H(1SO)	0.9120
C(2S)-H(2S3)	0.9800	O(2S)-Na(1)#12	2.371(4)
C(3S)-O(3S)	1.402(7)	O(2S)-Na(2)#7	2.842(5)
C(3S)-H(3S1)	0.9800	O(2S)-H(2SO)	0.8737
C(3S)-H(3S2)	0.9800	O(3S)-Na(2)#13	2.394(4)
C(3S)-H(3S3)	0.9800	O(3S)-Na(1)#14	2.496(4)
Na(1)-O(1B)#2	2.346(3)	O(3S)-H(3SO)	0.63(5)
Na(1)-O(2S)#3	2.371(4)		
Na(1)-O(2B)#4	2.471(4)	C(2)-C(1)-O(3)	125.0(4)
Na(1)-O(3S)#5	2.496(4)	C(2)-C(1)-C(10)	120.1(5)
Na(1)-O(1)	2.544(4)	O(3)-C(1)-C(10)	114.9(4)
Na(1)-O(2)	2.562(4)	C(1)-C(2)-C(3)	120.6(4)
Na(1)-O(1B)#4	2.606(4)	C(1)-C(2)-H(2A)	119.7
Na(1)-C(12B)#4	2.826(5)	C(3)-C(2)-H(2A)	119.7
Na(1)-Na(2)#6	3.148(2)	C(4)-C(3)-C(8)	119.4(4)
Na(1)-Na(2)#2	3.192(2)	C(4)-C(3)-C(2)	122.8(4)
Na(2)-O(1)#7	2.237(4)	C(8)-C(3)-C(2)	117.8(4)
Na(2)-O(1S)#3	2.302(4)	C(5)-C(4)-C(3)	120.9(4)
Na(2)-O(1B)#8	2.371(4)	C(5)-C(4)-H(4A)	119.6
Na(2)-O(3S)#9	2.394(4)	C(3)-C(4)-H(4A)	119.6
Na(2)-O(2B)#3	2.460(4)	C(4)-C(5)-C(6)	122.1(4)
Na(2)-O(2S)#2	2.842(5)	C(4)-C(5)-H(5A)	119.0
Na(2)-Na(1)#10	3.148(2)	C(6)-C(5)-H(5A)	119.0
Na(2)-Na(1)#7	3.192(2)	C(7)-C(6)-C(5)	117.0(4)
O(1)-Na(2)#2	2.237(4)	C(7)-C(6)-C(11)	122.8(4)
O(1B)-Na(1)#7	2.346(3)	C(5)-C(6)-C(11)	120.2(4)
O(1B)-Na(2)#11	2.371(4)	C(6)-C(7)-C(8)	122.8(4)
O(1B)-Na(1)#1	2.606(4)	C(6)-C(7)-H(7A)	118.6

Table B.2. *Continued.*

C(8)-C(7)-H(7A)	118.6	C(2B)-C(1B)-C(10B)	127.6(7)
C(9)-C(8)-C(3)	119.3(4)	C(2B)-C(1B)-O(3B)	121.7(7)
C(9)-C(8)-C(7)	122.9(4)	C(10B)-C(1B)-O(3B)	110.7(5)
C(3)-C(8)-C(7)	117.8(4)	C(1B)-C(2B)-C(3B)	115.6(6)
C(10)-C(9)-C(8)	121.0(4)	C(1B)-C(2B)-H(2B)	122.2
C(10)-C(9)-H(9A)	119.5	C(3B)-C(2B)-H(2B)	122.2
C(8)-C(9)-H(9A)	119.5	C(4B)-C(3B)-C(8B)	127.7(6)
C(9)-C(10)-C(1)	121.0(5)	C(4B)-C(3B)-C(2B)	120.0(6)
C(9)-C(10)-H(10A)	119.5	C(8B)-C(3B)-C(2B)	112.3(5)
C(1)-C(10)-H(10A)	119.5	C(3B)-C(4B)-C(5B)	114.9(7)
C(6)-C(11)-C(12)	111.1(4)	C(3B)-C(4B)-H(4BA)	122.5
C(6)-C(11)-C(13)	111.2(4)	C(5B)-C(4B)-H(4BA)	122.5
C(12)-C(11)-C(13)	111.5(4)	C(4B)-C(5B)-C(6B)	125.2(7)
C(6)-C(11)-H(11A)	107.6	C(4B)-C(5B)-H(5BA)	117.4
C(12)-C(11)-H(11A)	107.6	C(6B)-C(5B)-H(5BA)	117.4
C(13)-C(11)-H(11A)	107.6	C(7B)-C(6B)-C(5B)	118.5(6)
O(1)-C(12)-O(2)	123.1(4)	C(7B)-C(6B)-C(11B)	121.1(6)
O(1)-C(12)-C(11)	118.8(4)	C(5B)-C(6B)-C(11B)	120.4(6)
O(2)-C(12)-C(11)	118.0(4)	C(6B)-C(7B)-C(8B)	118.7(7)
O(1)-C(12)-Na(1)	61.1(2)	C(6B)-C(7B)-H(7BA)	120.7
O(2)-C(12)-Na(1)	62.0(2)	C(8B)-C(7B)-H(7BA)	120.7
C(11)-C(12)-Na(1)	178.8(3)	C(9B)-C(8B)-C(3B)	131.0(7)
C(11)-C(13)-H(13A)	109.5	C(9B)-C(8B)-C(7B)	114.1(6)
C(11)-C(13)-H(13B)	109.5	C(3B)-C(8B)-C(7B)	114.9(6)
H(13A)-C(13)-H(13B)	109.5	C(8B)-C(9B)-C(10B)	114.5(7)
C(11)-C(13)-H(13C)	109.5	C(8B)-C(9B)-H(9BA)	122.7
H(13A)-C(13)-H(13C)	109.5	C(10B)-C(9B)-H(9BA)	122.7
H(13B)-C(13)-H(13C)	109.5	C(1B)-C(10B)-C(9B)	118.9(6)
O(3)-C(14)-H(14A)	109.5	C(1B)-C(10B)-H(10B)	120.5
O(3)-C(14)-H(14B)	109.5	C(9B)-C(10B)-H(10B)	120.5
H(14A)-C(14)-H(14B)	109.5	C(6B)-C(11B)-C(13B)	113.0(5)
O(3)-C(14)-H(14C)	109.5	C(6B)-C(11B)-C(12B)	111.3(4)
H(14A)-C(14)-H(14C)	109.5	C(13B)-C(11B)-C(12B)	108.8(4)
H(14B)-C(14)-H(14C)	109.5	C(6B)-C(11B)-H(11B)	107.8

Table B.2. *Continued.*

C(13B)-C(11B)-H(11B)	107.8	H(3S1)-C(3S)-H(3S2)	109.5
C(12B)-C(11B)-H(11B)	107.8	O(3S)-C(3S)-H(3S3)	109.5
O(1B)-C(12B)-O(2B)	124.0(4)	H(3S1)-C(3S)-H(3S3)	109.5
O(1B)-C(12B)-C(11B)	118.1(4)	H(3S2)-C(3S)-H(3S3)	109.5
O(2B)-C(12B)-C(11B)	117.9(4)	O(1B)#2-Na(1)-O(2S)#3	123.02(15)
O(1B)-C(12B)-Na(1)#1	67.0(3)	O(1B)#2-Na(1)-O(2B)#4	82.60(12)
O(2B)-C(12B)-Na(1)#1	60.9(2)	O(2S)#3-Na(1)-O(2B)#4	144.84(14)
C(11B)-C(12B)-Na(1)#1	156.6(3)	O(1B)#2-Na(1)-O(3S)#5	81.42(13)
C(11B)-C(13B)-H(13D)	109.5	O(2S)#3-Na(1)-O(3S)#5	79.91(13)
C(11B)-C(13B)-H(13E)	109.5	O(2B)#4-Na(1)-O(3S)#5	81.07(13)
H(13D)-C(13B)-H(13E)	109.5	O(1B)#2-Na(1)-O(1)	136.00(13)
C(11B)-C(13B)-H(13F)	109.5	O(2S)#3-Na(1)-O(1)	82.91(14)
H(13D)-C(13B)-H(13F)	109.5	O(2B)#4-Na(1)-O(1)	94.31(13)
H(13E)-C(13B)-H(13F)	109.5	O(3S)#5-Na(1)-O(1)	141.71(13)
O(3B)-C(14B)-H(14D)	109.5	O(1B)#2-Na(1)-O(2)	85.83(12)
O(3B)-C(14B)-H(14E)	109.5	O(2S)#3-Na(1)-O(2)	105.73(13)
H(14D)-C(14B)-H(14E)	109.5	O(2B)#4-Na(1)-O(2)	99.27(13)
O(3B)-C(14B)-H(14F)	109.5	O(3S)#5-Na(1)-O(2)	167.10(14)
H(14D)-C(14B)-H(14F)	109.5	O(1)-Na(1)-O(2)	51.18(11)
H(14E)-C(14B)-H(14F)	109.5	O(1B)#2-Na(1)-O(1B)#4	130.57(8)
O(1S)-C(1S)-H(1S1)	109.5	O(2S)#3-Na(1)-O(1B)#4	94.57(13)
O(1S)-C(1S)-H(1S2)	109.5	O(2B)#4-Na(1)-O(1B)#4	51.74(11)
H(1S1)-C(1S)-H(1S2)	109.5	O(3S)#5-Na(1)-O(1B)#4	74.49(13)
O(1S)-C(1S)-H(1S3)	109.5	O(1)-Na(1)-O(1B)#4	73.09(11)
H(1S1)-C(1S)-H(1S3)	109.5	O(2)-Na(1)-O(1B)#4	115.93(12)
H(1S2)-C(1S)-H(1S3)	109.5	O(1B)#2-Na(1)-C(12B)#4	108.79(14)
O(2S)-C(2S)-H(2S1)	109.5	O(2S)#3-Na(1)-C(12B)#4	120.80(14)
O(2S)-C(2S)-H(2S2)	109.5	O(2B)#4-Na(1)-C(12B)#4	26.49(12)
H(2S1)-C(2S)-H(2S2)	109.5	O(3S)#5-Na(1)-C(12B)#4	81.60(14)
O(2S)-C(2S)-H(2S3)	109.5	O(1)-Na(1)-C(12B)#4	78.31(13)
H(2S1)-C(2S)-H(2S3)	109.5	O(2)-Na(1)-C(12B)#4	104.51(13)
H(2S2)-C(2S)-H(2S3)	109.5	O(1B)#4-Na(1)-C(12B)#4	26.23(12)
O(3S)-C(3S)-H(3S1)	109.5	O(1B)#2-Na(1)-C(12)	111.04(13)
O(3S)-C(3S)-H(3S2)	109.5	O(2S)#3-Na(1)-C(12)	94.94(14)

Table B.2. *Continued.*

O(2B)#4-Na(1)-C(12)	97.20(13)	O(3S)#9-Na(2)-O(2B)#3	83.36(12)
O(3S)#5-Na(1)-C(12)	167.19(14)	O(1)#7-Na(2)-O(2S)#2	78.76(13)
O(1)-Na(1)-C(12)	25.50(12)	O(1S)#3-Na(2)-O(2S)#2	109.00(16)
O(2)-Na(1)-C(12)	25.69(12)	O(1B)#8-Na(2)-O(2S)#2	88.72(12)
O(1B)#4-Na(1)-C(12)	94.40(12)	O(3S)#9-Na(2)-O(2S)#2	143.18(13)
C(12B)#4-Na(1)-C(12)	91.20(14)	O(2B)#3-Na(2)-O(2S)#2	59.95(11)
O(1B)#2-Na(1)-Na(2)#6	48.46(9)	O(1)#7-Na(2)-Na(1)#10	131.16(11)
O(2S)#3-Na(1)-Na(2)#6	126.91(12)	O(1S)#3-Na(2)-Na(1)#10	124.81(11)
O(2B)#4-Na(1)-Na(2)#6	50.17(9)	O(1B)#8-Na(2)-Na(1)#10	47.78(9)
O(3S)#5-Na(1)-Na(2)#6	48.52(9)	O(3S)#9-Na(2)-Na(1)#10	51.36(9)
O(1)-Na(1)-Na(2)#6	144.30(11)	O(2B)#3-Na(2)-Na(1)#10	50.47(8)
O(2)-Na(1)-Na(2)#6	122.43(10)	O(2S)#2-Na(2)-Na(1)#10	97.76(9)
O(1B)#4-Na(1)-Na(2)#6	84.19(9)	O(1)#7-Na(2)-Na(1)#7	52.36(10)
C(12B)#4-Na(1)-Na(2)#6	69.64(10)	O(1S)#3-Na(2)-Na(1)#7	142.07(13)
C(12)-Na(1)-Na(2)#6	138.14(11)	O(1B)#8-Na(2)-Na(1)#7	53.42(9)
O(1B)#2-Na(1)-Na(2)#2	177.38(12)	O(3S)#9-Na(2)-Na(1)#7	136.31(12)
O(2S)#3-Na(1)-Na(2)#2	59.28(11)	O(2B)#3-Na(2)-Na(1)#7	86.62(9)
O(2B)#4-Na(1)-Na(2)#2	94.79(9)	O(2S)#2-Na(2)-Na(1)#7	45.82(8)
O(3S)#5-Na(1)-Na(2)#2	98.06(11)	Na(1)#10-Na(2)-Na(1)#7	90.44(5)
O(1)-Na(1)-Na(2)#2	44.14(8)	C(12)-O(1)-Na(2)#2	169.4(4)
O(2)-Na(1)-Na(2)#2	94.76(9)	C(12)-O(1)-Na(1)	93.4(3)
O(1B)#4-Na(1)-Na(2)#2	46.94(8)	Na(2)#2-O(1)-Na(1)	83.50(12)
C(12B)#4-Na(1)-Na(2)#2	68.59(10)	C(12)-O(2)-Na(1)	92.3(3)
C(12)-Na(1)-Na(2)#2	69.35(9)	C(1)-O(3)-C(14)	117.7(4)
Na(2)#6-Na(1)-Na(2)#2	129.46(7)	C(12B)-O(1B)-Na(1)#7	132.6(3)
O(1)#7-Na(2)-O(1S)#3	101.50(14)	C(12B)-O(1B)-Na(2)#11	137.9(3)
O(1)#7-Na(2)-O(1B)#8	83.38(13)	Na(1)#7-O(1B)-Na(2)#11	83.75(11)
O(1S)#3-Na(2)-O(1B)#8	162.19(17)	C(12B)-O(1B)-Na(1)#1	86.8(3)
O(1)#7-Na(2)-O(3S)#9	135.14(16)	Na(1)#7-O(1B)-Na(1)#1	130.66(14)
O(1S)#3-Na(2)-O(3S)#9	81.47(15)	Na(2)#11-O(1B)-Na(1)#1	79.64(11)
O(1B)#8-Na(2)-O(3S)#9	83.08(14)	C(12B)-O(2B)-Na(2)#12	130.9(3)
O(1)#7-Na(2)-O(2B)#3	136.38(14)	C(12B)-O(2B)-Na(1)#1	92.7(3)
O(1S)#3-Na(2)-O(2B)#3	104.56(15)	Na(2)#12-O(2B)-Na(1)#1	79.36(11)
O(1B)#8-Na(2)-O(2B)#3	82.32(12)	C(14B)-O(3B)-C(1B)	114.5(6)

Table B.2. *Continued.*

C(1S)-O(1S)-Na(2)#12	137.8(3)
C(1S)-O(1S)-H(1SO)	105.7
Na(2)#12-O(1S)-H(1SO)	116.0
C(2S)-O(2S)-Na(1)#12	132.2(3)
C(2S)-O(2S)-Na(2)#7	104.8(3)
Na(1)#12-O(2S)-Na(2)#7	74.90(13)
C(2S)-O(2S)-H(2SO)	116.8
Na(1)#12-O(2S)-H(2SO)	106.0
Na(2)#7-O(2S)-H(2SO)	64.2
C(3S)-O(3S)-Na(2)#13	114.1(4)
C(3S)-O(3S)-Na(1)#14	132.6(4)
Na(2)#13-O(3S)-Na(1)#14	80.12(12)
C(3S)-O(3S)-H(3SO)	105(5)
Na(2)#13-O(3S)-H(3SO)	115(5)
Na(1)#14-O(3S)-H(3SO)	108(5)

Symmetry transformations used to generate equivalent atoms:

#1 x+1,y+1,z-1 #2 -x+1,y-1/2,-z+1 #3 x,y-1,z

#4 x-1,y-1,z+1 #5 x-1,y-1,z #6 x-1,y,z+1

Table B.3. Anisotropic displacement parameters ($Å^2x10^3$) for methanol solvate of sodium naproxen, anisotropic displacement factor exponent takes the form: $-2\pi^2$ [h^2 $a^{*2}U^{11}$+...2 h k $a^*b^*U^{12}$].

	U^{11}	U^{22}	U^{33}	U^{23}	U^{13}	U^{12}
C(1)	47(3)	35(3)	36(3)	-4(2)	9(2)	-2(2)
C(2)	40(2)	37(3)	43(3)	7(2)	13(2)	4(2)
C(3)	27(2)	31(2)	41(3)	4(2)	8(2)	5(2)
C(4)	33(2)	30(2)	43(3)	4(2)	12(2)	-1(2)
C(5)	32(2)	33(2)	31(3)	1(2)	5(2)	-3(2)
C(6)	26(2)	27(2)	36(3)	5(2)	4(2)	5(2)
C(7)	33(2)	30(2)	36(3)	1(2)	10(2)	-6(2)
C(8)	35(2)	32(2)	43(3)	3(2)	2(2)	-1(2)
C(9)	45(3)	40(3)	45(4)	-6(2)	10(2)	-13(2)
C(10)	44(3)	48(3)	38(3)	-4(2)	6(2)	-7(2)
C(11)	30(2)	35(2)	36(3)	5(2)	3(2)	1(2)
C(12)	31(2)	23(2)	34(3)	-2(2)	9(2)	-3(2)
C(13)	45(3)	79(4)	49(4)	25(3)	0(3)	16(3)
C(14)	86(4)	64(4)	40(4)	-6(3)	23(3)	-23(3)
C(1B)	41(3)	81(5)	98(6)	53(5)	13(3)	-1(3)
C(2B)	105(6)	64(5)	72(5)	11(4)	-14(4)	11(4)
C(3B)	59(3)	43(3)	52(4)	5(3)	-11(3)	-4(3)
C(4B)	80(5)	74(5)	101(6)	21(5)	-30(4)	-12(4)
C(5B)	132(6)	73(5)	33(4)	7(3)	28(4)	34(4)
C(6B)	75(4)	61(4)	48(4)	22(3)	12(3)	29(3)
C(7B)	85(5)	111(6)	46(4)	34(4)	27(4)	35(5)
C(8B)	59(4)	43(3)	116(6)	6(4)	-27(4)	-4(3)
C(9B)	103(6)	74(5)	91(6)	12(4)	-33(5)	-21(5)
C(10B)	93(5)	78(5)	63(5)	4(4)	31(4)	-7(4)
C(11B)	56(3)	49(3)	25(3)	4(2)	10(2)	14(3)
C(12B)	37(2)	27(2)	33(3)	-1(2)	9(2)	-2(2)
C(13B)	61(4)	96(5)	61(4)	10(4)	-14(3)	4(4)
C(14B)	45(3)	74(5)	132(7)	-3(5)	-14(4)	-4(3)
C(1S)	74(4)	40(3)	66(4)	-10(3)	34(3)	-11(3)
C(2S)	63(3)	51(3)	45(4)	-5(3)	12(3)	-20(3)

Table B.3. *Continued.*

	U^{11}	U^{22}	U^{33}	U^{23}	U^{13}	U^{12}
C(3S)	49(3)	73(4)	69(4)	14(4)	-6(3)	-12(3)
Na(1)	34(1)	27(1)	37(1)	-1(1)	7(1)	5(1)
Na(2)	39(1)	24(1)	47(1)	3(1)	17(1)	1(1)
O(1)	43(2)	31(2)	59(2)	5(2)	19(2)	-6(2)
O(2)	39(2)	28(2)	57(2)	-3(2)	11(2)	5(2)
O(3)	65(2)	51(2)	39(2)	-7(2)	13(2)	-7(2)
O(1B)	42(2)	26(2)	43(2)	-5(2)	11(2)	-3(1)
O(2B)	51(2)	26(2)	35(2)	-2(1)	3(1)	7(2)
O(3B)	70(3)	96(4)	66(3)	4(3)	10(2)	18(3)
O(1S)	81(3)	28(2)	98(4)	-5(2)	56(3)	-11(2)
O(2S)	82(3)	36(2)	47(2)	-5(2)	25(2)	-22(2)
O(3S)	40(2)	25(2)	48(2)	2(2)	8(2)	0(2)

Table B.4. Hydrogen coordinates (x 10^4) and isotropic displacement parameters ($Å^2$ x 10^3) for methanol solvated form of sodium naproxen.

	x	y	z	U(eq)
H(2A)	5243	1061	5380	47
H(4A)	5710	1928	6959	42
H(5A)	5343	1950	8406	38
H(7A)	2806	-993	7828	39
H(9A)	2407	-2034	6284	52
H(10A)	2731	-1968	4834	52
H(11A)	3976	1784	9432	41
H(13A)	5145	-505	9736	87
H(13B)	4174	-1783	9604	87
H(13C)	4254	-492	10410	87
H(14A)	4834	519	3112	94
H(14B)	5557	348	4024	94
H(14C)	4711	1829	3889	94
H(2B)	9289	10459	5582	98
H(4BA)	10975	10701	4761	105
H(5BA)	11800	10226	3492	93
H(7BA)	9340	7683	2316	95
H(9BA)	7779	7472	3063	110
H(10B)	6872	7861	4368	92
H(11B)	11439	7274	2020	52
H(13D)	12736	9171	2630	111
H(13E)	12190	10642	2039	111
H(13F)	12721	9096	1580	111
H(14D)	7308	10042	6890	128
H(14E)	8068	11096	6319	128
H(14F)	8413	9270	6668	128
H(1S1)	6988	10131	2446	88
H(1S2)	6133	9296	1742	88
H(1S3)	6334	11273	1725	88
H(2S1)	879	9205	7299	79

Table B.4. *Continued.*

	x	y	z	U(eq)
H(2S2)	-26	7938	6921	79
H(2S3)	1024	7235	7457	79
H(3S1)	6980	9739	9260	96
H(3S2)	7347	7994	8873	96
H(3S3)	7679	9717	8440	96
H(1SO)	7388	8846	1102	56
H(2SO)	-210	7368	8394	56
H(3SO)	8500(40)	8500(70)	9760(40)	22(16)

Table B.5. Torsion angles [°] for methanol solvated form of sodium naproxen.

O(3)-C(1)-C(2)-C(3)	177.2(4)
C(10)-C(1)-C(2)-C(3)	-3.6(7)
C(1)-C(2)-C(3)-C(4)	-178.3(5)
C(1)-C(2)-C(3)-C(8)	1.4(7)
C(8)-C(3)-C(4)-C(5)	-2.5(7)
C(2)-C(3)-C(4)-C(5)	177.3(4)
C(3)-C(4)-C(5)-C(6)	-1.1(7)
C(4)-C(5)-C(6)-C(7)	3.3(6)
C(4)-C(5)-C(6)-C(11)	-177.1(4)
C(5)-C(6)-C(7)-C(8)	-2.1(6)
C(11)-C(6)-C(7)-C(8)	178.4(4)
C(4)-C(3)-C(8)-C(9)	-179.0(5)
C(2)-C(3)-C(8)-C(9)	1.2(6)
C(4)-C(3)-C(8)-C(7)	3.6(6)
C(2)-C(3)-C(8)-C(7)	-176.2(4)
C(6)-C(7)-C(8)-C(9)	-178.6(5)
C(6)-C(7)-C(8)-C(3)	-1.3(7)
C(3)-C(8)-C(9)-C(10)	-1.7(7)
C(7)-C(8)-C(9)-C(10)	175.5(5)
C(8)-C(9)-C(10)-C(1)	-0.4(8)
C(2)-C(1)-C(10)-C(9)	3.2(8)
O(3)-C(1)-C(10)-C(9)	-177.6(5)
C(7)-C(6)-C(11)-C(12)	-29.5(6)
C(5)-C(6)-C(11)-C(12)	151.0(4)
C(7)-C(6)-C(11)-C(13)	95.3(5)
C(5)-C(6)-C(11)-C(13)	-84.2(5)
C(6)-C(11)-C(12)-O(1)	94.1(5)
C(13)-C(11)-C(12)-O(1)	-30.5(7)
C(6)-C(11)-C(12)-O(2)	-83.3(5)
C(13)-C(11)-C(12)-O(2)	152.1(5)
C(6)-C(11)-C(12)-Na(1)	6(15)
C(13)-C(11)-C(12)-Na(1)	-119(15)
C(10B)-C(1B)-C(2B)-C(3B)	-1.0(11)

Table B.5. *Continued.*

O(3B)-C(1B)-C(2B)-C(3B)	179.3(5)
C(1B)-C(2B)-C(3B)-C(4B)	-177.0(7)
C(1B)-C(2B)-C(3B)-C(8B)	0.2(8)
C(8B)-C(3B)-C(4B)-C(5B)	3.1(11)
C(2B)-C(3B)-C(4B)-C(5B)	179.9(6)
C(3B)-C(4B)-C(5B)-C(6B)	-3.2(10)
C(4B)-C(5B)-C(6B)-C(7B)	2.3(10)
C(4B)-C(5B)-C(6B)-C(11B)	-176.4(6)
C(5B)-C(6B)-C(7B)-C(8B)	-1.0(9)
C(11B)-C(6B)-C(7B)-C(8B)	177.8(5)
C(4B)-C(3B)-C(8B)-C(9B)	179.4(8)
C(2B)-C(3B)-C(8B)-C(9B)	2.4(10)
C(4B)-C(3B)-C(8B)-C(7B)	-2.0(10)
C(2B)-C(3B)-C(8B)-C(7B)	-179.0(5)
C(6B)-C(7B)-C(8B)-C(9B)	179.6(7)
C(6B)-C(7B)-C(8B)-C(3B)	0.8(9)
C(3B)-C(8B)-C(9B)-C(10B)	-3.9(11)
C(7B)-C(8B)-C(9B)-C(10B)	177.5(6)
C(2B)-C(1B)-C(10B)-C(9B)	-0.5(12)
O(3B)-C(1B)-C(10B)-C(9B)	179.2(6)
C(8B)-C(9B)-C(10B)-C(1B)	2.7(10)
C(7B)-C(6B)-C(11B)-C(13B)	172.7(6)
C(5B)-C(6B)-C(11B)-C(13B)	-8.6(8)
C(7B)-C(6B)-C(11B)-C(12B)	49.9(8)
C(5B)-C(6B)-C(11B)-C(12B)	-131.4(5)
C(6B)-C(11B)-C(12B)-O(1B)	-122.7(5)
C(13B)-C(11B)-C(12B)-O(1B)	112.2(6)
C(6B)-C(11B)-C(12B)-O(2B)	60.0(6)
C(13B)-C(11B)-C(12B)-O(2B)	-65.2(6)
C(6B)-C(11B)-C(12B)-Na(1)#1	140.5(7)
C(13B)-C(11B)-C(12B)-Na(1)#1	15.3(11)
O(1)-C(12)-Na(1)-O(1B)#2	169.7(3)
O(2)-C(12)-Na(1)-O(1B)#2	-11.6(3)
C(11)-C(12)-Na(1)-O(1B)#2	-101(15)

Table B.5. *Continued.*

O(1)-C(12)-Na(1)-O(2S)#3	-62.0(3)
O(2)-C(12)-Na(1)-O(2S)#3	116.6(3)
C(11)-C(12)-Na(1)-O(2S)#3	27(15)
O(1)-C(12)-Na(1)-O(2B)#4	84.9(3)
O(2)-C(12)-Na(1)-O(2B)#4	-96.4(3)
C(11)-C(12)-Na(1)-O(2B)#4	174(15)
O(1)-C(12)-Na(1)-O(3S)#5	3.5(8)
O(2)-C(12)-Na(1)-O(3S)#5	-177.8(6)
C(11)-C(12)-Na(1)-O(3S)#5	93(15)
O(2)-C(12)-Na(1)-O(1)	178.7(5)
C(11)-C(12)-Na(1)-O(1)	89(15)
O(1)-C(12)-Na(1)-O(2)	-178.7(5)
C(11)-C(12)-Na(1)-O(2)	-90(15)
O(1)-C(12)-Na(1)-O(1B)#4	32.9(3)
O(2)-C(12)-Na(1)-O(1B)#4	-148.4(3)
C(11)-C(12)-Na(1)-O(1B)#4	122(15)
O(1)-C(12)-Na(1)-C(12B)#4	59.0(3)
O(2)-C(12)-Na(1)-C(12B)#4	-122.3(3)
C(11)-C(12)-Na(1)-C(12B)#4	148(15)
O(1)-C(12)-Na(1)-Na(2)#6	119.1(3)
O(2)-C(12)-Na(1)-Na(2)#6	-62.2(3)
C(11)-C(12)-Na(1)-Na(2)#6	-152(15)
O(1)-C(12)-Na(1)-Na(2)#2	-7.5(3)
O(2)-C(12)-Na(1)-Na(2)#2	171.2(3)
C(11)-C(12)-Na(1)-Na(2)#2	82(15)
O(2)-C(12)-O(1)-Na(2)#2	71.0(18)
C(11)-C(12)-O(1)-Na(2)#2	-106.3(16)
Na(1)-C(12)-O(1)-Na(2)#2	72.3(16)
O(2)-C(12)-O(1)-Na(1)	-1.4(5)
C(11)-C(12)-O(1)-Na(1)	-178.7(4)
O(1B)#2-Na(1)-O(1)-C(12)	-13.9(4)
O(2S)#3-Na(1)-O(1)-C(12)	117.5(3)
O(2B)#4-Na(1)-O(1)-C(12)	-97.7(3)
O(3S)#5-Na(1)-O(1)-C(12)	-178.7(3)

Table B.5. *Continued.*

O(2)-Na(1)-O(1)-C(12)	0.7(3)
O(1B)#4-Na(1)-O(1)-C(12)	-145.5(3)
C(12B)#4-Na(1)-O(1)-C(12)	-118.9(3)
Na(2)#6-Na(1)-O(1)-C(12)	-92.7(3)
Na(2)#2-Na(1)-O(1)-C(12)	169.9(3)
O(1B)#2-Na(1)-O(1)-Na(2)#2	176.24(17)
O(2S)#3-Na(1)-O(1)-Na(2)#2	-52.33(13)
O(2B)#4-Na(1)-O(1)-Na(2)#2	92.44(13)
O(3S)#5-Na(1)-O(1)-Na(2)#2	11.4(3)
O(2)-Na(1)-O(1)-Na(2)#2	-169.12(19)
O(1B)#4-Na(1)-O(1)-Na(2)#2	44.66(11)
C(12B)#4-Na(1)-O(1)-Na(2)#2	71.22(13)
C(12)-Na(1)-O(1)-Na(2)#2	-169.9(3)
Na(2)#6-Na(1)-O(1)-Na(2)#2	97.45(17)
O(1)-C(12)-O(2)-Na(1)	1.4(5)
C(11)-C(12)-O(2)-Na(1)	178.7(4)
O(1B)#2-Na(1)-O(2)-C(12)	169.1(3)
O(2S)#3-Na(1)-O(2)-C(12)	-67.7(3)
O(2B)#4-Na(1)-O(2)-C(12)	87.3(3)
O(3S)#5-Na(1)-O(2)-C(12)	177.8(6)
O(1)-Na(1)-O(2)-C(12)	-0.7(3)
O(1B)#4-Na(1)-O(2)-C(12)	35.5(3)
C(12B)#4-Na(1)-O(2)-C(12)	60.8(3)
Na(2)#6-Na(1)-O(2)-C(12)	135.6(3)
Na(2)#2-Na(1)-O(2)-C(12)	-8.3(3)
C(2)-C(1)-O(3)-C(14)	-5.4(8)
C(10)-C(1)-O(3)-C(14)	175.4(5)
O(2B)-C(12B)-O(1B)-Na(1)#7	-124.0(4)
C(11B)-C(12B)-O(1B)-Na(1)#7	58.8(6)
Na(1)#1-C(12B)-O(1B)-Na(1)#7	-146.5(3)
O(2B)-C(12B)-O(1B)-Na(2)#11	93.2(6)
C(11B)-C(12B)-O(1B)-Na(2)#11	-84.0(6)
Na(1)#1-C(12B)-O(1B)-Na(2)#11	70.6(4)
O(2B)-C(12B)-O(1B)-Na(1)#1	22.6(5)

Table B.5. *Continued.*

C(11B)-C(12B)-O(1B)-Na(1)#1	-154.7(4)
O(1B)-C(12B)-O(2B)-Na(2)#12	54.4(6)
C(11B)-C(12B)-O(2B)-Na(2)#12	-128.4(4)
Na(1)#1-C(12B)-O(2B)-Na(2)#12	78.2(3)
O(1B)-C(12B)-O(2B)-Na(1)#1	-23.8(5)
C(11B)-C(12B)-O(2B)-Na(1)#1	153.4(4)
C(2B)-C(1B)-O(3B)-C(14B)	-7.8(9)
C(10B)-C(1B)-O(3B)-C(14B)	172.5(7)

Symmetry transformations used to generate equivalent atoms:

#1 x+1,y+1,z-1 #2 -x+1,y-1/2,-z+1 #3 x,y-1,z

#4 x-1,y-1,z+1 #5 x-1,y-1,z #6 x-1,y,z+1

#7 -x+1,y+1/2,-z+1 #8 -x+2,y-1/2,-z #9 x,y-1,z-1

#10 x+1,y,z-1 #11 -x+2,y+1/2,-z #12 x,y+1,z

#13 x,y+1,z+1 #14 x+1,y+1,z

TableB.6. Hydrogen bonds for methanol solvated form of sodium naproxen [Å and °].

D-H...A	d(D-H)	d(H...A)	d(D...A)	<(DHA)
O(1S)-H(1SO)...O(2)#7	0.91	1.89	2.731(5)	152.0
O(2S)-H(2SO)...O(2B)#2	0.87	1.82	2.670(5)	163.3

Symmetry transformations used to generate equivalent atoms:

#1 x+1,y+1,z-1 #2 -x+1,y-1/2,-z+1 #3 x,y-1,z

#4 x-1,y-1,z+1 #5 x-1,y-1,z #6 x-1,y,z+1

#7 -x+1,y+1/2,-z+1 #8 -x+2,y-1/2,-z #9 x,y-1,z-1

#10 x+1,y,z-1 #11 -x+2,y+1/2,-z #12 x,y+1,z

#13 x,y+1,z+1 #14 x+1,y+1,z

REFERENCES

Atkins, P. Physical Chemistry. 6th ed. Oxford University Press. New York, New York. 1999.

Bauer, J.; Spanton, S.; Henry, R.; Quick, J.; Dziki, W.; Porter, W.; Morris J. Ritonavir: An Extraordinary Example of Conformational Polymorphism. *Pharmaceutical Research* **2001**, (18), 6, 859-866.

Bechtloff, B.; Sordhoff, S.; Ulrich, J, Pseudopolymorphs in Industrail Use. *Crystal Research and Technology* **2001**, 36, (12), 1315-1328.

Beiny, D.H.; Mullion, J.W., Solubilities of Higher Normal Alkanes in M-Xylene. *Journal of Chemical and Engineering Data* **1987**, (32), 1, 9-10.

Braun, D.E.; Gelbrich, T.; Kahlenberg, V.; Tessadri, R.; Wieser, J.; Griesser, U.J., Stability of Solvates and Packing Systems of Nine Crystal Forms of the Anhtipsychotic Drug Aripiprazole. *Crystal Growth & Design* **2009**, (9), 2, 1054-1065.

Braun, D.E.; Kahlenberg, V.; Gelbrich, T.; Ludescher, J.; Griesser, U. J., Solid State Characterization of four solvates of R-cinacalcet Hydrochloride. *CrystEnfComm* **2008**, 10, 1617-1625.

Brittain, H. G.; Byrn S. R. Structural Aspects of Polymorphism In Polymorphism in Pharmaceutical Solids. Brittain, H.G. Eds. Marcel Dekker, Inc. New York, New York. 1999. pp. 73-124.

Brown, S.D.; Burgess, J.; Fawcett, J.; Parsons, S. A.; Russell, D.R.; Wiltham, E. Three Polymorphic Forms of 2-Ethyl-3-hydroxy-4-pyranone (Ethyl Maltol). *Acta Crystallographica Section C* **1995** C51, 1335-1338.

Burger, A.; Ramberger, R. Polymorphism of Pharmaceutical and Other Molecular-Crystals 1.Theory of Thermodynamic Rules. *Mikrochimica Acta* **1979**, (2), 34, 259-271.

Byrn, S. R.; Lin, C. T., Effect of Crystal Packing and Defects on Desolvation of Hydrate Crystals of Cafferine and L-7(-)-1,4-Cyclohexadiene-1-anine. *Journal of the American Chemical Society* **1976**, (98), 13, 4004-4005.

Chavez, K.J.; Rousseau, R.W., 'Characterization of a Novel Methylated Form of Sodium Naproxen: *proceedings of the 17th International Symposium on Industrial Crystallization*, Maastricht, 17-18 September 2008.

Chen, Z. N.; Deng, R. W.; Wu, J. G. Synthesis, Characterization, and Antiinflammatory Activity of Naproxen Complexes with Rare Eath (III). *Journal. of Inorgnaic Biochemistry* **1992**, 47, 81-87.

Cox, J. S. G.; Woodard, G. D.; McCrone, W. C. Solid-state chemistry of cromolyn sodium (disodium cromoglycate) *Journal of Pharmaceutical Sciences* **1971** 60, 1458-1465.

Di Martino, P,; Barthelemy, C.; Palmieri, G.F.; Martelli, S., Physical Characterization of Naproxen Sodium Hydrate and Anhydrate Forms. *European Journal of Pharmaceutical Science* **2001**, (14), 4, 293-300.

Di Martino, P.; Barthelemy, C.; Joiris, E.; Capsori, D.; Masic, A.; Massarotti, V.; Gobetto, R.; Bini, M.; and martelli, S., A New Tetrahydrated Form of Sodium Naproxen. *Journal of Pharmaceutical Sciences* **2007**, (96), 1, 156-167.

Domiano, P.; NarDelli, M.; Balsamo, A.; Macchia, B.; Macchia, F., Crystal and Molecular Structure of Para-Methoxybenzyl 2-Aplpha-Methyl-2-Beta-[(R) Acetoxy(Methoxy)Methyl]-6-Beta-Phenoxyacetamidopenam-3-Alpha-Carboxylate. *Acta Crystallographica, Section B-Structural Science* **1979**, (35), JUN, 1363-1372.

Florey, K., Cephradine. In *Analytical Profiles of Drug Substances*, Florey, K., Ed. Academic Press: New York, 1973; Vol. 2, pp 1-62.

Görbitz, C. H.; Hersleth, H-P. On the inclusion of solvent molecules in the crystal structure of organic compounds. *Acta Crystallographica*, *Sect. B* **2000**, B56, 526-534.

Griesser, U. J., The Importance of Solvates In Polymorphism in the Pharmaceutical Industry. Hilfiker, R. Eds. WILEy-VCH Verlag GmbH & Co. KGaA. Weinheim, Germany. 2006. pp. 211-233.

Harrington, P.J.; Lodewijk, E., Twenty Years of Naproxen Technology. *Organic Process Research & Development* **1997**, 1, 72-76.

Hiramatsu, Y.; Suzuke, H.; Kuchiki, A.; Nakagawa, H.; Fujii, S. X-Ray Structural Studies of Lomeridine Dihydrochloide. *Journal of Pharmaceutical Sciences* **1996**, 85, 761-765.

Jacobsen, N.E., NMR Spectroscopy Explained: Simplified Theory, Applications and Examples for Organic Chemistry and Structural Biology. Wiley: New York, 2007; p 75-76.

Khanhari, R.K.; Grant, D. J. W., Pharmaceutical Hydrates. *Thermochimica Acta* **1995**, 248, 61-79.

Khanhari, R.K., Law, D., Grant, D.J.W. Determination of Water-Content in Pharmaceutical Hydrates by Differential Scanning Calorimetry. **1992** 82, 117-127.

Kim, Y.B.; Park, I.Y.; Lah, W.R. The Crystal Structure of Naproxen Sodium, ($C_{14}H_{13}O_3Na$), A non-steroidal anti-inflammatory Agent. *Archives of Pharmacal Research* **1990** 13, (2), 166-173.

Kim, Y-S. (2005) *Crystallization and Solid-state Transformation of Pseudopolymorphic Forms of Sodium Naproxen*. PhD Thesis Georgia Institute of Technology.

Kim, Y-S., Rousseau, R.W., Characterization and Solid-State Transformation of the Pseudopolumorphic Forms of Sodium Naproxen. *Crystal Growth & Design* **2004**, 4, (6), 1211-1216.

Kim, Y-S. ; Mendez del Rio, J. ; Rousseau, R.W., Solubility and Prediction of the Heat of Solution of Sodium Naproxen in Aqueous Solutions. *Journal of Pharmaceutical Sciences* **2005**, 94, 1941-1948.

Kim, Y.-S.; VanDerveer, D.; Rousseau, R.W.; Wilkinson, A.P. Anhydrous Sodium Naproxen. *Acta Crystallographica Section E: Metal-Organic Papers* **2004**, E60, m419-m420.

Kitaigorodski, A. I. (1961). *Organic Chemical Crystallography*. New York: Consultants Bureau.

Kuhnertb, M.; Gasser, P., Solvates and Polymorphic Modifications of Steroid Hormones. 1. *Microchemical Journal* **1971**, (16), 3, 419.428.

Long, F. A.; McDevit, W.F. Activity Coefficients of Nonelectrolyte Solutes in Aqueous Salt Solutions. *Chemical Reviews* **1952**, 51, 339-169.

Macrae, C. F.; Bruno, I. J.; Chisholm, J.A.; Edgington, P.R.; McCabe, P.; Pidcock, E.; Rodriguez-Monge, L.; Taylor, R.; van de Streek, J.; Wood, P.A., Mercury CSD 2.0 - New Features for the Visualization and Investigation of Crystal Structures *Journal of Applied Crystallography*, **2008**, 41, 466-470.

Méndez del Rio, J. R. (2004) *Solubility and phase transitions in batch and laminar-flow tubular crystallizers.* PhD Thesis Georgia Institute of Technology.

Moore, D. E.; Chappuis, P. P., A comparative-study of the photochemistry of the non-steroidal anti-inflammatory drugs, naproxen, benoxaprofen, and indomethacin. *Photochemistry and Photobiology* **1988**, 47, (2), 173-180.

Morris, K.R. Structural Aspects of Hydrates and Solvates. In *Polymorphism in Pharmaceutical Solids*, Brittain, H.G., Ed. Marcel Dekker: New York, 1999; pp 125-181.

Mullin, J.W. Crystallization. 4th ed. Burlington, MA: Elsevier Butterworth-Heinemann, 2004.

Myrdal, P. B.; Jozwiakowski, M. J. In *Water-Insoluble Drug Formulation*; Lui, R. Ed.; CRC Press LLC; Boca Raton, Florida, 2000; pp 531-554.

Ostwald, W., Studdien über die Bildung und Umwandlung fester Körper. *Zeitschrift für Physikalische Chemie* **1897**, 22, 289-330.

Phan, H. V.; Allen, R. H,; Coats, R. A. Sodium (S)-2-(6-Methoxy-2-Naphthyl)Propionate Monohydrate. US005874614A, FEB 23, 1999.

Pha, H, V.; Young, R. E. Preparation of high purity sodium (S)-2(6-methoxy-2-naphthyl)propionate. US5859292, JAN 12, 1999.

Poole, J. W.; Owen, G.; Silverio, J.; Freyhof, J.N.; B., R. S., Physiochemcial Factors Influencing the Absorption of the Anhydrous and Trihydrated Forms of Ampicilin. *Current Therapeutic Research, Clinical and Experimental* **1968**, 10, (6), 292-303.

Prausnitz, J.M.; Lichtenthaler, R.N.; Azevedo, E.G., *Molecular Thermodynamics of Fluid-Phase Equilibria*. 3rd ed.; Prentice-Hall PTR: Upper Saddle River, N.J., 1999.

Qu, H.; Louhi-Kultanen, M.; Kallas, J., Solubility and Stability of Anhydrate/Hydrate in Solvent Mixtures. *International Journal of Pharmaceutics* **2006**, 321, 101-107.

Ravikumar, K.; Rajan, S.S.; Pattabhi, V., Structure of Naproxen, $C_{14}H_{14}O_3$. *Acta Crystallographica Section C-Crystal Structure Communications* **1985**, 41, (FEB), 280-282.

Ressler, C., Solid-State dehydrogenation of S-1,4-Cylohexadiene-1-anine hydrate to L-phenylananine. *Journal of Organic Chemistry* **1972**, 37, (19), 2933.

Rocco, W. L.; Morphet, C.; Laughlin, S. M., Solid-state Characterization of Zanoterone. *International Journal of Pharmaceutics* **1995**, 122, 17-25.

Schmidt, A.C.; Niederwanger, V.; Griesser, U. J., Solid-state Forms of Prilocaine Hydrochloride: Crystal Polymorphs of Local Anesthetic Drugs, Part II. *Journal of Thermal Alnalysis and Calorimetry* **2004**, 77, 639-652.

Smith, J.M.; Van Ness, H.C.; Abbott, M.M. Introduction to Chemical Engineering Thermodynamics. 5th ed; McGraw-Hill: New York, NY, 1996.

Van de Streek, J. All series of multiple solvates (including hydrates) from the Cambridge Structural Database. *CrystEngComm*. **2007**, 9, 350-352.

Wirth, D. D.; Stephenson, G. A., Purification of Dirithromycin. Impurity Reduction and Polymorph Manipulation. *Organic Process Research & Development* **1997**, 1, 55-60.

Yaws, Carl L. (2003). Yaws' Handbook of Thermodynamic and Physical Properties of Chemical Compounds. Knovel. Online version available at: http://knovel.com.www.library.gatech.edu:2048/web/portal/browse/display?_EXT_KNOVEL_DISPLAY_bookid=667&VerticalID

Zhu, H.; Yuen, C.; Grant D.J.W., Influence of water activity in organic solvent + water mixtures on the nature of crystallizing drug phase. 1. Theophylline. *International Journal of Pharmaceutics* **1996,** 135, 151-160.

Zhu, H.; Grant D.J.W., Influence of water activity in organic solvent + water mixtures on the nature of crystallizing drug phase. 2. Ampicillin. *International Journal of Pharmaceutics* **1996**, 13, 33-43.